Peripheral discomfort glare and its influence on task performance on display screen equipment

May 28th
2019

Mads Klogborg Mårbjerg
Aalborg University Copenhagen

Supervisor
Henrik Clausen

Aalborg University Copenhagen

Semester: 10th semester, Master Thesis

Title: Peripheral discomfort glare and its influence on task performance on display screen equipment

Project Period: 1st February 2019 - 28th May 2019

Semester Theme: Master Thesis

Aalborg University Copenhagen
Frederikskaj 12,
DK-2450 Copenhagen SV
Semester Coordinator: Georgios Triantafyllidis
Secretary: Lisbeth Nykjær

Supervisor(s): Henrik Clausen

Project group no.: N/A

Members: Mads Klogborg Mårbjerg

Abstract:

Peripheral discomfort glare is considered an undesirable attribute of light, and despite almost 100 years of research effort, it still eludes researchers to an extend. This thesis sought to understand the issues from the bottom-up by reviewing the literature on the visual system, discomfort glare, regulation of lighting, the development of glare prediction models, and why they are still imprecise. The review led to ask if discomfort glare could be measured to have an influence on task performance on display screen equipment in an experiment built for this thesis and how. If yes, where in the visual field would it influence the most. An experiment was carefully planned and performed, but also showed the difficulties of the process. The results turned out rather inconclusive, partly because of mistakes made in the experimental design, which could have an influence, and partly because of the Stroop task was doubted to fit as a performance testing method for an external stimuli. Despite inconclusive results, four measures were presented to improve the visual environment in offices by improving workflow and strategies between architects, interior and lighting designers. This included future revisions of lighting standards, a better general understanding of what influence lighting, future of lighting simulation analysis, and the importance of specifications for implementation of a lighting design.

Table of Contents

1. Introduction 8

2. Problem statement 9

2.1 Vision .9

2.2 Issue statement .9

2.3 Methods .9

2.4 Proposal .9

3. Literature Review 10

3.1 The Human Vision 10

3.2 Light and Glare 17

3.3 Light and Glare Regulation 18

3.3.1 Illuminance, Em 19

3.3.2 Uniformity, U0 20

3.3.3 Discomfort glare, UGR_L 20

3.3.4 Glare Shielding 22

3.3.5 Veiling Reflections and Reflected Glare 22

3.3.6 Flicker and Stroboscopic Effects 22

3.3.7 Work Stations with Display Screen Equipment (DSE) 24

3.4 Predictive Glare Models. 24

3.5 Background luminance and glare source size. 28

3.6 Immediate surround and non-uniform glare sources 30

3.7 Position Index In Predictive Glare Models 31

4. Methodology 41

4.1 Hypothesis 42

4.2 Initial experimental design 42

4.3 Modelling. 43

4.4 Glare sources 46

4.5 Electronics 47

4.6 Construction 48

4.7 Light Lab design 49

4.8 Performance task 50

4.8.1 Cognitive demand of the visual task 50

4.8.2 Experimental bias. 51

4.9 The Stroop task 53

4.10 Participants. 54
4.11 Pilot experiments 54
4.12 Challenges 55
5. Analysis 55
5.1 Response time (RT) 55
5.2 Number of errors and error rate (ER) 56
5.3 Stroop interference (SI) 56
5.4 Sample Standard Deviation (SSD) 57
5.5 Coefficient of Variation (CV). 57
6. Results 58
6.1 Questionnaire 58
6.2 Stroop task 58
6.3 Deviation from mean 60
7. Discussion 62
7.1 Unbalanced lighting. 62
7.2 Misplacement of glare sources 62
7.3 Manual on/off order. 63
7.4 Benchmark tests 63
7.5 Unbalanced Stroop task. 64
7.6 Stroop task design 65
8. Lighting Design Guidelines 67
8.1 Revised regulation. 67
8.2 The visual environment. 69
8.3 Digital analysis. 70
8.4 Specifications. 71
9. Conclusion 73
10. References 76

List of Tables

Table 1 DGP value categorization in ranges (*DS/EN 17037:2018,* Danish Standard, 2018). 22

Table 2 Transformation of the interpretation scale from BRS/BGI scale to the IES-GI scale and compared to Hopkinson's multiple criterion scale. The IES-GI scale was considered more intuitive. 26

Table 3 Centre of glare sources positioned in radial angle and angular distance to fit the BCD (III) curve as defined by Kim and Kim (2010b, 2010c). Positions are marked on the polar coordinate diagram from Figure 21. 45

Table 4 Illuminance adjustment study by Logadóttir et al. (2011a). The mean adjustment of the participants always ends up relatively close to the centre of range demonstrating a stimulus or centring bias. Unit = lux. 52

Table 5 CCT adjustment study by Logadóttir et al. (2011b). The mean adjustment of the participants always ends up relatively close to the centre of range demonstrating a stimulus or centring bias. The is true for both controller types. The difference between mean adjustment and centre of range is written in parenthesis. Unit = kelvin.. 52

Table 6 Stroop interference between self-reported glare sensitives and self-reported glare insensitives. Red colour marks the two maximum Stroop interference values for each group.. 60

Table 7 Response time for congruent conditions along with sample standard deviation (SSD) and coefficient of variation (CV). 61

Table 8 Response time for incongruent conditions along with sample standard deviation (SSD) and coefficient of variation (CV). 61

Table 9 Analysis of types of wrong answers in the Stroop tasks.. 65

List of Figures

Figure 1 Illustration of the anatomy of the eye. (Boyce, Fig. 2.4, 2014) 10
Figure 2 Refractive conditions (Remington, Fig. 1-4, 2012).. 11
Figure 3 Retinal cells and layers. The 10 retinal layers are indicated (Remington, Fig. 4-11, 2012). 11
Figure 4 Schematic showing regions of retina and corresponding histologic architecture (Remington, Fig. 4-26, 2012).. 12
Figure 5 The visual pathway (Remington, Fig. 13-1, 2012). 14
Figure 6 Characteristics of a sine wave (amplitude, period/cycle, time) (*Sine Wave*, chegg.com). 16
Figure 7 The CIE 1931 xy chromaticity diagram with the MacAdam ellipses plotted 10 times larger (*MacAdam ellipse*, Wikipedia.com).. 16
Figure 8 Danish office lighting regulation (*DS/EN 12464-1:2011*, Danish Standard, 2011). 19
Figure 9 Illustration of the components of a solid angle calculation (Sørensen, 2012). . . 20
Figure 10 Modulation values in the grey area minimises visual discomfort (*IEEE Std. 1789-2015, Fig. 20,* IEEE-SA, 2015). 23
Figure 11 Experimental device: (A) experimental equipment, (B) cross-section of the device; 1: LED light source, 2: incandescent lamp, 3: halogen lamp and 4: the headrest. (Kim and Kim, 2010) 29
Figure 12 S-shaped curve for determination of exponent c. At 5 sr, c = 0. The curve extended down to 0.0003 sr (Kim and Kim, 2010a). 30
Figure 13 Chart for determining position index located at various positions in the visual field.(Luckiesh and Guth, 1949) 31
Figure 14 Experimental apparatus. "Position index for a glare source located below the line of vision" Iwata et al. 32
Figure 15 Points of fixation and positions of glare sources (Iwata and Tokura, 1997). . . . 34
Figure 16 New position index chart (Iwata and Tokura, 1997). 34
Figure 17 (A) Experimental setup by Luckiesh and Guth (1949). (B) Experimental setup by Kim and Kim (2010b, 2010c). 36
Figure 18 Average visual field as a function of the radial angle (Kim and Kim, 2010b).. . . 36
Figure 19 Average visual field of thirty-two subjects (Kim and Kim, 2010b). 37
Figure 20 BCD luminance at the line of sight (Kim and Kim, 2010b). 37
Figure 21 Comparison between the equal BCD curves obtained from the experiment and the Guth's equal BCD curves (Kim and Kim, 2010b). 38
Figure 22 BCD luminance in the line of sight (Kim and Kim, 2010c). 39
Figure 23 The visual field limits of single and both eyes (Kim and Kim, 2010c).. 39
Figure 24 The BCD curves based on the averages of the left and right eyes and position index (Kim and Kim, 2010c).. 40
Figure 25 Plan layout and photograph of the lighting chamber used in this study (Kent, Fotios, and Altomonte, Fig. 1, 2018).. 43
Figure 26 3D model showing sphere of vision and line of sight. 43
Figure 27 Final model of the experimental setup. 44
Figure 28 3D model showing polar coordinates mapped on the sphere of vision. 44
Figure 29 3D model showing the visual field mapped in a work context. 44
Figure 30 View directions with projected areas of the glare sources onto the sphere of vision.. 45

Figure 31 The experiment setup model in a 3D model of the Light Lab. 46
Figure 32 Light test 1 46
Figure 33 Light test 2. 46
Figure 34 Light test. 46
Figure 35 Pulse Width Modulation (PWM) dimming (Davis, -). 47
Figure 36 Constant Current dimming (CC) (Davis, -). 47
Figure 37 (A:) Glare sources boxes with aluminium foil inside. (B) Standing screen wall. (C) Staircase mounting of the glare source boxes. (D) Final construction. 48
Figure 38 Light setup in Light Lab. 49
Figure 39 Finished experimental setup.. 50
Figure 40 Task area. 50
Figure 41 Glare source positions marked on the polar coordinate diagram from Figure 21. The blue spots marks the constructed position, indicating the error. 62
Figure 42 Conditions used in PsychoPy. 64
Figure 43 Office lighting regulation from the DS/EN 12464-1 revision (public hearing version). $E_{m,r}$ = min. maintained illuminance. $E_{m,u}$ = upper maintained illuminance. U_0 = min. uniformity. R_a = min. colour rendering index. R_{UGL} = max. UGR limit. E_z = min. cylindrical illuminance. $E_{m,wall}$ = min. average illuminance on walls. $E_{m,ceiling}$ = min. average illuminance on ceilings. 69

1. Introduction

The experience of discomfort glare is something most people can relate to and find unpleasant. It can slow productivity, cause health issues and lead to creative solutions to correct the lighting environment. Often these impromptu solutions are inefficient in correcting the problem and are visually unappealing in terms of design. In order to prevent discomfort glare in the first place, careful planning in the early design phase is crucial but most importantly is understanding the challenges to full extend. Discomfort glare has been a subject of research for almost 100 years. In that period of time lighting technology has developed from the traditional filament bulb to the LED technology being installed in this day and age. Discomfort glare is highly influenced by the lighting technology in place and LED technology has made it possible to emit increasingly brighter light from a decreasing size area.

This has been a huge paradigm shift for how to research and predict discomfort glare. Research from before LED technology is still relevant but experiences might change as quickly as design for luminaires changes and since LED chips are relatively really small, manufacturers can get really creative in their design, which is not always for greater good. Changing design and experiences makes it more unpredictable for lighting designers to know how luminaires will behave in a design. Trusting the UGR value in programs such as DIALux is an important and regulated guideline, but lighting designers also know this metric is imprecise and how the measurements are set up can vary. From personal experience, during internship and student job, getting a UGR value for a space up to regulation can become a challenge in projects with many other variables to consider between architects, interior designers and lighting designers. It is important for all parts in such a debate to understand what causes discomfort glare, or at least trust the insight of the lighting designer, to reach the optimal compromise between the variables.

Poor design choices will be revealed after implementation and can be costly to correct. Along with employee satisfaction, health and productivity, this should create enough incentive for clients to invest in better designs and get it right the first time. The best method to achieve this is to design with knowledge. Following the flow of research with a critical mindset is essential to stay updated on how technology trends influence users and to be able to implement them wisely. Discomfort glare has proven a complex subject to research since it involves physiology, psychology and the physics of light. It is challenging to design experiments trying to quantify the individual experiences users have, but it is a necessity to keep researching in order to develop better prediction methods. This master thesis will use a bottom-up approach to understand discomfort glare and its intricacies through literature, design an experiment to uncover the considerations inspired by related research, analyse and interpret the results to contribute to the field. The knowledge gained from this process will be translated into specific measures for architects, interior designers and lighting designers to implement in workflow and design to prevent discomfort glare in office spaces.

2. Problem statement

2.1 Vision

I imagine a world where the challenges with office lighting are a thing of the past and occupant issues related to lighting are non-existent, whether it be health issues or inadequate impromptu solutions to an uncomfortable lighting environment.

2.2 Issue statement

Discomfort glare is an undesired attribute of light in working environments such as offices that can cause great distraction and even health related issues. It is generally considered to be caused by an imbalance of brightness between the task area, where focus of sight is maintained, and the peripheral area, filling up the rest of the visual field. Despite extensive research and modern technology, prediction of discomfort glare is still a great challenge in early lighting design requiring multi-disciplinary knowledge and workflows to overcome.

2.3 Methods

By reviewing the literature on discomfort glare from the perspective of an aspiring lighting designer with little preliminary knowledge of the topic, it might be possible to gain insight into and understand its complexity. The following research questions are asked to guide this process:

- **RQ 1:** How does the human visual system function?
- **RQ 2:** What is discomfort glare and how does the human visual system respond?
- **RQ 3:** How does building codes regulate discomfort glare?
- **RQ 4:** How did the research develop and transform the glare prediction models?
- **RQ 5:** What are the shortcomings of the current glare prediction model?

2.4 Proposal

I propose that by developing a more cooperative workflow between architects, interior designers and lighting designers, and emphasise design choices based on scientific knowledge, office environments can become more pleasant to occupy for workers. Clearer design and workflow strategies can help avoid typical, modern challenges of lighting, particularly discomfort glare.

3. Literature Review

The literature review will follow the order in which the research questions are asked. This should provide a bottom-up approach to understand the complexity of peripheral discomfort glare, how it is currently regulated and predicted.

3.1 The Human Vision

Understanding the intricacies of visual perception requires a foundational basic knowledge and understanding of the human visual system. The process of vision is a matter of taking in information through the medium of light, relay, filter and interpret it. During this process light rays are converted in the eye to neural signals and sent through a complex pathway in the central nervous system to form the view humans perceive and can interpret consciously. In this chapter, this process will be revealed, with an attempt at keeping it brief, relatively simple and relevant, and therefore leave out a sizeable amount of information parts of the anatomy. Focus will be on the optics, conversion of light to neural signal, and where this signal is interpreted. The source material for this chapter is by Remington (2012) if nothing else is specifically mentioned.

The first mechanism of vision is the front of the eye, where the light rays enters through the cornea and lens (see Figure 1). The cornea is protected by a thin tear film which, among other functions, hydrates and oxygenates the eye, and keeps the light scattering and distortion of the incident light to a minimum by smoothing out the surface of the cornea. The light gets refracted as it passes through the tear film and cornea, which makes up about 70% of the total refractive power. The optical power is attributed to the change in refractive index from air to tear film and the curvature of the cornea. In this process, the visible incident light has only been scattered less than 1%

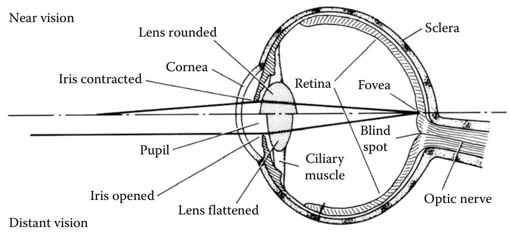

Figure 1: Illustration of the anatomy of the eye. (Boyce, Fig. 2.4, 2014)

The light then passes through the liquid (aqueous humor) in the so-called anterior chamber between the cornea, pupil and lens, which again causes refraction. The iris colour is determined by the tissue composition by the outer and inner layers of the iris. If the outer layer contains much pigmentation, it will appear brown. If it is only lightly pigmented, it will typically appear blue, green or grey depending on the combination of tissue in both the outer and inner layers. In the case of albinos, the iris will only get its colour from the inner layer rendering it pink. The light passes through the biconvex lens and travels through the so-called vitreous chamber filled with a gel-like substance (vitreous humor) until it reaches the retina. The lens makes up the last 30% of the total optical power. It is in this refractive process errors can occur from an imperfect shape of the eye or cornea causing either farsightedness (hyperopia) or nearsightedness (myopia), so a clear vision (emmetropia) cannot be achieved. This is corrected by placing a convex or concave lens, respectively, in front of the eye in the form of glasses or contact lenses to control the convergence or divergence of the light on the eye lens (see Figure 2). Glasses and contact lenses help achieving a normal focus of the light rays on the retina in the back of the eye.

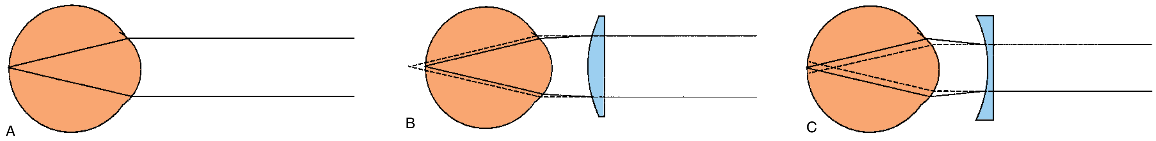

Figure 2: Refractive conditions (Remington, Fig. 1-4, 2012).

The light passes through cell layers on the retina, which decrease absorption and scattering in the eye, while the back of the retina particularly filters out ultraviolet light/radiation to protect the photosensitive cells. These cell layers consist of three different cell types, photoreceptor cells, collector cells and ganglion cells (see Figure 3). The photons carried by the light rays are reflected back and absorbed by photoreceptor cells called rods and cones. These cells contain different kinds of visual pigment (photopigment) defining their spectral sensitivity. The photopigment gets excited by the photons and starts a series of biochemical changes in a process called phototransduction. This creates an electrical current flow as an output which is send to the first of the collector cells, a neuron called a bipolar cell. There are 11 types of bipolar cells, one known type for rods and 10 for cones, and each rod or cone can have contact to several bipolar cells improving the sensitivity. Bipolar cells act as a relaying station, where neural signals from cones gets relayed to ganglion cells, while neural signals from rods gets relayed first to amacrine cells (another collector cell) and then to ganglion cells. Ganglion cells are the first cells in the visual pathway which can respond with an action potential by sending a signal to higher central nervous system (CNS) locations. Entangled with the rods, cones, bipolar and amacrine cells are horizontal cells and interplexiform neurons, the last two collector cells, which conveys information and feedback in between these layers. All the ganglion cell axons in the eye accumulate at the so-called optic disc and exits the eye through the optic nerve. The optic disc has no photoreceptor cells and does not elicit a response from light, therefore being a physiological blind spot in the eye.

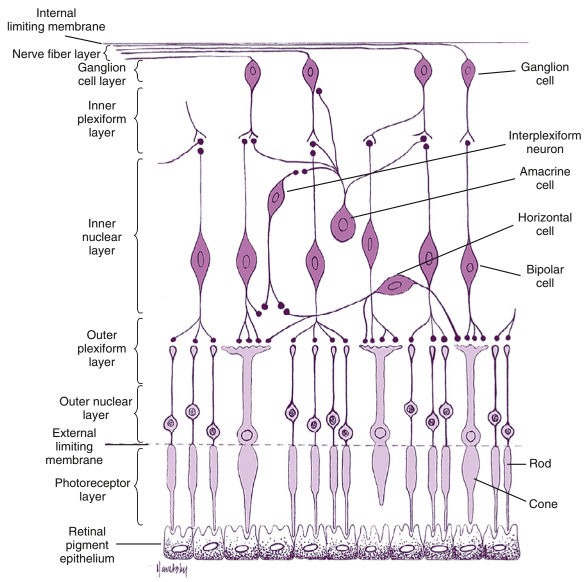

Figure 3: Retinal cells and layers. The 10 retinal layers are indicated (Remington, Fig. 4-11, 2012).

The human vision has been adapted to two scenarios, night and day. During the night, where only dim light is present, light detection is dominated by extremely light sensitive rod photoreceptors. This is called scotopic vision which emphasises detection of objects in low level illumination while sacrificing colour vision, so objects are perceived in a shade of grey. The adaption luminance for scotopic vision is less than 0.005 candelas/m^2 (cd/m^2). During the day, light detection is dominated by three types of cone photoreceptors sensitive to bright illumination and which can absorb specific wavelengths of either red (peak at 588 nm), green (peak at 531 nm) or blue (peak at 420 nm). This is called photopic vision which emphasises visual acuity and colour discrimination while sacrificing low illuminance detection. The adaption luminance for photopic vision is higher than 5 cd/m^2. The human colour vision is of the trichromatic type (three components of light, RGB) which has been shown to provide an accurate description of surface colours under most lighting conditions. Having a colour vision based on inputs from more than three photoreceptors would demand more of the neural capacity of the visual system, possibly not a worthy trade-off in the human evolution. Between the two states of vision, the mesopic vision is found when it is neither below 0.005 cd/m^2 or above 5 cd/m^2 in adaption luminance. Both rods and cones are active until one of the other states is reached and one type will take over. The pattern of emphasis and sacrifice can be seen in the number connections between rods and cones and individual ganglion cells. A single ganglion cell can be connected to 5,000 bipolar cells further connected to 75,000 rods to achieve an even higher sensitivity, when gathering the information about a dim lit environment. In contrast, a single ganglion cell can be connected to a small number of bipolar cells further connected to a small number of cones to achieve an even higher ability to discriminate details and colours when gathering information.

The focal point on the retina is called the central retina and consists of an area of approximately 9 mm in diameter occupied by useful colour vision (see Figure 4). From the centre and out lies the foveola (approximate diameter 0.35 mm), the fovea (approximate horizontal diameter 1.5 mm), parafoveal area (width 0.5 mm) and perifoveal area (width 1.5 mm). The fovea contains a depression at the centre, called the clivus, sloping to the floor, called the foveola. The fovea has highest density of cones from 199,000-300,000 cones

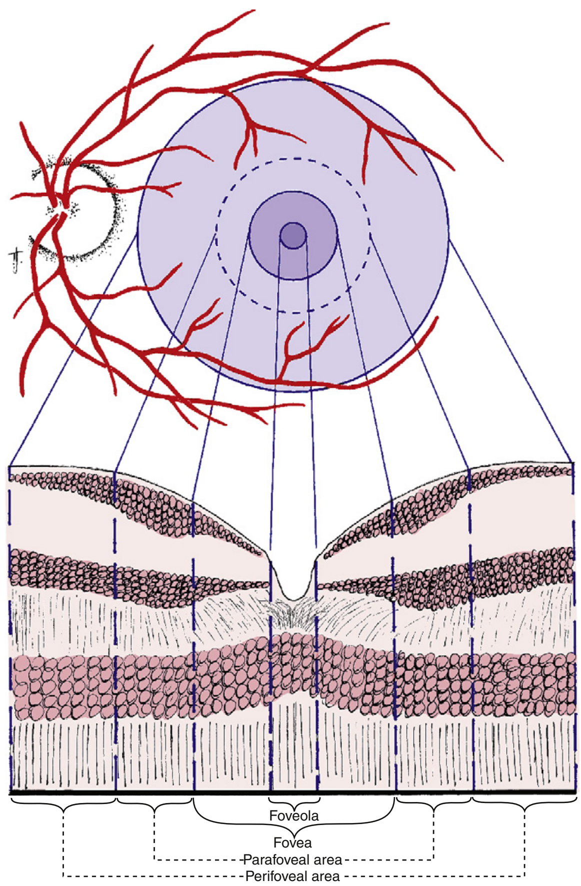

Figure 4: Schematic showing regions of retina and corresponding histologic architecture (Remington, Fig. 4-26, 2012).

per mm^2 at centre and decreasing rapidly moving outwards. At the centre, in a diameter of 0.57 mm is a zone where only cones are present, which represents approximately 1° of visual field. The parafoveal area contains the largest accumulation of bipolar and ganglion cells, a maximum density of ganglion cells of 40,000 cells per mm^2.

A wider term of retinal processing, which in recent years has come into the light of glare researchers, are receptive fields (Scheir et al., 2018). The term covers an area of the retina that elicits a retinal neuron response when stimulated by light. The receptive field of a single bipolar cell consists of the photoreceptors it is in direct contact with and all the photoreceptors and horizontal cells that can influence it. Since horizontal cells are entangled as previously described they greatly extend the receptive field beyond the photoreceptor connections of the bipolar cell. The arrangement of receptive fields in the retina is a so-called centre-surround pattern. This allow each bipolar cell to not only respond to a direct message it receives, but also to gather signals from neighbouring areas and take in information about the bigger picture before relaying its information. This process assists in detecting edges and in recognition of contrast, while maximising the retinal contrast sensitivity in a wide range of background illuminations. Because of this, receptive fields have become a special area of interest in newer research of vision and glare, potentially promising a new way of predicting discomfort glare (Scheir et al, 2018).

Visual perception through the mechanism of the eye is not a stationary mechanical process but involves a process of keeping focus and adjusting to brightness. This is called visual accommodation and adaption. The ciliary muscle attached to the lens reshapes it to adjust the focal length, a common analogy being a camera lens. The lens is rounded by relaxing the ciliary muscle to bring objects near the eye into focus and flattened by contracting the ciliary muscle to bring distant objects into focus. The iris acts as a diaphragm and the centre aperture, the pupil, regulates the illumination of the retina deeper in the eye with a constriction and a dilation muscle. The pupil diameter can be from 1-9 mm depending on light conditions, where brightly lit conditions produces the small (miotic) state and dim lit conditions produces the large (mydriatic) state. The background illumination affects the adaption time and significant changes can prolong this. When going from bright sunlight to complete dark, adaption time can be up to 30 minutes, since rods can take some time to reach their maximum functionality. When going from complete dark to bright sunlight, adaption time can be 5-10 minutes, since cones are quicker to reach maximum functionality than rods. The iris plays only a minor role in adaption, while neural processes account for practically all the transitory changes in the sensitivity of the eye at luminance values commonly associated with electrically lit environments, which is luminances below 600 cd/m^2.

From the accumulation point, the optic disc, the ganglion axons exit the eye as the nerve fibres in a collection called the optic nerve. It consists of between 1-2.2 million optic nerve fibres of different thickness. The optic nerve from each eye cross in the optic chiasm and passes through the optic tracts and is routed to the opposite side of the brain (see Figure 5). Approximately 10% of the nerve fibres will be projected to areas controlling pupil response (pretectal nucleus) or circadian rhythm (hypothalamus) while 90% will end in the lateral geniculate nucleus (LGN) in the thalamus. All sensory signals, except smells, passes through the thalamus, in the vertebrate brain, where visual information is processed by the LGN before being passed on. The LGN gathers input from cortical and subcortical centres of the cerebral cortex, the largest site of neural integration in the CNS, performs complex visual processing and regulates the flow of visual information to the primary visual cortex (striate cortex).

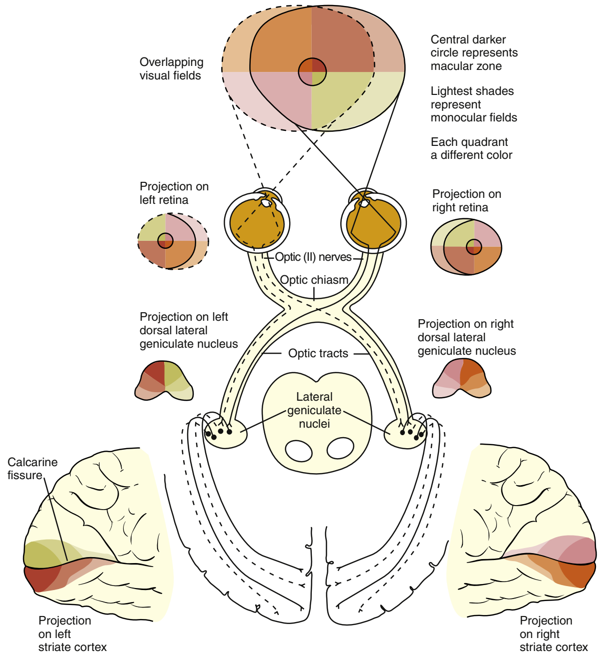

Figure 5: The visual pathway (Remington, Fig. 13-1, 2012).

In the striate cortex (see Figure 5), in the occipital lobe, certain areas are active when processing different information, e.g. motion stimulation and colour vision. The magnocellular areas of the LGN likely process movement detection and low-spatial frequency contrast sensitivity, while the parvocellular areas likely process colour and high-spatial-frequency contrast sensitivity to oversimplify. Other functions of the striate cortex worth mentioning is contour analysis and binocular vision. The processing of low- and high-spatial frequency contrast sensitivity is a recent field of interest in relation to discomfort glare, as Boyce (2018) suggests needs to be further explored. The striate cortex communicates with the superior colliculus and the frontal eye fields. The superior colliculus, in the midbrain, does not analyse sensory information for perception but assist in visual orientation, foveation (bringing an object into focus), and control of saccadic eye movements (rapid eye movement to direct the fovea onto an object). The frontal eye fields, in the frontal lobe, receives input from the superior colliculus contributing to control of conjugate eye movements (coordinated eye movement) while also processing voluntary and reflex ocular movements (muscles controlling eye movement), as well as pupillary responses to near objects. The striate cortex transmits the analysed visual information to the higher visual association areas, called the extrastriate cortex, for further interpretation. Studying the visual system in the brain requires magnetic resonance imaging (MRI) techniques sensitive to changes in blood flow and oxygenation occurring with neural activity and is out of scope for this thesis.

The human visual system is limited in its capabilities like every other system in the human body. Commonly the thresholds of the visual system are measured by opticians to test how well the vision of the patient is with certain threshold measurement tests, but producers of lighting equipment also test the thresholds as part of their design process and quality control. These threshold measurements can be divided into spatial, temporal and colour categories. It is usually assumed, when doing threshold measurements, that the observer is fully adapted, the target is presented in on field of uniform luminance and that the observer's accommodation is correct. A threshold is usually defined by a stimulus which is detected a certain percentage of times when presented, often 50% (Boyce, 2014).

Spatial threshold measures relate to the ability to detect a target from its background or discriminate detail within the target, usually assumed the target does not vary over time. This is typically measurements of luminance contrast and visual acuity. The luminance contrast of a target quantifies the visibility of the target against its immediate background. Higher luminance contrast means it is easier to see the target. There are three types of luminance contrast commonly used for uniform luminance targets seen against a uniform luminance background (Boyce, 2014). Formula (1) and (2) is used for uniform luminance targets seen against a uniform luminance background while (3) is used for targets that have a repeating pattern of luminance. Tests for visual acuity can be a Snellen chart or Landolt rings (Boyce, 2014).

$$C = \frac{L_t - L_b}{L_b} \quad (1) \qquad C = \frac{L_t}{L_b} \quad (2) \qquad C = \frac{L_{max} - L_{min}}{L_{max} + L_{min}} \quad (3)$$

where

C is the luminance contrast [cd/m^2]

L_t is the luminance of the target [cd/m^2]

L_b is the luminance of the background [cd/m^2]

L_{min} is the minimum luminance [cd/m^2]

L_{max} is the maximum luminance [cd/m^2]

Temporal threshold measures relate to the ability to detect fluctuations in luminance, usually assumed the target is fixed in position. Fluctuations in luminance can be viewed as waveforms and is measured in frequency and amplitude of the waveforms (see Figure 6). One period or cycle can be viewed as the waveform performing one oscillation and returning to its initial point. The frequency is the number of periods/cycles/oscillations performed per sec. in the unit of hertz (Hz = period/sec.). The amplitude in temporal threshold measures can then be expressed formula (4) (Boyce, 2014), known as peak-to-peak contrast or Michelson contrast and is equal to percent flicker or just modulation (*IEEE Std. 1789-2015,* IEEE-SA, 2015).

$$M = 100\frac{L_{max}-L_{min}}{L_{max}+L_{min}} \quad (4)$$

where
M is the modulation [%]
L_{min} is the minimum luminance [cd/m²]
L_{max} is the maximum luminance [cd/m²]

A simple temporal threshold measure is the detection of a flash of light against a uniform luminance background. Bloch's Law states that the product of the luminance and the duration of exposure is constant, which means the photon energy required to stimulate the visual system is the same. That is to say a stimulus of a certain luminance over a certain time would stimulate the visual system as much as a stimulus of half the luminance over twice the time. This phenomenon is called temporal summation. This rule breaks down at a certain point when the duration is fixed and luminance is varied, this point is called the critical duration. For adaptation luminances corresponding to scotopic vision, the critical duration is 0.1 sec., and for adaptation luminances corresponding to photopic vision, the critical duration is 0.03 sec. Longer than the critical duration, the difference in luminance between the flash and the background will determine the ability to detect the flash, as well as time interval between flashes (Boyce, 2014). Temporal threshold measures are especially important in electrical lighting when the electrical current (AC) supplied to the light sources causes them to flash, and when those flashes become visible, they are said to be flickering. Producers of electrical drivers are designing and testing their products to make sure flickering does not occur.

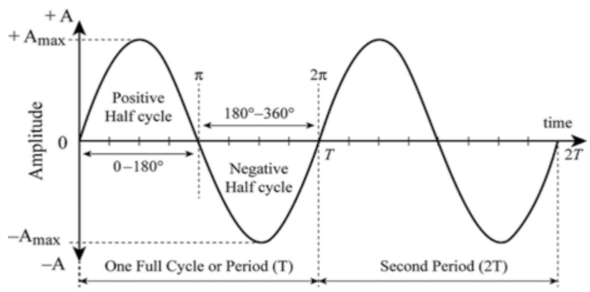

Figure 6: Characteristics of a sine wave (amplitude, period/cycle, time) (*Sine Wave*, chegg.com)

Colour threshold measures relate to the ability to discriminate colours. Colour threshold measures are performed on LED during quality control to ensure the LEDs are sorted into matching categories so LEDs of the same category will emit the same colours. For this, three- to seven-step MacAdam ellipses representing three to seven standard deviations in chromaticity coordinates (see Figure 7). The MacAdam ellipses can be plotted on the CIE 1931 chromaticity diagram (Boyce, 2014). Colour threshold measures is not included in the scope of this thesis to discuss further.

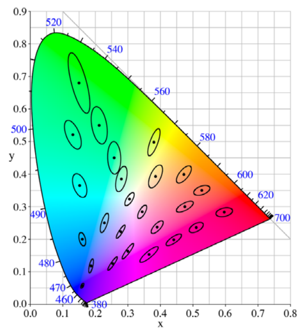

Figure 7: The CIE 1931 xy chromaticity diagram with the MacAdam ellipses plotted 10 times larger (*MacAdam ellipse*, Wikipedia.com).

This concludes the examination of the human visual system which revealed a very complex pattern of information gathering and processing. Usually it is not given much thought when going about our daily lives, but when light is impairing our sight or distracting us, most would probably agree that an awareness sets in. If our visual system cannot adapt to the circumstances then our mind actively wants to find a solution, e.g. change position or posture, and becomes frustrated over time if none is found. Researching and designing our environments with this in mind will help limit the occurrence of these scenarios.

3.2 Light and Glare

Glare is a product of an individual's experience and contextual lighting. It arises when light is interacting within an environment in such a way that a given individual would deem it unpleasant or just inconvenient. When discussing glare, it is often in relation to a task of a given kind and the function of the environment the light is supporting. An unpleasant experience may or may not have a task at hand, or the task is simply to not feel unpleasant, e.g. outdoor lighting in parks or a waiting room. An experience is mostly inconvenient and/or unpleasant when there is a task to do and the lighting is preventing this to a certain extent, e.g. road lighting for driving or office lighting for working. In their book, Tregenza and Loe (2014) briefly categorises four types of glare: Dazzle, disability glare, discomfort glare, and veiling reflection.

- Dazzle could also more fittingly be called blinding glare, since that is what it basically is. Dazzle occurs when a light source of significantly higher luminance, than what the visual system can adapt to, is present in the visual field, causing a temporary inability to see. This is most often an attribute of direct or reflected sunlight, since a single source of such luminance would not be beneficial in an environment designed for working people.
- Disability glare occurs when one or more bright light sources are in direct view or causing bright reflections on surfaces but not on the task. This causes a reduction in apparent contrast, making it more difficult to discriminate the task details, since the visual system attempts to adapt to the bright light source. Disability glare can be attributed to reflected sunlight, dim enough not to be blinding, and electrical lighting.
- Discomfort glare occurs when one or more bright light sources are in direct view or causing specular reflection. Discomfort glare can effectively be attributed to the same sources as disability glare, but the luminance is usually lower. This can be experienced as light dim enough to not be impairing, but the discomfort can gradually increase with time and become a nuisance that must be dealt with before the task can be completed efficiently. Several factors can influence this experience.
- Veiling reflection occurs when experiencing bright reflections on the task itself, e.g. glossy images or text in a book. This causes a reduction of actual contrast on the

surface of the task.

When the visual system has been operating on its limit for a prolonged period, the eyes and the brain can begin to show signs of discomfort. These signs can be either physiological and psychological symptoms such as red, itchy or watering eyes, pain in and around the eyes, headaches, nausea and fatigue. When people complain about discomfort glare by mentioning these symptoms, it is important to identify the right cause, though it can be difficult since it depends on the individual person's physiology and psychology. Each person has a personal definition and expectation of comfort and discomfort defined by previous experiences (Boyce & Wilkins, 2018).

Boyce and Wilkins (2018) has defined three underlying causes of visual discomfort: Poor visibility, overstimulation and distraction.

- A task is suffering from poor visibility when the information becomes too difficult to extract because of stimuli within the visual field being close to the detection threshold. This may increase the neural demands on the visual system for processing and cause discomfort.
- The visual cortex (striate and extrastriate cortex) is suffering from overstimulation when stimulated by large-field, spatially or temporarily repetitive patterns in the visual field. Prolonged periods of working under such conditions can cause discomfort.
- The visual system can suffer from distraction when bright, moving or fluctuating objects close to the temporal threshold are present in the peripheral field of vision. The peripheral field is particularly sensitive to this and the visual system wants to focus the fovea on these objects, if they cannot be ignored. An active thought process of ignoring the objects can become a distraction and cause discomfort.

These definitions of discomfort are based on the reaction of the visual system but is does not identify any aspect of lighting. Poor visibility of a task is usually caused by insufficient illuminance, inappropriate distribution, shadows, light spectrum, or veiling reflections. Overstimulation can be caused by fluctuating light output, systematic or temporal. Distraction would usually be more sudden experiences of light than just fluctuations, appearing out of nothing and demanding attention. It is important to remember that light is highly contextual and interacts with the geometry and materials of the environment. Designing environments without discomfort glare is about controlling the environmental parameters influencing the physics of light.

3.3 Light and Glare Regulation

The built environment is under strict regulation in Europe and lighting regulation been revised several times since 2000. This enforces work environments to be designed and built with a balance of productivity, health and energy in mind. The scope of this thesis mainly concerns office lighting because it has been extensively studied and has relatively high demands, generally only superseded by tasks involving very detail-oriented work. Office work is often stationary at a desk working with a computer with little room to adjust seating and posture in relation to light. The computer screen and desk space for reading is rather fixed, so poor lighting can be impairing on productivity and health. In most of Europe, different aspects of electrical lighting are regulated by the EN 12464-1 standard (*DS/EN 12464-1:2011*, Danish Standard, 2011) (see Figure 8), with a revision in the works, while daylight is regulated by the new EN 17037 standard (*DS/EN 17037:2018*, Danish Standard, 2018) and individual countries may have different supplementary regulation. In this chapter, the regulation of electrical office lighting and how it influences glare will be examined in relation to the three definitions set by Boyce and Wilkins (2018).

Table 5.26 — Offices

Ref. no.	Type of area, task or activity	E_m lx	UGR_L –	U_o –	R_a –	Specific requirements
5.26.1	Filing, copying, etc.	300	19	0,40	80	
5.26.2	Writing, typing, reading, data processing	500	19	0,60	80	DSE-work, see 4.9.
5.26.3	Technical drawing	750	16	0,70	80	
5.26.4	CAD work stations	500	19	0,60	80	DSE-work, see 4.9.
5.26.5	Conference and meeting rooms	500	19	0,60	80	Lighting should be controllable.
5.26.6	Reception desk	300	22	0,60	80	
5.26.7	Archives	200	25	0,40	80	

Figure 8: Danish office lighting regulation (*DS/EN 12464-1:2011*, Danish Standard, 2011).

3.3.1 Illuminance, Em

The first cause of visual discomfort is poor visibility (Boyce & Wilkins, 2018). One of the most general aspects of lighting, when discussing poor visibility, is illuminance, describing the rate at which light falls on a surface in lumens/m^2 or lux (Tregenza & Loe, 2014).

- In the EN 12464-1 standard, the required illuminance on the defined task area is 500 lux (*DS/EN 12464-1:2011*, writing and reading, ref. no. 5.26.2, Danish Standard, 2011) (see Figure 8).
- The immediate surrounding area of the task area, defined as a band with a width of at least 0.5 m, the required illuminance is 300 lux (*DS/EN 12464-1:2011,* section 4.3.4, table 1, Danish Standard, 2011).
- The background area, defined as a band with a width of at least 3 m, requires 1/3 of the illuminance in the immediate surrounding area, which is 100 lux (*DS/EN 12464-1:2011,* section 4.3.5, Danish Standard, 2011).

These are minimum illuminance requirements, but Boyce and Wilkins (2018) points out, these tend to exceed what is actually necessary to provide effective visibility. Also, a maximum requirement is markedly absent despite massive focus on electricity consumption, which is an interesting observation. Excessive light is mostly a daylighting issue, but it is interesting from a utilities point-of-view.

3.3.2 Uniformity, U0

If the minimum illuminance requirements are followed in their respective areas, it should prevent poor visibility, but it is not necessarily enough. Uniformity is a measure of light distribution across a space, with exception of a band of 0.5 m from walls, to exclude usually darker zones. It is a measure of the minimum illuminance divided by the average illuminance in the space. In an office environment, a uniformity of 0.60 is required (see Figure 8). An office space should be uniformly lit to provide a pleasant contrast range between darkness and brightness. The larger the contrast range gets in the visual field, the closer the eyes will get to their adaption limit, which can cause disability glare (Tregenza & Loe, 2014). The background area is equally important as the immediate surrounding area, always in relation to the task area, since the visual field is covering it all in some portion.

Luminance is the aspect of light describing the light flowing in a particular direction, measured in cd/m^2. The luminance of a piece of matt white paper with an illuminance of 500 lux emit a luminance of 130 cd/m^2. Luminance can be called objective brightness, which can be measured with a luminance meter, while apparent brightness is the experience through the visual system (Tregenza & Loe, 2014). Achieving uniformity is about controlling the objective brightness in the visual field of people to not impair their vision with poor contrast ratio.

3.3.3 Discomfort glare, UGR_L

Discomfort glare is regulated by using the Unified Glare Rating formula introduced by the CIE (International Commission on Illumination).

$$UGR = 8\log_{10}\frac{0.25}{L_b}\sum\frac{L^2\omega^1}{P^2} \quad (5)$$

where

L_b is the background luminance [cd/m^2]

L is the luminance of the glare source in the direction of the observer's eye [cd/m^2]

ω is the solid angle of each glare source at the observer's eye in steridians [sr]

P is Guth's position index of each glare source which relates to its displacement from the line of sight[-]

The solid angle of a source at the observer's eye is the portion of the visual field the source occupies (see Figure 9). Imagine a sphere around the observer's head of the observer with the radius r (in meters) corresponding to the distance between the eyes to the centre of the luminous part of a source. The projected area of the source onto this sphere is the area A (in m^2). The solid angle

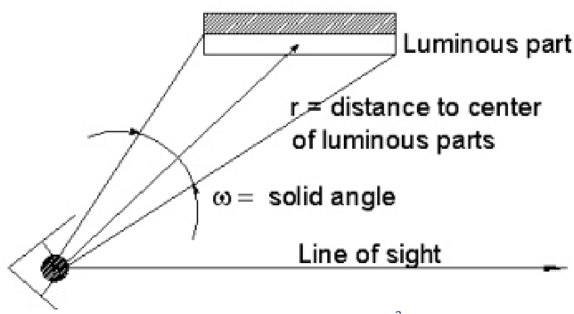

Figure 9: Illustration of the components of a solid angle calculation (Sørensen, 2012).

is measured in steridians (sr), which is a standard dimensionless unit (*Planning and calculation tips...*, Fagerhult, *2019)*. If the observer holds a 1 m^2 sheet of paper at 1 meter distance it would subtend a 1 sr solid angle of the observer's eye. If the distance was doubled to two meters, the solid angle would be 0.25 sr (Tregenza and Loe, 2014).

$$\omega = \frac{A}{r^2} \quad \textbf{(6)}$$

where
ω is the solid angle of each glare source at the observer's eye in steridians [sr]
A is the ...
r is the ...

UGR is evaluated in a series of values: 10, 13, 16, 19, 22, 25, 28. Each single step is considered the smallest detectable difference and a step of three is a noticeable step in difference of glare. A value of 10 is considered imperceptible while 28 is considered intolerable. The formula includes the background luminance L_b, tying it to both illuminance and uniformity, which are influencing the background luminance. Additionally, it includes the source luminance L, source solid angle ω (portion of the visual field) and position in the visual field (position index, P) tying it to both the sources of light and to the individual point-of-view of every person in the space. These connections show how complicated discomfort glare is to quantify and standardise. If the equation of discomfort glare is solved in a space, then the more severe types of glare are usually considered to be solved as well. In an office environment, this means designing for a UGR value of 19 (see Figure 8), but since a notable difference is only felt at 22, values in between should not be noticeable from 19.

EN 12464-1 is, as of writing this, still the current standard and mentions there is currently no standardised method for rating discomfort glare from windows. The new EN 17037 changes this by referring to the Daylight Glare Probability (DGP), which is applicable for positions near vertical or inclined daylight openings but not for horizontal daylight openings (*DS/EN 17037:2018,* Danish Standard, 2018). The DGP value is an estimation of the fraction of dissatisfied people in a space (see Table 1).

$$DGP = 5.87 \times 10^{-5} E_v + 0.0918 \log\left(1 + \sum_i \frac{L_{si}^2 \omega_{si}}{E_v^{1.87} P_i^2}\right) + 0.16 \quad \textbf{(7)}$$

where
L_{si} is the luminance of source i [cd/m2]
ω_{si} is the solid angle of source i [sr]
E_v is the vertical luminance at the eye [cd/m2]
P_i is the position factor of source I

Table 1: DGP value categorization in ranges (*DS/EN 17037:2018,* Danish Standard, 2018).

DGP value	Perception of glare
DGP ≤ 0.35	Mostly not perceived
0.35 < DGP ≤ 0.40	Perceived but mostly not disturbing
0.40 < DGP ≤ 0.45	Perceived and often disturbing
0.45 < DGP	Perceived and mostly intolerable

The topic of prediction models will be discussed more in-depth later but will focus on glare models for electrical lighting as it is the only scope of this thesis. Even though there are similarities between daylight glare models and electrical glare models, the issues are the glare size source and uniformity of luminance across the source, which in electrical lighting is usually less complicated than windows, although it is a relevant topic of research in LED lighting as well. Researching daylight glare tends to be more difficult, since daylight is usually fluctuating more and cannot be held as constant as electrical lighting. Additionally, personal preferences might be even more influential since people tend to tolerate daylight issues differently possibly because it is a natural phenomenon our biology is connected to.

3.3.4 Glare Shielding

To further regulate glare, the EN 12464-1 standard requires luminaires within certain intervals of luminance to have certain minimum shielding angles in the visual field. A luminaire of 20,000 to 50,000 cd/m^2 requires minimum 15° shielding from the source. A luminaire of 50,000 to 500,000 cd/m^2 requires minimum 20° shielding from the source. A luminaire of 500,000 cd/m^2 or higher requires minimum 30° shielding from the source. This does not apply to upwards emitting luminaires mounted above normal eye level and luminaires only emitting downwards and mounted below normal eye level (*DS/EN 12464-1:2011,* Danish Standard, 2011).

3.3.5 Veiling Reflections and Reflected Glare

The EN 12464-1 standard (and EN 17037) recommends preventing or minimising veiling reflections and reflected glare by arranging work station wisely with respect to light sources, restrict luminance of luminaires, and be cautious with surface finishes such as bright ceilings and walls (*DS/EN 12464-1:2011* and *DS/EN 17037:2018,* Danish Standard, 2011 and 2018). Achieving this requires coordination between interior and lighting designers.

3.3.6 Flicker and Stroboscopic Effects

The EN 12464-1 standard highly recommends that lighting systems should be designed to avoid flicker and stroboscopic effects, since they may cause distraction, headache and in worst case dangerous situations with perceived motion (*DS/EN 12464-1:2011,* Danish Standard, 2011). As Boyce and Wilkins (2018) mentions, distraction by bright, moving or fluctuating objects in the peripheral visual field can become visual discomfort by distraction and should be avoided (*DS/EN 12464-1:2011,* Danish Standard, 2011). The temporal threshold of the visual system, as mentioned earlier, is what determines when a source is flickering. If the flashes of light cannot be perceived the source is not considered to be flickering, but a source will always flash, or modulate light, to some degree usually as a consequence of being powered by alternating current (AC) (*IEEE Std. 1789-2015,* IEEE-SA, 2015). With LEDs, it primarily comes down to how the light source is powered and controlled by its electrical driver. LEDs are powered by direct current (DC) and flicker in LEDs is dependent on how AC is transformed to DC in the driver. Generally, AC with a frequency of less than 60 Hz creates visible flickering for most people according to the IEEE-SA (*IEEE Std. 1789-2015,* 2015), which is a well-acknowledged third-party developer of industry standards for a vast variety of technologies. The frequency where flickering light fuses into an apparently constant light source is called the critical fusion frequency (CFF) and occurs generally in the range of 60 to 100 Hz. Flicker might also be invisible and above 100 Hz but sensed nonetheless, which can still cause health issues. For comparison, AC in Europe has a frequency of 50 Hz. This is of course below 60 Hz which goes directly against the logic of the previous statement of the IEEE, but normally in lighting the frequency is doubled in the transformation from AC to DC by full-wave rectification. This can be expressed as $f = 2 \cdot f_{AC}$ and the IEEE-SA (*IEEE Std. 1789-2015,* 2015) recommends that $f > CFF$ in two levels.

$Modulation\ [\%] < 0.08 \cdot f$ for low risk level (LRL)

$Modulation\ [\%] < 0.0333 \cdot f$ for no observable effect level (NOEL)

For a European country this means $f_{AC} = 50\ Hz$ and $f = 2 \cdot f_{AC} = 100\ Hz$ which IEEE recommends:

$Modulation\ [\%] < 0.08 \cdot 100\ Hz = 8\%$ for low risk level (LRL)

$Modulation\ [\%] < 0.0333 \cdot 100\ Hz = 3\%$ for no observable effect level (NOEL)

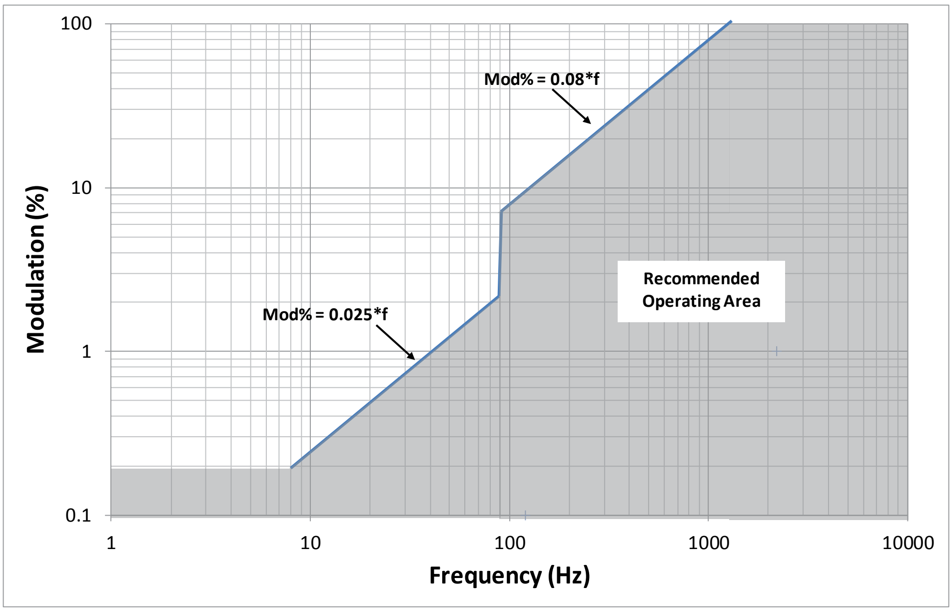

Figure 10: Modulation values in the grey area minimises visual discomfort (*IEEE Std. 1789-2015, Fig. 20,* IEEE-SA, 2015).

This recommendation can also be found in Figure 10. For the variable frequencies it is recommended to keep operating frequencies at modulation percentages according to the marked grey area to limit biological effects and detection of flicker in general illumination. An easy way to ensure this is specifying LED drivers certified by the IEEE in accordance with the 1789 standard. This only becomes more important when dimmable and tunable white LED sources are used, since flicker from such sources with bad drivers for various reasons are technically more prone to flickering (Hulsmans, 2019).

3.3.7 Work Stations with Display Screen Equipment (DSE)

The EN 12464-1 standard (and EN 17037) recommends caution when designing light for environments with DSE, since reflections in DSE and sometimes keyboards can cause disability or discomfort glare. The location of lighting in relation to DSE should be planned to avoid this for all types of tasks performed on DSE (*DS/EN 12464-1:2011* and *DS/EN 17037:2018,* Danish Standard, 2011 and 2018).

The standard also specifies luminaire luminance limits to limit reflections on DSE which are vertical or inclined at angles up to 15°. Screens are split into two groups, high luminance screens (L > 200 cd/m^2) and medium luminance screens (L ≤ 200 cd/m^2). The high state luminance of screens is the maximum luminance measured on the white part of the screen. In normal office conditions, high luminance screens set the luminaire luminance limit at ≤ 3000 cd/m^2 while medium luminance screens set the luminaire luminance limit at ≤ 1500 cd/m^2. A more detail-oriented task sets lower limits, ≤ 1500 cd/m^2 and ≤ 1000 cd/m^2 respectively (*DS/EN 12464-1:2011,* Danish Standard, 2011).

TCO Certified is a world-leading third-party sustainability certification scheme and would be a go-to source for product certification for DSE equipment and notebooks (with DSE) with more than 3,500 products certified across 27 brands (*TCO Certified,* TCO development, 2018). In their recent editions from December 2018 for displays (*TCO Certified... for displays,* TCO development, 2018) and notebooks (*TCO Certified... for notebooks,* TCO development, 2018), they do not include criteria for glare or glossiness of the screens. The only apparent criteria that can be related to glare is glossiness of keyboard and its reflection in the screen of towards the eye in the notebook edition. TCO Certified is referring to the ISO 9241 standard for ergonomics of human-computer interaction, but it is uncertain if this standard includes criteria or testing methods for glare in DSE. The EN 12464-1 standard is referring to EN ISO 9241-307 for visual qualities of DSE (*DS/EN 12464-1:2011,* Danish Standard, 2011).

3.4 Predictive Glare Models

Luckiesh and Holladay were among the pioneers with a study in 1925 studying the sensation to discomfort glare (study unobtainable). This study revealed that glare sensation changed according to the position of the source in the visual field (Kent, Fotios, & Altomonte, 2018). Luckiesh and Guth (1949) later made various experiments through the 1940's and developed Guth's position index, P. The subjects evaluated and defined the borderline between comfort and discomfort (BCD), which was interpreted as a relatively definite sensation. The position index became instrumental in future predictive glare models.

Petherbridge and Hopkinson (1950) investigated the relation between glare sensation and glare source attributes further. As Luckiesh and Guth (1949) in the USA, Petherbridge and Hopkinson (1950) in Great Britain also speculated how the variance of sensation between groups of subjects might be attributed to other unrecognised psychological and physiological phenomenon. They generally advised to demonstrate caution when glare sources were within the visual field. Petherbridge and Hopkinson (1950) developed a predictive glare model through their experiments called the British Research Station (BRS) formula (Kent, 2018; Petherbridge and Hokinson, 1950; Robinson et al. (1962)) [1,2,3], later named the British Glare Index (BGI).

$$BGI = \frac{L_s^{1.6} \cdot \omega^{0.8}}{L_b \cdot p^{1.6}} \quad \mathbf{(8)}$$

where

L_b is the background luminance [cd/m2]

L_s is the luminance of the glare source in the direction of the observer's eye [cd/m2]

ω is the solid angle the glare source at the observer's eye in steridians [sr]

P is Guth's position index of the glare source which relates to its displacement from the line of sight [-]

In their experiments, Petherbridge and Hopkinson (1950) used the so-called multiple criterion scale for subjective evaluation of the glare sensation instead of the BCD. The scale steps are from worst to least sensation of glare were (A) just intolerable, (B) just uncomfortable, (C) just acceptable, and (D) just imperceptible. The glare constant calculated from the BRS/BGI formula would correspond to a step on this scale, so a BGI of 600 was equal to (A), a BGI of 150 was equal to (B), a BGI of 35 was equal to (C), and a BGI of 8 was equal to (D).

About a decade later the Illuminating Engineering Society (IES) panel, looking into the problem of glare in interior lighting, sought to add an assessment tool to the revision of their code (Robinson et al., 1962). They based their IES Glare Index (GI) on the BGI formula with some additions. The first addition was to allow summation of glare (BGI) constants for each individual luminaire. Additionally, the IES panel did not find the BGI formula glare constant intuitive because of the large exponential increase in the steps of the scale. Because of this, the second addition to the formula was to multiply the sum of the glare constants for all luminaires with 10 log10 and the steps of 8, 35, 150, and 600 were adjusted to 10, 40, 160, and 640 (Robinson et al., 1962). With an extra addition of a constant later, the IES had transformed the BGI to the IES Glare Index (IES-GI)(Kent, 2018). The transition of interpretation scales can be found in Table 2.

$$IES - GI = 10\log_{10} \cdot 0.478 \cdot \sum \frac{L_s^{1.6} \cdot \omega^{0.8}}{L_b \cdot p^{1.6}} \tag{9}$$

where

L_b is the background luminance [cd/m²]

L_s is the luminance of the glare source in the direction of the observer's eye [cd/m²]

ω is the solid angle the glare source at the observer's eye in steridians [sr]

P is Guth's position index of the glare source which relates to its displacement from the line of sight [-]

Table 2: Transformation of the interpretation scale from BRS/BGI scale to the IES-GI scale and compared to Hopkinson's multiple criterion scale. The IES-GI scale was considered more intuitive.

BRS/BGI	IES-GI v1	IES-GI v2	Multiple criterion scale
600	640	28	Just intolerable (A)
150	160	22	Just uncomfortable (B)
35	40	16	Just acceptable (C)
8	10	10	Just imperceptible (D)

The transformation of the multiple criterion scale was now BGI 640 equal to IES-GI 28 interpreted as (A) just intolerable, BGI 160 equal to IES-GI 22 interpreted as (B) just uncomfortable, BGI 40 equal to IES-GI 16 interpreted as (C) just acceptable, and BGI 10 equal to IES-GI 10 interpreted as (C) just imperceptible.

Based on the work of Luckiesh, Holladay and Guth from 1925 to 1964 (Bay et al., 2017), the Visual Comfort Probability (VCP) model was developed and published in the IES Lighting Handbook in 1984 (Boyce, 2014; Bay et al., 2017). This model is rather different and does not seem relevant to development of the European standards of today and will be excluded from review in this thesis.

In 1975, Einhorn (1979) was asked by the CIE to devise comprehensive formula which should balance all the essential glare facts to form a basis for assessing existing methods and formulate new simplified models (Einhorn, 1979). He developed the CIE Glare Index (CGI) in 1979 and with additional adjustments with regards to the constants applied, it was published by the CIE in 1983 (Einhorn, 1979; Bay et al., 2017). The CGI scale ranges from 28, where values above are considered as intolerable, to 13, where values below are considered imperceptible.

$$CGI = 8\log_{10} 2 \cdot \left(\frac{1+\frac{E_d}{500}}{E_d+E_i}\right) \cdot \sum_{i=1}^{n} \frac{L_s^2 \cdot \omega_s}{P^2} \tag{10}$$

where

E_d is the direct vertical illuminance at the eye due to all sources [lux]
E_i is the indirect vertical illuminance at the eye ($E_i = \pi$ x Lb) [lux]. This corresponds to L_b in the other models.
L_s is the luminance of the glare source [cd/m^2]
ω is the solid angle of the glare source at the observer's eye in steridians [sr]
P is the Guth's position index of the glare source which relates to its displacement from the line of sight [-]
n is the number of glare sources

The CGI model is split into two parts. One part is fairly similar to the BGI and IES-GI model expressing the properties of each glare source and their respective relation to each other, calculated separately and added together. The relation between the source luminance L_s and source solid angle ω was changed from $L_s^{1.6}$ x $\omega^{0.8}$, used in both BGI and IES-GI, to L_s^{2} x ω^{1}. Einhorn (1979) argued that the exponent of 2 for the source luminance was based on "experimental evidence and forms a simple expression of the work of numerous research results studied" (Einhorn, 1979, p. 91). The exponent of 1 for the source solid angle, he argues, "is mathematically essential for additivity and subdivisibility" (Einhorn, 1979, p. 91), saying no matter how the glare source is subdivided the results will be consistent (Einhorn, 1979; Bay et al., 2017). The position index is still based on the work by Luckiesh and Guth (1949), although Einhorn (1979) suggests an expression for use on computers. The background luminance L_b is removed, which is the major difference from the previously mentioned models. Instead, the model includes a separate expression for adaptation which takes both the direct vertical illuminance at eye level E_d (the glare source contribution) and the indirect vertical illuminance at eye level E_i (the background contribution) into account (Einhorn, 1979; Bay et al., 2017). As Einhorn (1979) describes it, the adaptation level is determined by the luminance in the visual field, both background and source luminance (Bay et al., 2017). The separate expression is specifically balanced to have the right sensitivity in illuminance, according to the research, and implies a direct relationship between glare and direct illumination at the eye level (Kent, 2018; Bay et al., 2017).

In 1987, Sørensen proposed the Unified Glare Index to the CIE to replace the CIE Glare Index (CGI) (Kent, 2018; Boyce, 2014). It combines aspects of BGI and CGI and serves as a compromise between other models and simplifies the expression for easier application (Kent, 2018; Einhorn, 1979; Boyce, 2014). The CIE adapted the UGR model in 1995 (Bay et al., 2017).

$$UGR = 8\log_{10}\frac{0.25}{L_b}\sum\frac{L^2\omega^1}{P^2} \quad (11)$$

where
L_b is the background luminance [cd/m^2]
L_s is the luminance of the glare source in the direction of the observer's eye [cd/m^2]
ω is the solid angle the glare source at the observer's eye in steridians [sr]
P is Guth's position index of the glare source which relates to its displacement from the line of sight [-]

Most notable difference between UGR and CGI is the simplification of the adaption expression. Sørensen has removed the indirect vertical lumination at eye level E_d and brought back the background luminance variable L_b instead of the indirect vertical illuminance at eye level E_i. This means that glare sources are not contributing to the adaption of the observer but the CIE states that this will have little effect when applied to spaces with illumination within the recommended ranges of working interiors (Bay et al., 2017). UGR keeps the expression from CGI, describing the glare source properties which are still calculated individually and added together. The exponents are the same as Einhorn chose for the CGI model. A UGR value above 28 is considered intolerable and a value below 13 is considered imperceptible.

As can be seen, the current method of UGR has much in common with what was developed back in the 1950's, nearly 70 years ago. With the current development of advanced computer simulation software, a simplified mathematical formula might not be what is needed, which was the goal of the UGR formula. If the complex relationship of the different variables in play could be established through advanced research, then computer simulations could do all the heavy lifting in the design pahse. Both Boyce (2014) and Clear (2012) states the variables in the model is based on the assumption that the variables describing the glare source properties is independent of each other, but as Boyce (2014) mentions, in practice they are interacting. This is a logical statement as it is not realistic to think lowering a source will not change the luminance distribution or change the solid angle in the visual field as well. This might be one of the challenges as to why it is difficult to experiment with it in a practical setting and most experiments are performed in laboratory settings. Isolating a variable is not possible thus it becomes a challenge to directly observe its influence. In the next chapter, the variables in the UGR formula will be examined in relation to current research and what the limits of the empirical data is.

3.5 Background luminance and glare source size

Discussing the importance of background luminance is fundamentally a discussion of how to express adaption in the eye and visual system. The visual system is adapting the range of luminance sensitivity according to the luminance sensed in the peripheral visual field and central visual field. If the range becomes too wide, discomfort glare may occur. In the UGR model, the part describing the luminous environment in the equation is expressed $0.25/L_b$, which indicates that the result will become smaller as the background luminance increases. As Kim and Kim (2010a) states, because the exponent of the background luminance is fixed at 1, the UGR value will grow smaller as a constant proportion to the increase in background luminance independent of the size of the glare source. In their study, Kim and Kim (2010a) set out to test if this would line up with reality in an experiment. They constructed a semi-sphere similar to what Luckiesh and Guth (1949) used in their studies and placed the test-subject's head at the centre, so their visual field was enclosed by the semi-sphere. The background luminance was provided by a mix of 12 incandescent lamps and three halogen lamps installed along the brim of the semi-sphere behind the test-subject (see Figure 11). At the centre of the semi-sphere was 0.5 x 0.5 m square circuit board of 56 x 56 white LED. A dimmer was installed for varying the background luminance and veil screens were used to vary the size of the glare source LEDs. The glare source distance to the head of the test-subject could also be adjusted to 0.5 m or 0.7 m. The glare source was set at a luminance of 3,000 cd/m² while the background luminance set at 10, 30, 100, 300, and 1,000 cd/m². The glare source size varied was set at solid angles of 0.001, 0.005, 0.01, 0.05, 0.1, 0.5, and 1 sr split between the distances of 0.5 m and 0.7 m. Solid angles of 0.05 sr and 0.1 sr overlapped between the two distances for verification of discomfort glare sensation. In total, 42 conditions were to be tested by each test-subject. They used the traditional multiple-criterion scale set by Hopkinson (1972), which had changed "(D) Just imperceptible" from the 1950 study (Petherbrige and Hopkinson, 1950) to "(D) Just perceptible". They added "intolerable" and "imperceptible" at each end making it a six-criteria scale. The experiment started by adjusting the glare source and turning it off, adjusting the background luminance to a random value of the five values to subvert

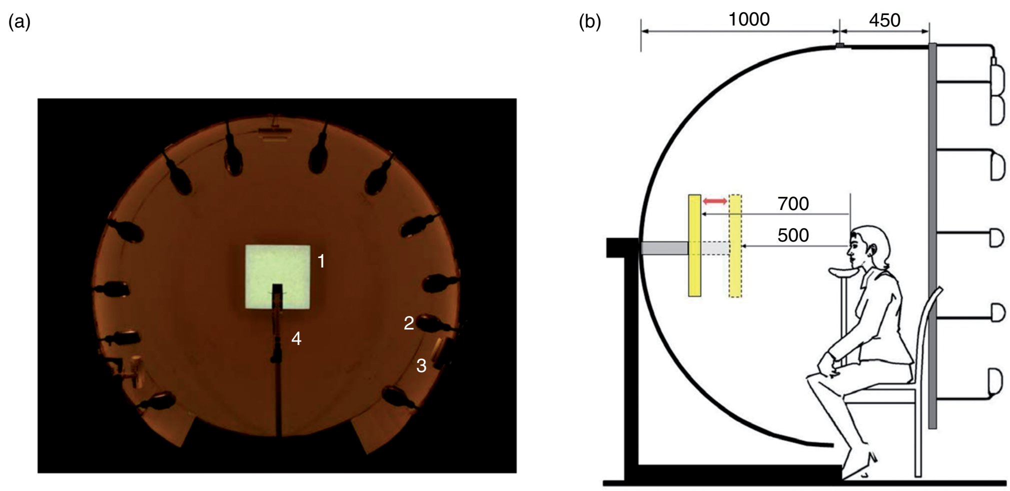

Figure 11: Experimental device: (A) experimental equipment, (B) cross-section of the device; 1: LED light source, 2: incandescent lamp, 3: halogen lamp and 4: the headrest. (Kim and Kim, 2010)

expectations of the test-subject, and turning the glare source on. The test-subject would then have 5 sec. to evaluate the discomfort level. Failing to evaluate within this time would restart the procedure. Once a solid angle was complete, a veil screen was mounted and the procedure would repeat until all solid angles and distances had been evaluated in relation to the background luminance. 27 test-subjects between age 21 and 29 participated (Kim and Kim, 2010a).

The result showed that the exponent of 1 of the background luminance in the UGR model for solid angles of 0.0003 to 0.1 sr was appropriate. For glare source with solid angles larger than 0.1 sr it would be difficult to chose one single value, so a variable exponent value would have to be determined. By plotting the data for solid angles in the range of 0.001 to 1 sr (see Figure 12), they could determine the maximum size of solid angle to be 5 sr, corresponding to the entire visual field with no background present. At 5 sr, the gradient called c, which was corresponding to the exponent of the background luminance, had become zero, indicating no influence of the background (Kim and Kim, 2010a). They developed an expression, which can be used to calculate the exponent of the background luminance for solid angles of the glare source of 0.0003 to 5 sr. This will expand the use of the UGR formula dramatically from 0.1 sr to 5 sr.

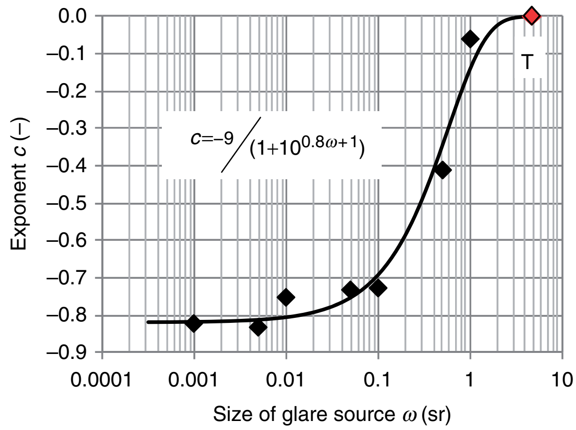

Figure 12: S-shaped curve for determination of exponent c. At 5 sr, c = 0. The curve extended down to 0.0003 sr (Kim and Kim, 2010a).

$$c = \frac{-9}{(1 + 10^{0.8\omega+1})} \quad \textbf{(12)}$$

where

ω is the solid angle the glare source at the observer's eye in steridians [sr]

Although Kim and Kim (2010a) verify the exponent c themselves, other studies have not been found verifying it. Before other studies has verified it for use with solid angles above 1 sr, its results should be used with caution.

3.6 Immediate surround and non-uniform glare sources

The UGR model is assuming the glare source is sufficiently small so the adaptation to the luminous environment is determined only by the background (Clear, 2012). The CGI model tried to include the glare source contribution, but this was removed since the CIE argued in would have little effect when applied to illumination within the recommended ranges (Bay et al., 2017). It is worth noting though, that Hopkinson in 1963 had included a fifth variable for the immediate surround to the glare source, besides the four already present in the BGI model. He argued that an immediate surround luminance balanced between the glare source luminance and the background luminance produced a reduction in glare sensation (Boyce, 2014). Since complex formulas are no longer a challenge to use with the computer-aided design (CAD) utilised today, it might be time to bring back the second and third variables to describe the luminous environment.

3.7 Position Index In Predictive Glare Models

The position index Luckiesh and Guth (1949) developed only account for glare sources located above the line of vision, since the aim was to assess electrical light sources typically mounted in the ceiling. They calculated the position index with two expressions, the vertical position factor V/R and the lateral position factor L/R. V is the vertical distance from the source perpendicular to the horizontal line of vision (looking straight ahead) and L is the lateral distance perpendicular to the horizontal line of vision, or simply put, the offset distance above and to the side of the line of vision. R is the horizontal distance from the eye to directly below the source. They presented this relationship graphically with position index curves as seen in Figure 13.

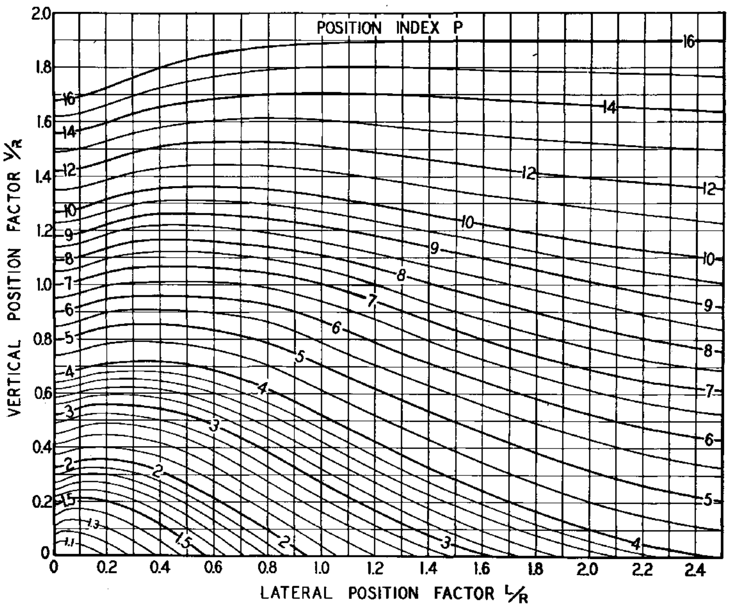

Figure 13: Chart for determining position index located at various positions in the visual field.(Luckiesh and Guth, 1949)

When Einhorn developed the CGI, he expressed this in formula (13) (Einhorn, 1979), which was considered to be of much higher precision than required though (Lowson, 1981).

$$\frac{1}{P} = \frac{d^2 e^x}{d^2 + 1.5d + 4.6} + 0.12(1 - e^x) \quad \textbf{(13)}$$

where

$$e^x = e^{\left(\frac{-0.18s^2}{d} + \frac{0.011s^3}{d}\right)} \quad \textbf{(14)}$$

where

d is the forward distance of the source/height

s is the sideways distance of the source/height

Iwata and Tokura (1997) set out to measure the difference in sensitivity to glare sources located above and below the line of vision, since glare sources could as well be located below. Their original motivation was glare from windows, since windows can take up a large portion of the visual field, but veiling reflections on surfaces of any kind can also be located on walls, floors and other surfaces around the visual field. Iwata together with a different team did also propose a modification for the position index for use in certain daylight glare indices but it presented some difficulties. Firstly, the visual field below the line of sight is larger than above which makes a modification of the formula difficult, and secondly, luminance from windows tend to be non-uniformly distributed (Iwata and Tokura, 1997).

Iwata and Tokura (1997) mentions only one other study by Sasaki and Muroi (unfortunately a source only in Japanese) with a similar goal of determining the position index below the line of sight. The method was similar to that of Luckiesh and Guth (1949) and the results were similar showing a glare source of a given brightness more effectively produced a sensation of glare in the upper visual field when displaced horizontally from the line of vision than when displaced the same angular distance vertically from the line of vision. The results deviated from Luckiesh and Guth (1949) in position index values obtained from angular distances above 40° in that they were smaller. They also found the effect of vertical displacement and horizontal displacement in the lower visual field to be similar, thereby being a different relationship than the upper visual field (Iwata and Tokura, 1997).

The experimental setup of the study by Iwata and Tokura (1997) is not described fully in detail as one would like and brings up questions. The apparatus was consisting of a plane of uniform luminance distribution illuminated by ten fluorescent lamps and a box (see Figure 14). The test subjects would be looking through two holes in the box, providing two visual fields each with a point of fixation at the centre of the visual field to fix the line of vision and off-axis glare sources. The distance (D) between eye and plane with glare source could be varied but the glare sources were arranged to always have a fixed solid angle of 0.0038 sr. One visual field was arranged with the "standard" glare source above the line of vision and the other visual field was arranged with the "test"

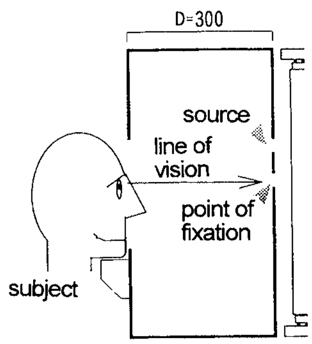

Figure 14: Experimental apparatus. "Position index for a glare source located below the line of vision" Iwata et al.

glare source below the line of vision. The vertical distance (H) from the horizontal line of vision would be the same but opposite, so the "test" source would move downwards (-H) as much as the "standard" source moved upwards (+H). The luminance of the "standard" source would remain constant while the "test" source could be adjusted with a dimmer by the test subjects. The background luminance was set to 1 cd/m^2 in both visual fields. From this description of the experimental setup and their illustration, it is not clear whether the box was closed of or had a divider between the visual fields. Without a divider of some kind between the fields it could be imagined that the glare source could interfere between fields. From the illustration (see Figure 14), the box looks closed off, but describing a "plane of uniform luminance" and "a box" sounds like the two items are not connected (Iwata and Tokura, 1997).

Six Japanese students between age 22 and 25 tested four glare source positions. Positions (a), (b), (c) would have a height to distance ratio (+H/D) of 0.2, 0.4 and 0.6 respectively for the "standard" source and a (-H/D) ratio of -0.2, 0.4 and -0.6 respectively for the "test" source. This would only test the vertical displacement of the glare source with luminance of 1,700 and 2,800 cd/m^2. At position (d), the "standard" source would be at (+H/D) ratio 0.4, while the "test" source would be horizontally displaced (Y) to a (Y/D) ratio of 0.4, not diagonally (H/D = 0.0), both with a source luminance of 1,700 cd/m^2. Before doing the experiment, test subjects were paired and would stay 15 min. in a separate room with less than one lux to adapt the eyes to mesopic conditions (between 0.005 cd/m^2 and 5 cd/m^2), making them sensitive to low luminance levels. In the experiment, the first subject of a pair was instructed to look at each field separately for one second periods at one second intervals while adjusting the "test" source to provide the same initial momentary sensation as the "standard" source. When the first subject was completely sure of this, the second subject of the pair would enter and make adjustments. This continued until the deviation of adjusted luminance between the two was less than 10%. Each pair had seven luminance conditions across the four positions presented in randomised order to avoid any effect of presentation order on the responses (Iwata and Tokura, 1997; Hirning, Isoardi, and Cowling, 2013).

The results showed that all test subjects adjusted the "test" source luminance lower than both 2,800 and 1,700 cd/m^2, indicating that sensitivity to glare was greater below the line of vision than above, where the "standard" source was placed. It was also found that the difference between vertical displacement (H/D = -0.4, Y/D = 0.0) and horizontal displacement (H/D = 0.0, Y/D = 0.4) below the line of vision was very small.

Because of large differences in results for individuals, Iwata and Tokura (1997) decided to conduct a larger experiment more test subjects and the constant method rather than the adjustment method. The experimental setup was the same in terms of glare source positions though two diagonal displaced glare sources were added as scenario (e) and (f) while scenario (d) was skipped. The "standard" source luminance varied from 2,205 to 2,765 cd/m^2 while the "test" source luminance varied from 473 to 2,795 cd/m². 35 Japanese students were split into groups of seven and presented to 30 luminance conditions across positions (a), (b), (c), (e), and (f) (see Figure 15). The procedure was repeated with 36 elderly subjects of age 66 to 83 but they were just presented to positions (a), (b), and (c). The constant method meant the subjects did not adjust themselves but assessed pre-adjusted levels. They assessed which field caused more glare and to which degree they were certain of this (Iwata and Tokura, 1997).

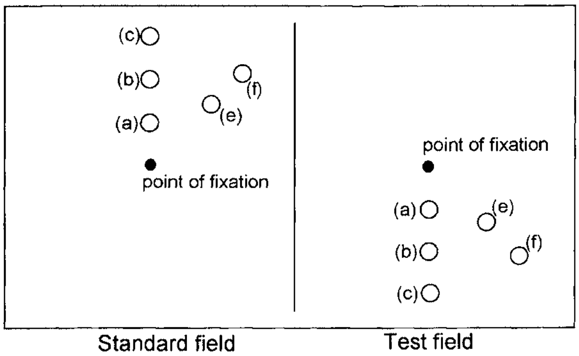

Figure 15: Points of fixation and positions of glare sources (Iwata and Tokura, 1997).

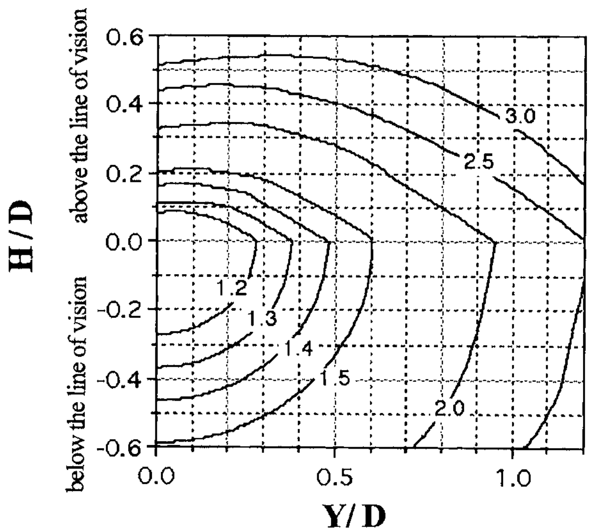

Figure 16: New position index chart (Iwata and Tokura, 1997).

Iwata and Tokura (1997) discussed if glasses could have an impact on the responses, but no variance analysis showed any significant differences in the results between those who used glasses (about 1/3 of the students) and those who did not. They speculate if distance (D) or glare sources was too small to make a difference. The criteria for when the "test" source was equal to the standard source was set to be when 50% of the subjects reported the "test" source was causing more glare than the "standard" source. The results showed when H/D = 0.2, a source below the line of vision requires 80% of the luminance of a source above the line of vision to cause the same sensation of glare. For H/D = 0.4 that number is 57% and for H/D = 0.6 it is 43%. It shows that the luminance ratio decreases with increasing H/D-ratio. This tendency was showed to be the same in the elderly subjects though the percentages was 91%, 38% and 27% respectively. It is speculated that this is caused by the upper edge of the visual field diminishing with age. The diagonal percentages for radius (R) to distance ratio (R/D) of 0.4 (H/D = ±0.283, Y/D = ±0.283) was shown to be 58% and for R/D = 0.6 (H/D = ±0.424, Y/D = ±0.424) to be 63%.

The results in both experiments were similar and showed no difference between the adjustment method and the constant method. The result did agree with the results found by Sasaki and Muroi (Iwata and Tokura, 1997). It was assumed that the position index above the line reported by Luckiesh and Guth (1949) was adequate and the team developed a new position index chart, although they themselves admitted it to not being precise (see Figure 16). They mainly argued this was caused by technical issues in relation to adaptation level of the subjects' eyes and the narrow range of the experimental setup (Iwata and Tokura, 1997). The exposure time can be an issue when the subjects used multiple viewings to adjust the source in the first experiment, and in the second when they can use multiple viewings to ensure their confidence in assessment. While Luckiesh and Guth (1949) argued short exposure was enough to get around this challenge and obtain the exact position index values, Iwata and Tokura (1997) used the adjustment and constant methods to derive a trend from.

In their published article in the "Lighting Research and Technology" scientific journal, H.D. Einhorn comments on their methods and results (Iwata and Tokura, 1997). He argues that the expansion into the lower field is valuable but whether it solves the challenge of glare from large sources is doubtful since it is based on experiments with small sources, which is an issue raised often in critique of glare models. He also argues that the background luminance of 1 cd/m^2 is not corresponding to real conditions and suggests a background luminance of 10 cd/m^2 to represent practical conditions better. Einhorn developed an expression to supplement the chart, based on the hypothesis that displacement downwards is as effective as sideways (Iwata and Tokura, 1997; Hirning, Isoardi, and Cowling, 2013).

$$P = 1 + 0.8 \cdot \frac{R}{D} \quad for \quad R < 0.6D \tag{15}$$

$$P = 1 + 1.2 \cdot \frac{R}{D} \quad for \quad R \geq 0.6D \tag{16}$$

$$R = \sqrt{H^2 + Y^2} \tag{17}$$

Einhorn also calls for more validity tests of the position index since the UGR model was recently introduced at that time (Iwata and Tokura, 1997). In 2009-2010, Kim and Kim extended their research on the effect of background luminance on discomfort glare in relation to glare source size to mapping the glare sensation over the entire visual field and develop a position index formula (Kim and Kim, 2010a, 2010b, 2010c). They mention Guth's position index as being expressed in the IES Lighting handbook from 2000 as (Kim and Kim, 2010c):

$$P = \exp\left[\left(35.2 - 0.31889\alpha - 1.22e^{\frac{-2\alpha}{9}}\right)10^{-3}\beta + (21 + 0.2667\alpha - 0.002963\alpha^2)10^{-5}\beta^2\right] \tag{18}$$

where

exp is e$^{[\,]}$

α is the angle on the vertical plane containing the source and the line of sight [°]

β is the angle between the line of sight (looking straight ahead) and the line from the observer's eye to the source [°]

The experimental apparatus is the same between the three studies with changes to how the glare source interacts with the observer. A semi-spherical screen 2 m in diameter extended with a cylinder with a cut-out for the observing subject to sit, so the entire visual field was covered, with similarities to Luckiesh and Guth's experiment. Incandescent lamps mounted on the edge of the cylinder behind the subject would irradiate the inside of the screen with a constant brightness serving as the background luminance. Where the first study had a LED circuit board at the centre as a glare source and varied the size and background luminance (Kim and Kim, 2010a), the second and third study (Kim and Kim, 2010b, 2010c) replaced this with a type of linear rail system upon which the location of the glare source could be mechanically adjusted in increments of 5°/s across the screen by a motor. The rail system itself could also be rotated 360° by a handle on the back making the glare source able to be located around the whole screen, though it was programmed for certain locations for consistency. The background luminance internally in the screen was set to 34.3 cd/m^2 as applied by the Luckiesh and Guth in their experiment (Kim and Kim, 2010b, 2010c) while the room itself had an average illumination of 30 lux for the convenience of the experimenter. The glare source had a solid angle of 0.0011 sr and luminance could be adjusted from 0 to 160,000 cd/m^2. A camera was also installed at the centre to observe the eyes of the subject.

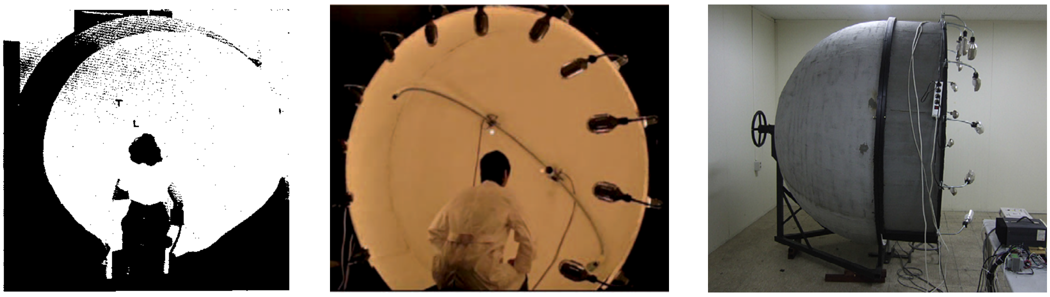

Figure 17: (A) Experimental setup by Luckiesh and Guth (1949). (B) Experimental setup by Kim and Kim (2010b, 2010c).

The procedure of the two studies on glare sensation mapping (Kim and Kim, 2010b, 2010c) was the same, only the number of subjects varied, with 32 subjects of age 20 to 30 in the first (Kim and Kim, 2010b) and eight subjects of age 20 to 31 in the second (Kim and Kim, 2010c), both consisting of students and researchers. Subject who wore glasses were tested without since the frame of the glasses could interfere. The experiment was split into three smaller experiments. The results and procedures of the first study (Kim and Kim, 2010b) will be discussed first, since it has the largest sample size. Afterwards the minor differences of the second study (Kim and Kim, 2010c) compared to the first (Kim and Kim, 2010b) will be discussed.

Visual field	Radial angle [°]	Limit of the vision [°]
Upper field	0	92
	22.5	82
	45	64
	67.5	54
	90	48
	112.5	53
	135	60
	157.5	78
Lower field	180	88
	−157.5	89
	−135	84
	−112.5	73
	−90	67
	−67.5	77
	−45	86
	−22.5	91

Figure 18: Average visual field as a function of the radial angle (Kim and Kim, 2010b).

The first experiment involved measuring the limit of the visual field with each eye individually and both eyes at once staring at a fixed point in the centre. The moveable light source was set to 1,000 cd/m² and was moved from outside the visual field towards the centre until the subject could detect it in the view. This was repeated randomly over 16 different radial angles in the first study (Kim and Kim, 2010b) to avoid prediction and obtain average values. The results from the first study (Kim and Kim, 2010b) showed the upper field vertically extending to 48° at the radial angle of 90° while the lower field extended to 67° at the radial angle of -90° (see Figure 18 and Figure 19). At the radial angle of 0° and 180° the fields extended to 90°. Kim and Kim (2010b) mentioned this being slightly lower than the standard set by the IES, which at the time of publishing was 60° and 70° for radial angles 90° and – 90° respectively, while being 90° for radial angles 0° and 180°. The total size of the visual field was measured to be 4.7 sr with a small difference between left and right eye, 2.3 sr and 2.4 sr respectively, which was accounted to individual eye dominance (Kim and Kim, 2010b). This did of course also show to be smaller than the 5 sr the IES standard suggests. It is interesting that neither the upper and lower field or right and left side of the visual field was found to be symmetrical.

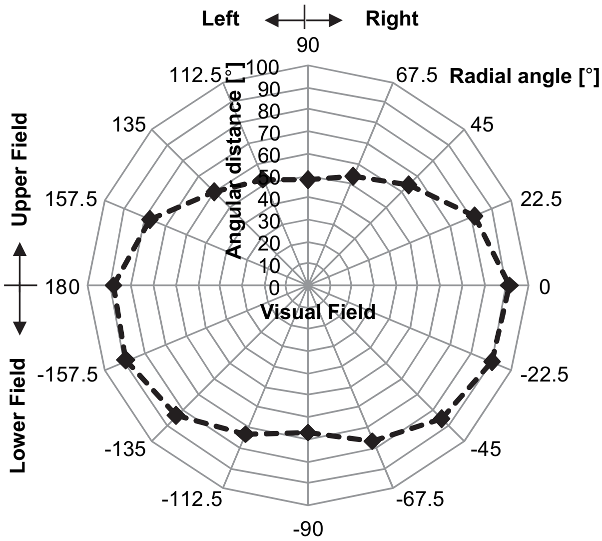

Figure 19: Average visual field of thirty-two subjects (Kim and Kim, 2010b).

The second experiment involved measuring the luminance which served as the borderline between comfort and discomfort (BCD) on the line of sight. A standard light source was placed at the centre of the semi-spherical screen and set to blink at 1 sec. intervals. The subjects then used a dimmer to increase the light level until they reached their BCD level which was repeated three times so average values could be obtained. They found BCD luminance ranging from 520 cd/m² to 5,500 cd/m² showing the large difference in tolerance between subjects, which was the same findings Luckiesh and Guth (1949) arrived at according to the team. Kim et al. decided to use the average value of 2,242 cd/m² (see Figure 20).

Subject no.	BCD luminance [cd/m²]	Subject no.	BCD luminance [cd/m²]
1	1180	17	817
2	1859	18	3303
3	3023	19	885
4	1780	20	1147
5	4550	21	4790
6	520	22	2080
7	573	23	2043
8	653	24	2923
9	2868	25	865
10	2194	26	2072
11	2519	27	2822
12	5500	28	1653
13	3013	29	2804
14	5450	30	2940
15	852	31	1189
16	2000	32	863
			Average: 2242

Figure 20: BCD luminance at the line of sight (Kim and Kim, 2010b).

The third and last experiment involved measuring the BCD luminance across the whole visual field. Four luminance levels were chosen based on the average BCD luminance value obtained through the second experiment, 3,000 (I), 5,000 (II), 10,000 (III) and 30,000 (IV) cd/

m². They were presented to the subject from highest luminance to lowest and from outside towards the centre on all 16 radial angles, as in the first experiment. The subjects had both eyes open and the radial angles were chosen randomly prevent prediction. When a spot that triggered a BCD sensation in the subject was found on all 16 radial angles, they could be connected to create the "equal BCD curve". Such a curve was found for all four luminance levels. For the 30,000 cd/m² luminance source the curve occupied 4.4 sr of the whole visual field, with the upper and lower field occupying 1.7 and 2.7 sr respectively. For the 10,000 cd/m² luminance source the curve occupied 3.2 sr of the whole visual field, with the upper and lower field occupying 1.2 and 2.0 sr respectively. For the 5,000 cd/m² luminance source the curve occupied 1.9 sr of the whole visual field, with the upper and lower field occupying 0.7 and 1.2 sr respectively. For the 3,000 cd/m² luminance source the curve occupied 0.8 sr of the whole visual field, with the upper and lower field occupying 0.3 and 0.5 sr respectively.

The curves continually showed that the lower field occupying more of the visual field than the upper field. The fields being asymmetrical also suggests that findings from experiments conducted only on the upper field cannot be used for the lower field. When compared to Guth's equal BCD curves, Kim and Kim (2010b) mentions the shape being similar as a suggestion of reliability. One special critique the researchers brings up themselves, are that of the kinetic testing method versus the stationary method. The kinetic testing method is used in the first and third experiment where subjects are required to find locations that cause discomfort in the visual field with moving (kinetic) objects of preselected size and luminance. The stationary testing method is used in the second experiment where subjects are required to find discomfort at preselected (stationary) locations with objects of varying luminance. Guth's data was obtained with the stationary method and to fully compare with that experiment would require the same method to be used. Kim and Kim (2010b) argue that time is a critical factor when the test source have high luminance. Kinetic testing was quicker since the stationary method which would have required resetting the adaption for every point on all of the 16 radial angles when the BCD luminance at each point was obtained. Repeating three times to obtain average values for all 32 participants, as was the method, would have drastically slowed down the experiment.

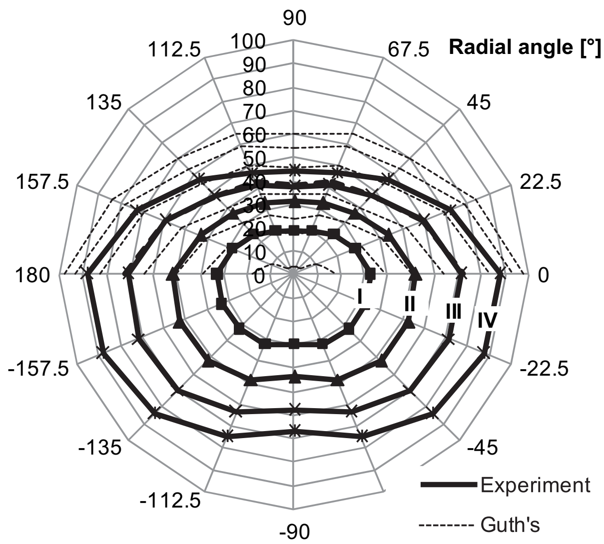

Figure 21: Comparison between the equal BCD curves obtained from the experiment and the Guth's equal BCD curves (Kim and Kim, 2010b).

The second study (Kim and Kim, 2010c) had similar procedures throughout the three experiments with minor differences. As mentioned, the sample size was four times smaller but around the same age. The first experiment only used eight radial angles to locate the limits of the visual field (0°, 45°, 90°, 135°, 180°, -45°, -90°, -135°). The second and third experiment was switched around this time seemingly to avoid the subject had to adjust to a high luminance source before mapping the BCD curves. In the second (previously third) experiment they mapped the BCD curves of the entire visual field using the same four luminance values for the light source and tested all 16 radial angles as before. The subject had the left and right eye tested individually as well as both eyes in the second experiment as an addition (see Figure 22). Despite criticising the kinetic testing method in the previous study, Kim and Kim (2010c) did not change this for the second study. In the third experiment (previously second) the subject was required to locate the BCD luminance at the line of vision but this time the experimenter was the one controlling the dimmer and the subject would just signal when the BCD luminance was reached. This was also done for each eye individually as well as both eyes (Kim and Kim, 2010c).

Subject no.	Left eye L ($cd \cdot m^{-2}$)	Right eye L ($cd \cdot m^{-2}$)	Both eye L ($cd \cdot m^{-2}$)
1	3503	4593	6457
2	2723	4167	7817
3	6117	7470	4257
4	3730	5023	6020
5	2873	2993	5803
6	2213	3183	3797
7	2197	3940	2620
Average	3336	4481	5253

Figure 22: BCD luminance in the line of sight (Kim and Kim, 2010c).

The sizes of the different fields were slightly smaller than what was found in the first study (Kim and Kim, 2010b) (see Figure 23). Although the limits of the visual field did not change much, the BCD curves changed much more. For the 30,000 cd/m² luminance source the curve occupied 2.67 sr of the whole visual field (previously 4.4 sr), with the upper and lower field occupying 0.92 and 1.75 sr respectively. For the 10,000 cd/m² luminance source the curve occupied 2.05 sr of the whole visual field (previously 3.2 sr), with the upper and lower field occupying 0.77 and 1.28 sr respectively. For the 5,000 cd/m² luminance source the curve occupied 1.02 sr of the whole visual field (previously 1.9 sr), with the upper and lower field occupying 0.37 and 0.65 sr respectively. For the 3,000 cd/m² luminance source the curve occupied 0.6 sr of the whole visual field (previously 0.8 sr), with the upper and lower field occupying 0.22 and 0.38 sr respectively. It might be that the new subjects were less sensitive and the BCD luminance in the line of vision actually show them to be more tolerant with a range between 2,620

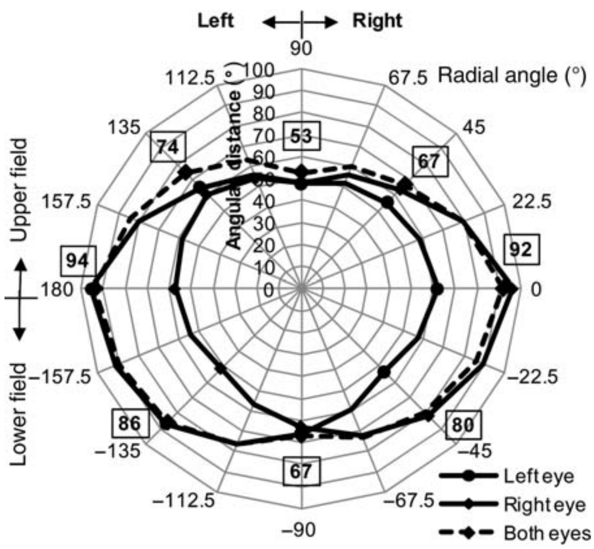

Figure 23: The visual field limits of single and both eyes (Kim and Kim, 2010c)..

and 7,817 cd/m² for both eyes and an average of 5,253 cd/m². Interestingly, the average BCD luminance of both eyes showed to be 1.6 and 1.2 times higher than the average BCD luminance of the left and right eye respectively (Kim and Kim, 2010c).

Kim and Kim (2010b, 2010c) supposedly used the data from both studies, a sample size of 40 subjects, to develop a new position index formula. The new average BCD luminance was 2,990 cd/m². The new position index formula could be expressed as (Kim and Kim, 2010c):

$$P = exp\left[\frac{\beta - (-0.000009\alpha^3 + 0.0014\alpha^2 + 0.0866\alpha + 21.663)}{-0.000009\alpha^3 + 0.0013\alpha^2 + 0.0853\alpha + 8.772}\right] \quad \textbf{(19)}$$

where

exp is $e^{[\,]}$

α is the angle on the vertical plane containing the source and the line of sight [°]

β is the angle between the line of sight (looking straight ahead) and the line from the observer's eye to the source [°]

If the BCD luminance in the centre (line of sight) at 2,990 cd/m² is position index 1 the other BCD curves can be calculated accordingly. The BCD curve for 3000 cd/m² is also position index 1. The BCD curve for 5,000 cd/m² is position index 1.7. The BCD curve for 10,000 cd/m² is position index 3.3. The BCD curve for 30,000 cd/m² is position index 10. The position index chart over the whole visual field is presented in Figure 24 (Kim and Kim, 2010c):

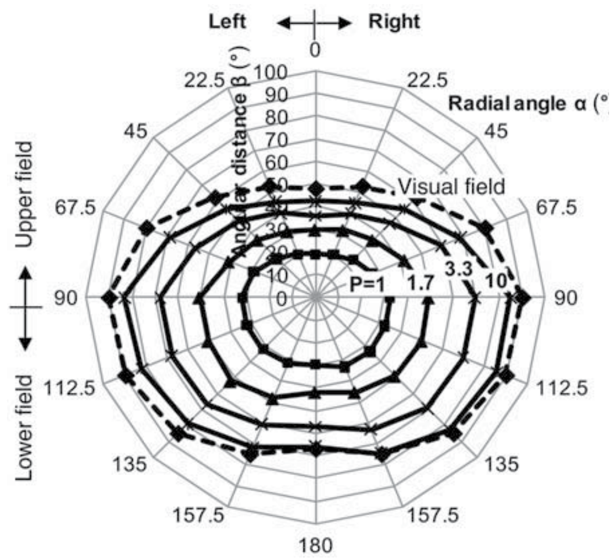

Figure 24: The BCD curves based on the averages of the left and right eyes and position index (Kim and Kim, 2010c).

According to these few studies it would seem that the human visual system is in fact more sensitive below the line of vision, but data collected in modern, practical settings with LED light and large groups of subjects are still too little. Additionally, the mentioned studies only assess and map the glare according to its position in the visual field, but it does not actually test if it affects task performance and to what degree.

4. Methodology

In order to fully comprehend the challenges of researching peripheral discomfort glare, an experiment will be designed and performed, and the considerations from the process will be presented. From the literature review, two additional research questions comes to mind.

- ▹ **RQ 6:** Does discomfort glare influence task performance and how can it be measured?
- ▹ **RQ 7:** If it does influence task performance, where in the visual field does it influence the most?

It seems there is general consensus in the literature that discomfort glare does influence the ability to concentrate 100% on a task. How much it impairs task performance and what influence placement of glare sources has appears to be relatively individual. In the literature, preference and performance are two different measurements to aim for but one do not seem easier than the other. While a relatively modern daylight glare prediction model has been developed, DGP, and the daylight regulation has been revised in 2018, the indoor electrical glare regulation in offices will still rely on the UGR model in the revision of 12464-1 standard to come. As previously suggested, this model has its shortcomings although it might still be the best model available for small sources. The discussion about position index and glare source placement in the visual field is highly relevant, though it seems the research by Kim and Kim (2010b, 2010c) are the only recent attempts at updating the index with modern data. Their conclusions are required to be tested further for any implementation to be realistic, but it does not look like the most popular subject to research. One of the conclusions by Kim and Kim (2010b, 2010c) suggests that people are more sensitive to glare in the lower part than the upper part of the visual field. It would be interesting to test this hypothesis in a Danish context and see if the Korean results and conclusion can be replicated or questioned. Such experiment could be designed to test both **RQ6** and **RQ7**: Can influence be measured and which position in the visual field have the most influence?

In their article, Luckiesh and Guth (1949, p. 651-651) writes: "Any comprehensive study of quality of lighting or the environmental brightness relationships must include:

- ▹ The brightness-level to which the eyes are adapted.
- ▹ The brightness of various areas in the visual field.
- ▹ The area and position of sources of brightness.
- ▹ The criticalness of the visual task to be performed."

This summarises the factors included in most tests reasonably well but are not elaborated well as complete guidelines to follow. For this experiment, the considerations will be thoroughly explained to justify the design choices.

4.1 Hypothesis

The expected answers to the experimental research questions is based on the conclusions by Kim and Kim (2010b, 2010c). The hypothesis to **RQ6** is that peripheral discomfort glare does have a negative influence on task performance and can be measured with a well designed experimental setup. The hypothesis to **RQ7** is that discomfort glare sources in the lower visual field will have more negative influence on task performance than discomfort glare sources in the upper visual field as suggested by Kim and Kim (2010b, 2010c).

4.2 Initial experimental design

A list of experimental design criteria grounded in the literature review was to be applied to the setup in an attempt to guide the process toward designing the best setup and achieve results of the best quality for later analysis and interpretation. The criteria correspond to the ones set by Luckiesh and Guth (1949, p. 650-651) but are more elaborated to guide the process more efficiently. As the criteria are considered henceforth, their prefix (C#) will be referenced.

- **(C1)** The visual task is required to be performed on a computer screen (Display Screen Equipment, DSE) to fit a modern work scenario.
- **(C2)** The surrounding view of the computer task visible in the peripheral visual field is required to be a uniform surface to create minimal stimuli.
- **(C3)** The glare sources are required to be placed in the peripheral visual field.
- **(C4)** The glare sources are required to be covering equal solid angles.
- **(C5)** The glare sources are required to be individually controlled and have equal output.
- **(C6)** The background luminance and glare source luminance are independent of each other just as the UGR prediction model is defining it.
- **(C7)** Adaption time should be minimised to lower total duration of the experiment.
- **(C8)** Personal and experimental bias should be kept at a minimum.

A study by Kent, Fotios and Altomonte (2018) used an experimental setup which could meet many of the criteria with some adjustments. The authors employed a screen wall to cover the whole visual field (**C2**), as shown in Figure 25. For the visual task they used DSE (**C1**) and for the glare source they used a projector to light up a diffusive screen in a hole in the wall. This made the glare source luminance independent of the background luminance (**C6**). The design was used as a starting point since it offered a setup reasonably easy to build from scratch.

The concept was to have a participant sitting at a table with DSE at 1 m distance from a similar wall screen. The visual field as presented in the study by Kim and Kim (2010b, 2010c) would be mapped as the perspective of the participant. Specific positions and solid angles of the glare sources would be calculated (**C3,C4**) to correspond to one of the BCD curves from the study in terms of position and luminance (3,000 (I), 5,000 (II), 10,000 (III) and 30,000 (IV) cd/m^2). It proved challenging to balance position and solid angle to a setup in development. As described earlier, solid angle ($\omega = A/r^2$, (6)) depends on the projected area *A* of the glare source onto the sphere of vision and the distance *r* to the centre of the glare source. This means different positions and distances can result in different sizes of holes in the screen wall. It was decided that it would be easier to plan and balance these variables in a digital model of the setup.

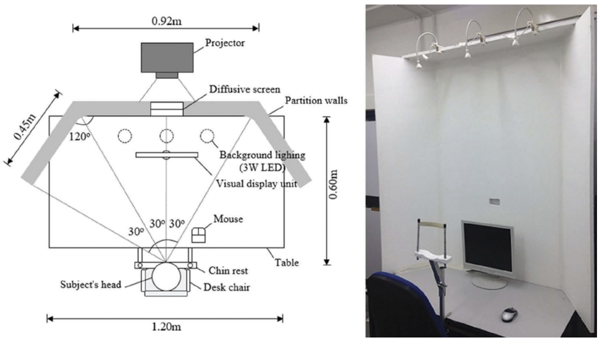

Figure 25: Plan layout and photograph of the lighting chamber used in this study (Kent, Fotios, and Altomonte, Fig. 1, 2018).

4.3 Modelling

The tools used to create the digital model was Rhinoceros 3D v.5 (Rhino) and the plugin Grasshopper. Rhino is a computer-aided design (CAD) program used to design 3D models. Grasshopper is an extension program and a visual programming environment used to develop models in Rhino through interconnected components dragged onto a canvas. This software combination allows the user to build a 3D model that can easily be adjusted based on defined parameters and optimises workflow.

The digital model began with a stand-in for the participant, a 3D seated participant with eye level at height 1,2 m as standard. To model the visual field as mapped by Kim and Kim (2010b, 2010c), a semi-sphere was modelled with centre at the eyes and a radius of 1 m, simulating the participant looking straight ahead (see Figure 26). The angular distances (0°, 10°, 20°, 30°, 40°, 50°, 60°, 70°, 80°, 90°) and radial angles (0°, 22.5°, 45°, 67.5°, 90°, 112.5°, 135°, 157.5°, 180°, -157.5°, -135°, -112.5°, -90°, -67.5°, -45°, -22.5°). This resulted in 144 polar points (see Figure 27). Sphere and points were then rotated 15° downwards around the observer point to simulate looking slightly downward at DSE.

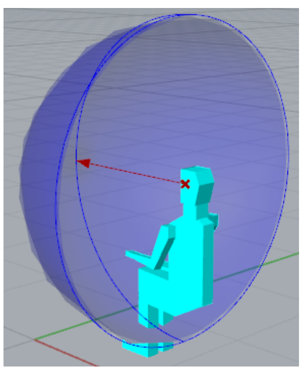

Figure 26: 3D model showing sphere of vision and line of sight.

The polar points were connected to match the visual field mapped by Kim and Kim (2010b, 2010c) and redundant points were removed. The angular distances were modelled with blue lines showing the 10° increments. The radial angles were modelled with white lines showing 22.5° increments. A simple table and computer screen was modelled so the centre of the screen was lining up with the 15° downward angle line (see Figure 29). Three walls were modelled with 1220x2440 mm (WxH) masonite plates and assembled with a rotation angle of 140° from the back wall (see Figure 28). A table custom table with a width of 920 mm was designed to fit the setup perfectly.

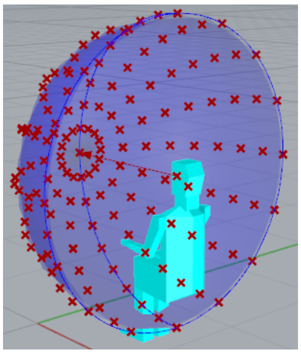

Figure 27: 3D model showing polar coordinates mapped on the sphere of vision.

To test the hypothesis to **RQ7**, that people are more sensitive to discomfort glare in the lower part of the visual field than the upper part, six glare sources was placed in the side walls (**C3**). Two below the line of sight (radial angles -22.5° and -157.5°), two on the line of sight (radial angles 0° and 180°) and two above the line of sight (radial angles 22.5° and 157.5°). To compare, a seventh glare source was placed in the centre wall above the computer screen (radial angle 90°) (**C3**).

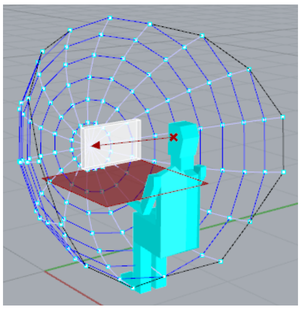

Figure 29: 3D model showing the visual field mapped in a work context.

In the study by Kent et al. (2018), they made evaluations in one half of their experiment. They chose four luminance levels to provide different levels of discomfort based on Hopkinson's multiple-criterion scale in a study by Hopkinson in 1960. The chosen luminance levels were 762 cd/m^2, 1,799 cd/m^2, 4,122 cd/m^2, and 9,819 cd/m^2 corresponding respectively to "just imperceptible" (IES-GI = 10), "just acceptable" (IES-GI = 16), "just uncomfortable" (IES-GI = 22), and "just intolerable" (IES-GI = 28). The luminance for this experiment was set to 10,000 cd/m^2 corresponding to the BCD (III) curve (see Table 3) in the study by Kim and Kim (2010b, 2010c), which compared to 9,819 cd/m^2, viewed as "just intolerable", seemed like a reasonable choice to be strong enough induce discomfort without becoming disability glare. Additionally, being able to create a diffuse discomfort glare source for seven positions with a luminance of 10,000 cd/m^2 was realistic, while brighter sources would become expensive and challenging. Following the BCD (III) curve, the angular distances were decided (**C3**) (see Table 3). Unfortunately an error was made with the two top glare sources resulting in them being placed at angular distance 70°, as the other four side wall sources, instead of 60°. The potential influence of this error will be discussed later.

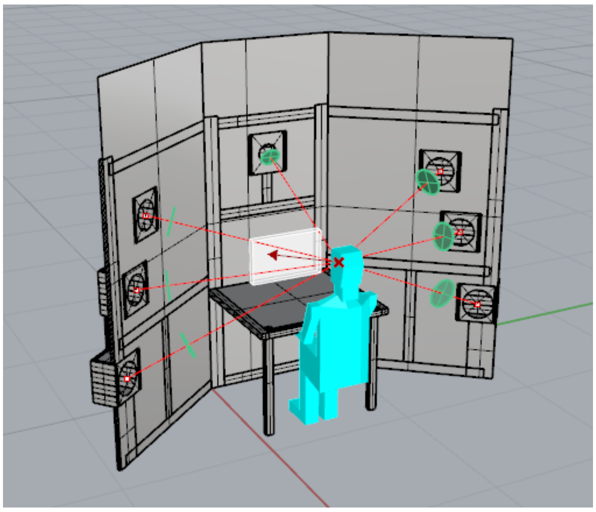

Figure 28: Final model of the experimental setup.

Table 3: Centre of glare sources positioned in radial angle and angular distance to fit the BCD (III) curve as defined by Kim and Kim (2010b, 2010c). Positions are marked on the polar coordinate diagram from Figure 21.

Glare source position	Radial angle	Angular distance
Left bottom	-157.5°	70°
Left middle	180°	70°
Left top	157.5°	60°
Centre	40°	90°
Right Top	22.5°	60°
Right middle	0°	70°
Right bottom	-22.5°	70°

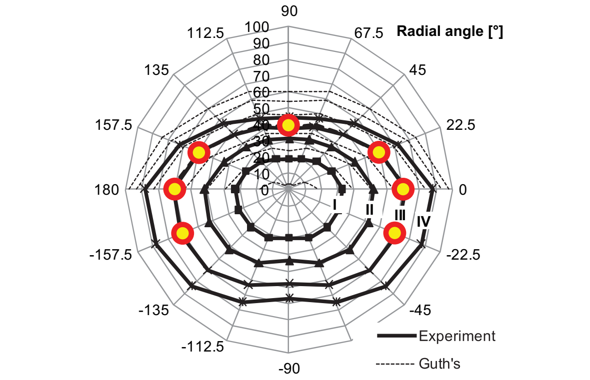

Calculating the solid angles of the glare sources proved a little complicated. Interestingly, studies tend to leave out how they reach their respective solid angles in their experiments. Kent et al. (2018) used a rectangular glare source 0.08 x 0.04 m (WxH) which equals an area of 0.0032 m^2 placed at a distance to the observer of 0.6 m. The solid angle they mention is 0.009 sr and this is similar to 0.0032/0.62 = 0.00889 sr ≈ 0.009 sr. This would indicate they used formula (6) which only appears applicable for circle sources. It was difficult to obtain information on rectangular solid angles, but on a mathematics forum a much more complex formula (20) was found (*How to calculate solid angle...*, 2015-2017). Another instance of this critique is the studies by Kim and Kim who used both squared (2010a) and round (2010b, 2010c) glare sources without describing the calculation. A definitive answer to the calculation of different types of solid angle has not been found and round sources was chosen as that method was certain.

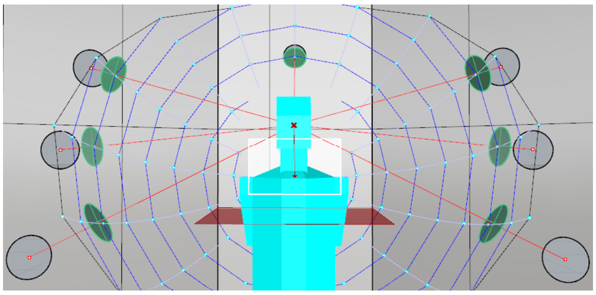

Figure 30: View directions with projected areas of the glare sources onto the sphere of vision.

$$\omega = 4sin^{-1}\left(\frac{lb}{\sqrt{(l^2+4d^2)(b^2+4d^2)}}\right) \qquad \textbf{(20)}$$

Kent et al. (2018) chose a solid angle of 0.009 sr arguing Luckiesh and Guth (1949) and Petherbridge and Hopkinson (1950) both used similar sizes in their studies. Kim and Kim (2010a, 2010b, 2010c) has used a solid angle of 0.011 sr in two of their studies. As long as the solid angle was within the threshold of the UGR model (0.0003-0.1 sr) it would be acceptable. It was chosen to follow Kent et al. (2018) and use a solid angle of 0.009 sr with round sources (see Figure 30). The bottom glare sources were 210 mm in diameter (0.08988 sr), the middle (0.09025 sr) and top (0.09028 sr) glare sources were 190 mm in diameter, and the centre glare source was 130 mm in diameter (0.008967 sr) (**C4**). The measurements of each positions from the edges can be found in annex A.

The experiment would takes place in the Light Lab at Aalborg University Copenhagen (AAU-CPH). It was measured and build in the model as well to make sure the setup would fit (see Figure 31). This also determined the model would be built in a modular way in the workshop preparing for easy assembling and disassembling because of a tight booking schedule for the Light Lab.

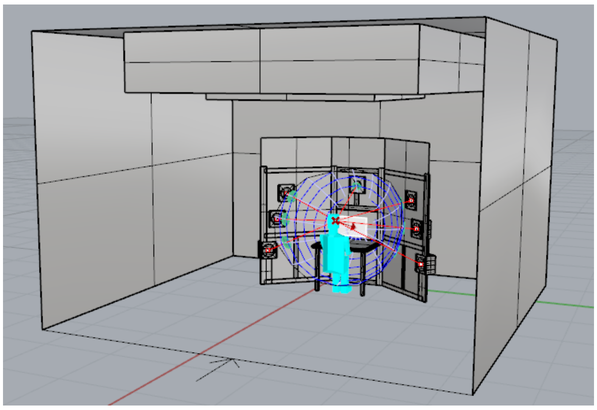

Figure 31: The experiment setup model in a 3D model of the Light Lab.

4.4 Glare sources

The glare sources was designed as a box to be mounted on the back of the wall screen. The boxes would be fitted powerful LED-strips and a reflective material on the inside surfaces to reflect and distribute the light. The opening of the boxes would be covered with a diffusive material as Kent et al. (2018) did. For the diffusive material, some decorative translucent paper was chosen as a relatively cheap and well-suited option. For the reflective material, aluminium tape was tested, but it was both expensive and worse at reflecting light than simple aluminium foil, which could be mounted with hobby glue stick.

For the LED-strips, an option of 2100 lumen/m, 25 W/m, 240 LED/m chip density, 4,000 K CCT, CRI 80, 120° spread angle, and with adhesive tap on the back was chosen. Building a custom design with LED chips would have risked wasting time and introducing errors by soldering components. LED-strips comes in 12 V DC version and are easy to use with a simple power supply. An electrician was consulted in this process.

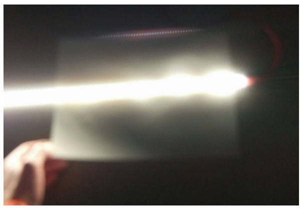

Figure 32: Light test 1

The distribution and transmission of light through the diffusive material was of great importance. A completely diffuse light emitting surface was necessary with no single spots of LEDs visible. A simple test of the distance between the LEDs and the diffusive material was carried out and it showed an installation depth of 150 mm would be sufficient (see Figure 32 and Figure 33).

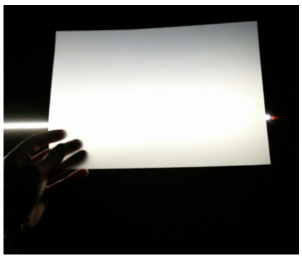

Figure 33: Light test 2.

The luminance meter (burrowed from the Danish Building Research Institute (SBI) in connection with AAU-CPH) showed the LED-strips had potential to reach the 10,000 cd/m² at around 1-1.2 m distance. A box was constructed with a depth of 150 mm and 300 mm of LED-strip was installed (see Figure 34). The diffusive material

Figure 34: Light test.

was shown to work as intended, but the LED-strip did not emit light close to 10,000 cd/m². Without the diffusing paper the LEDs had a luminance of 15,000-20,0000 cd/m2 but with the diffusing paper on top of the box it had 3,000-5,000 cd/m². It was decided to install 1,000 mm LED-strip in each box, over three times as much. The goal was to provide more than enough light and then dim it to the desired level instead (**C5**). The was also a product of the strict time schedule to construct this whole setup one person with limited time for testing this any further.

4.5 Electronics

The controls of the glare sources was kept relatively simple with a toggle switch for each glare source to turn them on and off manually (**C5**). To adjust the glare source luminance levels, a dimming function was needed, but dimming can cause flickering if the wrong technology is used. As described earlier, flickering is a product of fluctuations in the electric current supplied to the driver, but a reasonably good driver turns this alternating current (AC) into direct current (DC) making the fluctuations invisible. Dimming light potentially risks introducing flickering by other means.

A dimmer is essentially controlling the voltage supplied to the LEDs. One method of dimming is called Pulse Width Modulation (PWM) which turns the current on and off very fast, chopping the signal pulse into small parts in the process. It modulates the width of the signal pulse's on-parts, which regulates the average voltage supplied to the LEDs. Because of the on/off pattern, systematic flickering might occur and this was not the type of discomfort glare the experiment was designed to test and had to be ruled out. Another way of dimming is with a constant current (CC) regulator producing a straight voltage pulse instead of the jagged on/off pulse produced by PWM. This ensures the LEDs will not be turned on and off quickly, thus resulting in a steady light. CC still has problems with dimming to low light levels, but this setup did not require low dimming levels.

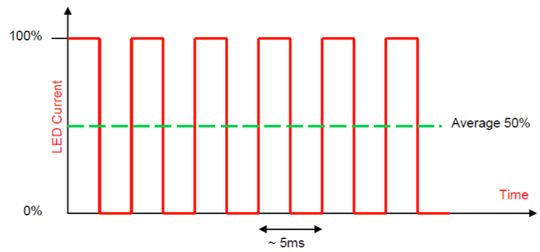

Figure 35: Pulse Width Modulation (PWM) dimming (Davis, -).

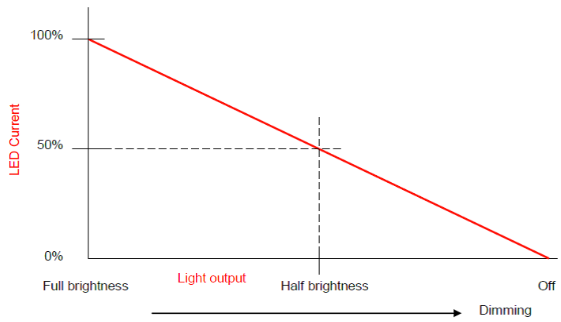

Figure 36: Constant Current dimming (CC) (Davis, -).

Power would be supplied from a computer power supply repurposed as a lab power supply providing 12V DC up to 18 A delivering up to 648 W. From the power supply, the voltage would be regulated by a constant current regulator with a watt meter display next to provide feedback on the voltage adjustments. From the watt meter display seven wires would be running to seven on/off toggle switches and on to the LED-strips in the glare source boxes (**C6**). The idea was to control the luminance output of all seven glare sources with one CC regulator to keep it simple and cheap. For this to work, the loss through the wires would have to be the same, requiring wiring to each source to be the same length. Additionally, to lose less power through the wiring and utilize most of the power of the LEDs, the gauge of the wires was set to 1,5 mm2. An electrician was consulted in this process.

4.6 Construction

One glare source box was built for testing first and once approved, the rest of the seven boxes were built. All five surfaces inside the boxes were covered with glue and aluminium foil with its most reflective side showing. In the process, the foil was smoothed out as much as possible to optimise reflection (see Figure 37A). The centre wall was cut to 920 mm width and all the glare source holes was traced on each segment. Each hole was then cut with a jigsaw. The skeleton support was mounted on the back of the masonite plates with screws and brackets as designed in the digital model. To ensure the correct angle of the screen wall, brackets were bent 40° before mounting. Simple feet were put on the segments to avoid them tipping over backwards (see Figure 37B)). Afterwards the wall segments were painted in a white matte to avoid reflections (**C2**) as in the study by Kent et al. (2018). The glare source boxes were mounted in a staircase design where the next box rested on the box below it (see Figure 37C). The bottom boxes fitted into a slot in the skeleton and rested on a bracket at on the bottom. The middle boxes then rested on a pole piece with a back piece keeping both box and pole in place. They were also mounted to the skeleton with a bracket on the side of the box. The top boxes were mounted with a similar pole and back piece to be rested on and nothing more. The centre box was mounted with brackets connected to the skeleton on both the top and bottom of the box. The staircase design served a purpose of minimising the use of screws run through the surface of the wall segments to keep the surface as unspoiled as possible. The screws had of course been painted with the same paint as the walls.

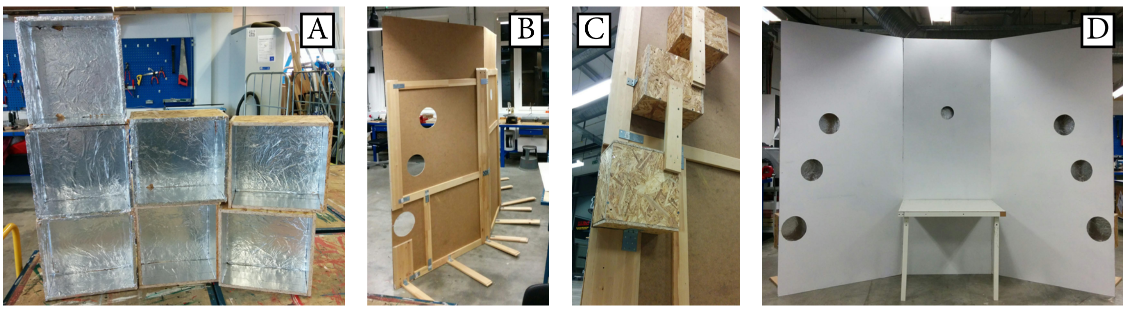

Figure 37: (A:) Glare sources boxes with aluminium foil inside. (B) Standing screen wall. (C) Staircase mounting of the glare source boxes. (D) Final construction.

4.7 Light Lab design

In the process of moving the setup to the Light Lab, the paint got scratched a little by its own screws unfortunately, but it was decided to not attempt cleaning or repairing it of fear of ruining it further. The Light Lab had a truss rig hanging in the ceiling to mount fixtures on for this purpose, but the available fixtures turned out not to be optimal. Since the LED-strips was 4,000 K CCT most of the fixtures were either warmer or with filters in the front. Additionally, most of the fixtures were spots and not wide angled. Luckily, four Iguzzini (model uncertain) recessed downlights were hanging in wires at the corners of the truss rig and with a little readjustment towards the ceiling and behind the screen wall, they created a reasonable general lighting in the lab with indirect light (see Figure 38). There was no option of dimming them, but the purpose was to create enough light to avoid adaption time in the experiment. The general luminance had to be higher than 5 cd/m^2 to avoid participants adjusting to either scotopic (>0.005 cd/m^2) or mesopic vision (0.005 > 5 cd/m^2). The general lighting was unfortunately uneven, but it was managed to get an average illuminance of 70 lux across the floor (see annex B). This is not exactly a realistic work scenario, as 70-80 lux barely makes corridor levels, but it achieves the goal of not entering scotopic or mesopic vision state and not requiring extensive adaption time in the experiment (**C7**). It is not optimal, but they were the best available option in terms of power, CCT, and spread.

The lighting on the screen wall had the same challenges. Only two of the available fixtures could be used in terms of CCT and spread. Two Erco (model uncertain) fixtures were mounted on the truss rig in the middle of the side walls and directed across the room to the opposite side wall segments (see Figure 38). They were also tested lighting the wall segments from the back of the room, but that would create a moving shadow of the participant, which was less ideal. Directing the light across to the opposite wall segment also cast some light on the centre wall segment and distributed the light as best as possible. The Erco fixtures fortunately had a built-in dimmer which was used to try to achieve a luminance of 34 cd/m^2. This was the background luminance used in the studies by Kim and Kim (2010b, 2010c). In the study by Iwata and Tokura (1997), Einhorn had commented a recommendation of raising the background luminance from "dark surroundings" to above 10 cd/m^2 to represent practical conditions. In the study by Kent et al. (2018), they used a mean luminance of 65 cd/m^2 which is probably closer to a real office scenario. Since the studies by Kim and Kim (2010b, 2010c)

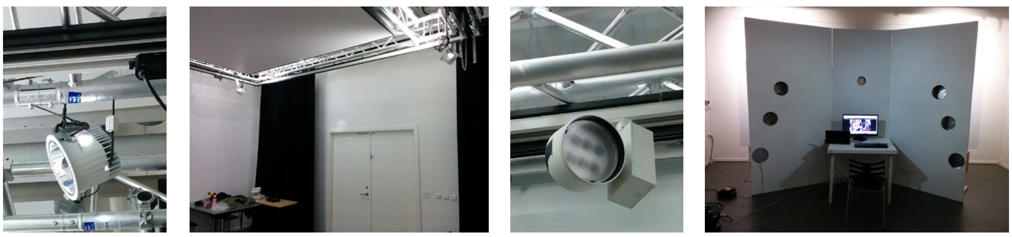

Figure 38: Light setup in Light Lab.

was the focus of the experiment, as it was testing their conclusions, 34 cd/m² was viewed as a good compromise to aim for. A few measurements were done of the walls of the lab still in view at the edge of the visual field (see annex B), and they had a mean luminance of 20 cd/m² (left lab wall) and 15 cd/m² (right lab wall). The wall segments had a mean luminance of 33 cd/m² (left), 32 cd/m² (centre), and 31 cd/m² (right). All-in-all, it was possible to fulfil the criteria set for the experimental setup with limited means (**C2**).

Unfortunately, due to time pressure to be ready to start the experiment, the LED-strips were not mounted with too much care which could have optimised their distribution and make the boxes completely identical. It was believed the reflective material would make up for this. The gaps in the screen wall was sealed with duct tape to cover the light behind the screen wall (**C2**). The leftover LED-strip was mounted on the floor below the table to try to shine more light at the bottom of the side wall segments to make the table shadow less intrusive and make the uniformity better. It was impossible to remove the shadow completely unfortunately. An attempt was made at covering the black parts of the computer screen with regular paper (see Figure 39), so it would not cast a shadow and to make everything white (**C2**). Only the keyboard was black and remained untouched. See final experimental setup in Figure 40.

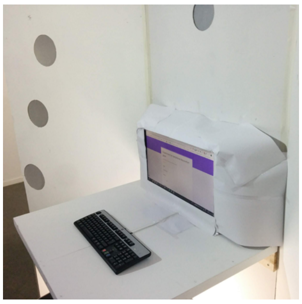

Figure 39: Task area.

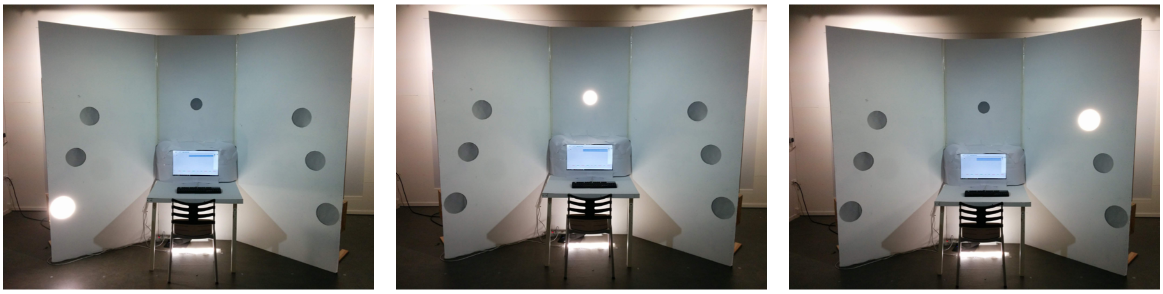

Figure 40: Finished experimental setup.

4.8 Performance task

The experiment was designed to assess the performance of participants exposed to discomfort glare, whether it influenced task performance negatively or not and what the circumstances were. In the literature, there are different approaches to test and analyse this.

4.8.1 Cognitive demand of the visual task

In the study by Kent et al. (2018) they hypothesised that a visual task requiring more cognitive attention, such as a text, would provide more distraction from discomfort glare than a less demanding task, such as a fixation task, and thus increasing the tolerance. Their experiment set out to test the hypothesis that instructing the participants to focus attention on a visual task demanding a greater degree of cognitive attention will lead to lower evaluations of discomfort glare than when instructed to focus attention toward a simple fixation mark. The visual task they chose to use was a pseudo text, which is a line of randomised letters not making any sense, that the participants had to read aloud. The fixation task was simply to focus on a circle.

They used two procedures to verify the evaluations from both visual tasks. The first was the well-known luminance adjustment method where the luminance of the source is evaluated according to Hopkinson's multiple-criterion scale ("just imperceptible", "just acceptable", "just uncomfortable", and "just intolerable"). The experimenter would adjust the luminance of the glare source on command from the participant from a low IES-GI value and upwards. The second method was category rating where four fixed luminance levels were rated on the multiple-criterion scale. 24 participants performed both visual tasks and evaluated each task with both procedures. The results demonstrated that when the participants were focus on the pseudo-text task, they were more tolerant to discomfort glare than when told to fixate on a simple mark. In the adjustment procedure, the luminance could be adjusted brigther while occupied with the pseudo-text than with the fixation task. Additionally, participants rated glare lower in the category rating procedure when occupied with the pseudo-text than with the fixation task. This proved their hypothesis. Learning from this, it is reasonable to consider the cognitive level of the visual task for the experiment. Since it aims at measuring task performance, the visual task is required to be cognitively demanding (**C1**,**C8**).

That said, there are challenges with the pseudo-text task and category rating task they chose to use. For instance, in their literature review (Kent et al, 2018), the researchers mention a study showing that different response scales may lead to different outcomes. Though this multiple-criterion scale by Hopkinson is the foundation of the UGR model, it can be challenging to fully trust it in an experimental setting since individuals can interpret response scales differently. This means it is not guaranteed, that doing an experiment with two different response scales will produce the same result and that testing for preference is made more complicated (**C1**,**C8**).

4.8.2 Experimental bias

Kent et al. (2018) raise other issues in their literature review, referring to two studies by Logadóttir, Christoffersen, and Fotios (2011a) and Logadóttir et al. (2011b). These two studies brought interesting conclusions stimulus range and anchor bias. The first study is focused on using the adjustment task to set the preferred illuminance of a workplace environment and the second study is focused on using the adjustment task to set preferred colour of ambient illumination. The studies were about preference and not performance, but they are highly relevant in terms of experimental design (**C8**).

The first study by Logadóttir et al. (2011a) found that the experimental design influenced the results. The results (see Table 4) showed a centring bias, where the preferred illuminance tended to fall in the centre of the stimulus range. This was the stimulus bias (**C8**). In the experiment, they started the experiment at different initial illuminances, called anchors. Each adjustment range was tested with three different anchors. The first anchor was around 70 lux, the second around 50% on the control dial, and the third around 90%. This was to not give the 36 participants the impression, that decreasing was the only option. The results showed the higher the anchor, the higher the preferred illuminance. This was the anchor bias (**C8**).

Table 4: Illuminance adjustment study by Logadóttir et al. (2011a). The mean adjustment of the participants always ends up relatively close to the centre of range demonstrating a stimulus or centring bias. Unit = lux.

Adjustment range	Centre of range	Mean adjustment	Difference
21-482	251.5	337	85.5
38-906	472	523	51
72-1307	689.5	645	44.5

The second study by Logadóttir et al. (2011b) again found that experimental design influenced results. The results (see Table 5) once again showed a centring bias. The anchors used were the same as the other study, though they suggest a 50% anchor as the best alternative refering to Boyce. The results showed the higher, the anchor the higher the preferred CCT, proving again that also anchor bias was in effect. The second study also investigated the effect of the controls used for the adjustment task. They used two controllers. The first was an analog potentiometer with a 360° turn accounting for a full range with physical limits at both ends of the range. The second was a digital incremental encoder meaning it could be turned indefinitely but set to cover the full range in three full turns. The experiment would show if physical limits to the stimulus range controller and its increments had an effect. The results and statistical analysis did not show any effect though (**C8**).

Table 5: CCT adjustment study by Logadóttir et al. (2011b). The mean adjustment of the participants always ends up relatively close to the centre of range demonstrating a stimulus or centring bias. The is true for both controller types. The difference between mean adjustment and centre of range is written in parenthesis. Unit = kelvin.

Adjustment range	50% anchor	Centre of range	Analog controller	Digital controller
2,736-3,530	3,204	3,133	3,289 (156)	3,283 (150)
3,284-4,014	3,625	3,649	3,630 (19)	3,647 (2)
2,736-4,014	3,405	3,375	3,461 (30)	3,486 (111)

What can be concluded from both the studies by Kent et al. (2018) and Logadóttir et al. (2011a, 2011b) is that using participants to adjust to preferential light settings or rate light settings is very difficult to design experiments around. Individual and experimental bias have to be eliminated and this often takes multiple runs of the same experiment as well as different methods and procedures to verify each other. This can end up becoming a lengthy affair for each participant and make it difficult to attract participants in the first place. This project cannot offer any attractive compensation for the time spent by participants. Additionally, the Light Lab, the only truly qualified place for the experiment to take place, is under a tight booking schedule without the sufficient time to accomplish this. These conclusions encourage to use a simple method of measuring task performance since this would not include individual assessments introducing bias of the kinds just discussed (**C7**,**C8**).

4.9 The Stroop task

In a study by Rodriquez, Garretón, and Pattini (2016), they tried to measure the effect of glare from daylight, not strictly discomfort glare, on task performance on a computer screen. Their hypothesis was that glare will become a distraction affecting the performance in a task requiring attention, a cognitive task, much like the hypothesis of this experiment. They also hypothesise that people, who consider themselves glare-sensitive, will be more distracted by a glare source than people who consider themselves glare-insensitive. This is an interesting hypothesis and will be added to the experiment as research question eight (**RQ8**). The experimental setup of their study is not of the greatest interest to this project since involves daylight, but the visual task they chose to use is quite interesting. They chose the so-called Stroop task, an apparent "gold standard" of cognitive attentional measures in the words of the researchers. The Stroop task is a visual task where a word is presented on the screen in a certain colour which is either in congruent condition (matching the meaning of the word, e.g. blue presented as blue) or incongruent condition (not matching the meaning of the word, e.g. blue presented as green). When the participant is supposed to report the actual colour of the word as quick as possible, incongruent conditions usually results in a slower response time and more errors than congruent conditions. The difference in response time between congruent and incongruent conditions is called the Stroop interference and can be viewed as an indicator of selective attention. This type of visual task leaves out luminance adjustments and glare evaluations, which can introduce bias, and is a rather easy task to understand while being surprisingly difficult to get completely right. This seemed to be the right choice of visual task for the experiment of this project and the study by Rodriguez et al. (2016) provided a blueprint (**C1**).

Even though the use of the Stroop task led to inconclusive results regarding glare and performance in the study by Rodriguez et al. (2016), this type of visual task did not seem widely used lighting studies. The researchers had used an open-source software program called PsychoPy (Peirce, 2019) to run the Stroop task. It was developed by a researcher in neuroscientific methods for other researchers in the field to quickly be able to build behavioural science experiments and easily extract the necessary data.

The task for this experiment was designed basically the same way as the experiment by Rodriguez et al. (2016). A single word written with capital letters (RED, GREEN or BLUE) with the Arial font (a letter being 20(H)x10(W) mm, 0.1 in PsychoPy) would be presented in the centre of the computer screen in either congruent or incongruent condition. The participant then have to report the actual colour and try to ignore the meaning of the word by pressing the arrow keys on a keyboard. The arrows would have coloured squares of tape on top for guidance (left = red, down = green, right = blue). Once a key had been pressed the program would store the response time and present the next word. This would go on until a certain number of words had been reported, which would make up a round. The words would be presented in random order from round to round. One round was needed for each of the seven glare sources, which was called a run. To avoid a single bad round to have too much impact on the result, it was decided to have two runs for each participant which made 14 rounds of Stroop tasks. The mean reaction times for each glare source could then be calculated based on the two rounds per source. It would be manually ensured that a glare source in the second run would not be turned on in the same order as the first run. Generally the last sources in the first run would be earlier in the second run, to avoid an experimental bias where focus might drop when doing 7 rounds in a row (**C8**). In order to reveal an influence the task performance, two benchmark rounds were introduced at the beginning of the experiment, totalling 16 rounds of Stroop tasks. A short introduction of the experiment and a questionnaire before the rounds would help gather relevant information for analysis as well as provide a little adaption time from daylight to the dimmer Light Lab (**C7**). A quick break was also introduced in between the two runs to prevent fatigue (**C8**). As mentioned before, focus was put on keeping the duration of the experiment relatively short to make it more attractive to participate. The total duration was set to be about 30 minutes, a realistic compromise between achieving accuracy and not be too time consuming for participant to partake in (**C7**).

4.10 Participants

A poster was produced to attract participants to the experiment on the university campus as well as digitally on Facebook, among friends, and LinkedIn, among professional connections. It was attempted to appeal to an experience most people know of, working on their computer while being subjected to annoying glare. Images of an annoyed worker and an early 3D model design were used to grab attention. Cake was offered as compensation, since nothing else would be possible. The poster can be found in annex C. 19 participants were gathered in total.

4.11 Pilot experiments

The days leading up to the start of the experiments had been stressful and brought illness. This resulted in the 1/9 days booked for testing being used to make the last hasty preparations. When measuring the glare source luminance, it showed the centre source was different than the six side sources. A separate CC regulator was installed on this to be able to adjust it by itself, in order to make the sources as similar as possible (**C5**). It was suspected that since the centre box had been the testing box, it was built with more attention to detail when installing the LEDs and distributing the light better outwards. Despite all the considerations and precautions in the process, it proved to be a challenge to get all sources to have equal output of 10,000 cd/m^2 (**C5**).

It was decided to use the first two participants scheduled on day 2 of 9 to become pilot studies in order to get the other 17 participants right. Initially the word count for each round was set to 30, which was deemed too few. The experiments were much shorter than 30 minutes and the participants made only one and two errors over the total 16 Stroop tasks respectively. The word count was increased to 78 per round, as a short test showed this would make the experiment run about 30 minutes. It was expected that stressing the participants with more words would increase the error rates and put more strain on their selective attention in the cognitive visual task (**C1**).

4.12 Challenges

On test day 3 and 4, the PsychoPy Stroop task program would not run the test on the laptop computer. This was a very critical moment for this to happen. The developers are running a forum for the community behind to help each other and for the developers to be informed of bugs and the issue was posted there in hope of assistance (*Nothing but background...*, 2019). They tried to help, but due to the critical timing it was not solved until the 5th test day, where a large stationary PC was tested and transported to campus. None had been scheduled on the lost days, but they were supposed to be used to recruit participants on campus. The experiment went as it was planned from this point through day 5 to 9 of 9 when it was ended. It was not possible to extent the experiment or assemble it for another period later since the Light Lab schedule was completely booked.

5. Analysis

In order to compare the results with the study by Rodriguez et al. (2016) to see if they were reasonable, the data had to be organised and analysed accordingly. The results would be compared to the results of their diffuse daylight scenario. Results were split into participants who had reported themselves as being glare sensitive and those who had reported themselves as being glare insensitive. To be able to compare the results, a mean response time, mean error rate, and Stroop interference for each glare source had to be calculated for each of the two groups. The standard deviation (SD) would also be calculated to analyse the distribution of the data, but it was found that the coefficient of variation (CV) would be easier to use. The data would also be tested with a Shapiro-Wilk normality test, as Rodriguez et al. (2016) did, to find out whether the data was normally distributed.

5.1 Response time (RT)

[1] Only the RT for correct answers were used, since it was considered that participants can have a quick response time while providing a wrong answer. This is dubbed the trigger-finger effect onwards. This will prevent quick, wrong answers from skewing the results, in line with other studies using the Stroop task in lighting experiments such as Moum and Högman (2015). [2] For each participant, a mean RT between the two runs of Stroop tasks (14

rounds) was calculated per glare source. [3] A mean RT for all participants was then calculated for each glare source using the results from [2]. A diagram of the mean RT for glare sensitives in incongruent and congruent conditions for each glare source can be found in Figure D3 (annex D). The same type of diagram can be found for glare insensitives in Figure D4 (annex D). In each diagram, the results from the study by Rodriguez et al. (2016) are marked by a horizontal line. The blue colour represents incongruent conditions and the green colour represents congruent conditions. A bright version of the colour represents glare sensitives, while a darker version represents glare insensitives. A comparison diagram of the mean RT from Figure D3 and Figure D4 can be found in Figure D5 (annex D) with same colour coding. Incongruent conditions and congruent conditions are here grouped for each glare source for easier comparison.

5.2 Number of errors and error rate (ER)

While errors are sorted out of the data set for RT, number of errors are a different but equally interesting measure of performance. This is in line with both the study by Rodriguez et al. (2016) and Moum and Högman (2015). Although is it not stated if Rodriguez et al. (2016) sorted out the errors when analysing the RT, they also did the analysis of number of errors. [1] The total number of errors each participant made in both runs (14 rounds) was calculated for each glare source. Through two runs a glare source had two rounds and a total of 156 words. [2] Using the results from [1], a mean number of errors for all participants was then calculated for each glare source. [3] The mean number of errors for each glare source could then be turned into an error rate (ER) measured in percentage. A diagram of the mean ER for glare sensitives in incongruent and congruent conditions for each glare source can be found in Figure D6 (annex D). The same type of diagram can be found for glare insensitives in Figure D7 (annex D). As with the RT, each diagram is marked by a horizontal line showing the results from the study by Rodriguez et al. (2016). The colour coding is also matching the logic of the RT diagrams. A comparison diagram of the mean ER from Figure D6 and Figure D7 can be found in Figure D8 (annex D). Incongruent conditions and congruent conditions are grouped for each glare source for easier comparison.

5.3 Stroop interference (SI)

Stroop interference (SI) is the difference between incongruent conditions (word not matching colour) and congruent conditions (word matching colour). This can be calculated for both reaction time (RT) and number of errors.

Finding the SI for RT starts after [2], where the individual means for each glare source has been calculated. [3] The difference between the individual mean RTs for incongruent and congruent conditions are calculated for each source. [4] From the results of [3] a mean SI for each glare source can then be calculated.

Finding the SI for ER starts after [3], where the individual mean number of errors per glare source has been calculated. [4] The difference between the individual mean ER for incongruent and congruent conditions are calculated for each source. [4] From the results of [3] a mean SI for each glare source can then be calculated.

In Figure D1 (annex D) the mean SI for RT is presented for glare sensitives (blue) and glare insentitives (orange). In Figure D2 (annex D) the mean SI for RT is presented for glare sensitives (blue) and glare insentitives (orange). Two horizontal lines represents the results for diffuse daylight obtained in the study by Rodriguez et al (2016) in each diagram in similar colours.

5.4 Sample Standard Deviation (SSD)

The standard deviation (SD) is a measure of how the data is spread compared to the mean of the data set (*Describing Variability*, 2019). Specifically, it is the average difference between the values of the data set and the mean. A small standard deviation signifies that the data is spread closer to the mean while a large standard deviation signifies a larger spread. It is normal to present the SD when presenting means and it can inform about how similar observations were. In this analysis, it will be used to compare data sets with Rodriguez et al. (2016) without having access to their data set. In their study, they do not clarify which type of standard deviation they calculate, but it is assumed to be the Sample Standard Deviation (SSD), since no population mean is presented, normally used in a Population Standard Deviation (PSD) calculation. The SSD can be calculated with the following formula [3]:

$$s = \sqrt{\frac{\sum(X - \bar{X})^2}{n - 1}} \quad \textbf{(21)}$$

where
X is the observation
$\overline{X}$ is the mean value of all n observations
n is the number of observations

5.5 Coefficient of Variation (CV)

The coefficient of variation is another measure of the spread of the data and is simply a ratio between the standard deviation and the mean value of the observations. It makes it easier to assess the mean and the standard deviation simultaneously with one value. Since the experiment is not following the methods by Rodriguez et al. (2016) to full extent it is more suitable to use a ratio for comparison. A low CV indicates the data is situated close to the mean while a high CV shows a larger deviations from the mean.

$$CV[\%] = \frac{SD}{\overline{X}} \cdot 100 \quad (22)$$

where
SD is the standard deviation
$\overline{X}$ is the mean value of all observations

6. Results

6.1 Questionnaire

The experiment had 19 participants in total. 2 participants were used for pilot studies. 1 participant misunderstood the instructions and reported the word instead of the colour and this data was left out of the analysis, leaving data from 16 participants to be analysed. Of the 16 participants, there were 12 male and 4 females of age 23 to 57, an average age of 28.9. Age 57 was an outlier in the data, and if that was sorted out hypothetically, the average age would drop to 27.1. Nationalities varied from Danish (n=12), Hungarian (n=1), Italian (n=1), Indian (n=1), and a multinational German/Swedish living in Denmark (n=1).

6 participants reported to be working professionally with light while 10 did not. 4 participants reported themselves as being glare-sensitive with a simple "Yes" while 10 reported as being glare-insensitive with a simple "No" (7 males, 3 females). One reported as "observant" and one reported "Yes, the sun can annoy me. Cold light can give me a headache." Both were included in the glare-sensitive group, resulting in 6 participants (5 males, 1 female). 3 participants wore glasses, 1 wore lenses and 12 did not use any eye correction. 13 participants report no other issues with eyesight. One reported to be left eye dominant because of a weak right eye but did not wear any correction anymore. One reported seeing correct colours but having focusing issues when green and red stand side-by-side, not an issue in this experiment although the colours might appear quickly after one another. One reported normal eyesight on the left eye while right eye is corresponding to +6 but did not use any correction. When asked how energized they felt on a scale from 1 (tired) to 5 (fresh), 5 participants answered "5", 6 answered "4", 4 answered "3", 1 answered "2" and 0 answered "1".

6.2 Stroop task

Reviewing the results of the Stroop tasks from a general perspective first, combining the results for all 16 participants and all 7 glare sources, the mean response time (RT) for both congruent and incongruent conditions was in the range of 0.378 s to 0.832 s. Separating them into conditions, the mean RT for incongruent conditions was 0.583 s and 0.568 s for congruent conditions resulting in a Stroop interference (SI) of 0.034 s. In comparison, Rodriguez et al. (2016) found a mean RT of 0.949 s for incongruent conditions, 0.869 s for congruent conditions, resulting in a SI of 0.080 s. The results more or less agree with each other although in an offset manner. The incongruent conditions had a slightly slower RT and the SI created by the Stroop task is proved the effect to be true, though the effect is larger with some glare sources than others. Interestingly, the mean error rate (ER) did not reflect this as participants generally made fewer errors in incongruent conditions (1.29%) than congruent conditions (1.48%).

Separating the results into the glare-sensitive and glare-insensitive groups, it was found that glare sensitives (n=6) had a mean RT of 0.682 s in incongruent conditions, 0.653 s in congruent conditions, resulting in a SI of 0.034 s. In comparison, glare insensitives (n=10) had a mean RT of 0.523 s in incongruent conditions, 0.517 s in congruent conditions, resulting in a SI of 0.024 s. Generally, the glare sensitives had a longer RT for all glare sources than the glare insensitives, on average 0.118-0.180 s longer for incongruent conditions, 0.123-0.159 s for congruent conditions, resulting in 0.009-0.040 s longer SI. This consistency can also be deduced from Figure D5 (annex D). Rodriguez et al. (2016) had the same findings with an mean RT of 0.183 s longer for incongruent conditions, 0.165 s longer for congruent conditions, resulting in a 0.017 s longer SI. The results once again agree with each other, but the sample size of the experiment was unbalanced between the two groups and half the size compared to Rodriguez et al. (2016). This suggests an answer to **RQ8**, that individuals who are self-perceived glare-sensitive are more impaired by discomfort glare than individuals who are self-perceived glare-insensitive.

When separated into the two groups, the mean ER differs. The glare sensitive made more errors in incongruent conditions (1.36%) and fewer errors in congruent conditions (1.14%). This was reversed in the case of the glare insensitive, as they made fewer errors in incongruent conditions (1.25%) and more errors in congruent conditions (1.68%). Figure D8 (annex D) also demonstrates this. Once again, the ER fails to definitively cooperate with the results of RT.

Finally, separating the results further into both groups and individual glare sources might reveal which position influence the task performance the most as **RQ7** asks. First, comparing the mean RT of each glare source for incongruent conditions to Rodriguez et al. (2016), the participants in this experiment were on average 0.358 s quicker for glare sensitives and 0.334 s quicker for glare insensitives. For congruent conditions, the participants were on average 0.298 s quicker for glare insensitives and 0.269 s quicker for glare insensitives. This of course suggests the same answer to **RQ8** as before, but also show that the participants generally were quicker than those who participated in the study by Rodriguez et al. (2016). There is no such definitive result in comparison of the error rates as can be deduced from Figure D8 (annex D) Error rates will not be reviewed any further in results.

Second, assessing the mean SI is the best way to measure a difference in performance between the individual glare sources. In Figure D1 (annex D), the mean SI can be interpreted between the two groups. It is clearly shown that the benchmark is the tallest of the bars in the chart both in RT and SI. This defeats the purpose of the benchmark as it was expected either to have a quicker RT and smaller SI than when a glare source in view, or at least have a similar RT and SI to show the glare sources made no difference. It was the tool to provide an answer to **RQ6**, asking whether discomfort glare influence task performance or not. This will be discussed later, and the benchmark will not be reviewed any further in the results.

Assessing the individual glare sources and the mean SI for glare sensitives (see Table 6), two sources stand out with have a maximum SI above 0.060 (right top at 0.064s and left middle at 0.060 s). For glare insensitives, the maximum SI of 0.031 s is shared between two sources (left bottom and centre both at 0.031 s). These values are both lower maximum values than Rodriguez et al. (2016) reported.

Table 6: Stroop interference between self-reported glare sensitives and self-reported glare insensitives. Red colour marks the two maximum Stroop interference values for each group.

	Glare sensitives		Glare insensitives	
	Mean Stroop interference (s)	Rank (#)	Mean Stroop interference (s)	Rank (#)
Benchmark	0.070	-	0.056	-
Left bottom	0.047	4/5	**0.031**	**1/2**
Left middle	**0.060**	**2**	0.023	4
Left Top	0.043	6	0.020	6
Centre	0.041	7	**0.031**	**1/2**
Right top	**0.064**	**1**	0.024	3
Right middle	0.048	3	0.016	7
Right bottom	0.047	4/5	0.022	5
Glare source mean	0.050	-	0.024	-
Rodriguez et al.	0.088	-	0.071	-

The benchmark mean RT has the maximum deviation from the mean for all the glare sources in both congruent and incongruent conditions for both groups (0.020 s for glare sensitives and 0.032 s for glare insensitives). Again, this becomes an issue when trying to answer **RQ6**. An answer to **RQ7**, where in the visual field discomfort glare influences task performance the most, is also uncertain. A difference between the groups can be measured, but the groups do not agree on which glare source creates a longer SI. It could be speculated that glare sources in the upper visual field influences task performance the most, since 3/4 of the maximum SI is measured there (right top, centre and left middle), but that is, admittedly, a far stretch. It is unlikely this result can be interpreted as other than the Stroop interference in effect.

6.3 Deviation from mean

Coefficient of Variation (CV) values for both glare sensitives and glare insensitives are within the range of 8-12% for congruent conditions (see Table 7). For incongruent conditions glare sensitives have a CV range of 8-11% while glare insensitives have a CV range of 10-15% (see Table 8). These are reasonably low CV values indicating that the participants reacted similarly with no distinct outliers in the data set. The glare insensitives have a little more variation in both conditions, but their sample size was 2.5 time larger, which probably is the reason. The results reported by Rodriguez et al. (2016) can calculated to a CV of 37-38% or glare sensitives and 17-18% for glare insensitives in both conditions. A CV of 37-38% is rather high, indicating more variation in the observations. This experiment had half the sample size, 16 participants compared to 32 in the study by Rodriguez et al. (2016), and it could be speculated that more participants will show more variation.

Table 7: Response time for congruent conditions along with sample standard deviation (SSD) and coefficient of variation (CV).

Congruent response time						
	Glare sensitives			Glare insensitives		
	Mean (s)	SSD	CV (%)	Mean (s)	SSD	CV (%)
Benchmark	0.723	0.089	12	0.545	0.068	12
Left bottom	0.676	0.059	9	0.517	0.051	10
Left middle	0.639	0.058	9	0.511	0.056	11
Left Top	0.640	0.038	6	0.510	0.048	9
Centre	0.665	0.066	10	0.522	0.059	11
Right top	0.663	0.062	9	0.526	0.048	9
Right middle	0.638	0.049	8	0.516	0.055	11
Right bottom	0.648	0.056	9	0.519	0.061	12
Rodriguez et al.	0.951	0.356	37	0.786	0.135	17

Table 8: Response time for incongruent conditions along with sample standard deviation (SSD) and coefficient of variation (CV).

Incongruent response time						
	Glare sensitives			Glare insensitives		
	Mean (s)	SSD	CV (%)	Mean (s)	SSD	CV (%)
Benchmark	0.783	0.094	12	0.601	0.094	16
Left bottom	0.709	0.063	9	0.529	0.080	15
Left middle	0.675	0.059	9	0.516	0.061	12
Left Top	0.683	0.041	6	0.520	0.066	13
Centre	0.699	0.047	7	0.527	0.074	14
Right top	0.653	0.051	8	0.534	0.062	12
Right middle	0.662	0.068	10	0.510	0.068	13
Right bottom	0.695	0.075	11	0.522	0.051	10
Rodriguez et al.	1.04	0.336	32	0.857	0.151	18

7. Discussion

Researching, designing, building, and performing the experiment as well as reviewing the results and post-researching it has brought revealed different issue to discuss. In order to validate or dismiss the results and experimental method, and suggest improvements in future studies on the subject, a critical review and discussion must take place.

7.1 Unbalanced lighting

The general lighting in the Light Lab was uneven due to limited access to suitable lighting fixtures. Under the circumstances, it was as good as it got. An important design element, as design criterion **C2** stated, was to have a uniform surface in the visual field, applying to both surface material, colour and light. This required mostly the screen wall to be uniformly lit, as well as the small part of the room side walls visible, to be as similar as possible. From the measurements it got close, but distribution could have been made more even throughout the room. With access to more and better fixtures, this could have been possible. It is not speculated to have had any special impact on the results, although it did not fully represent practical office lighting. Many other factors might have had a larger impact.

It was also a design criterion for the experimental setup to have equal luminance for all glare sources, but this proved difficult to achieve due to time pressure. Steps was skipped in the installation process of the LED-strips and resulted in some differences in luminance output as reported. It is a variable that should have been fixed within a certain range, which would be a goal for future experiments. It is not speculated to have any influence on the results since the luminance generally was close to the goal of 10,000 cd/m^2.

7.2 Misplacement of glare sources

An error occurred in the design phase of the experimental setup which led to the two top side glare sources being placed at 70° angular distance instead of 60° (see Figure 41). This meant they did not follow third BCD curve as mapped by Kim and Kim (2010b, 2010c) and were closer to the fourth BCD curve, meaning the luminance of 10,000 cd/m^2 (III) should have been closer to 30,000 cd/m^2 (IV) to provoke a sensation of discomfort. The misplacement is unfortunate since it makes it challenging to compare results. Despite this, the results do not seem to reflect the error since the right top glare

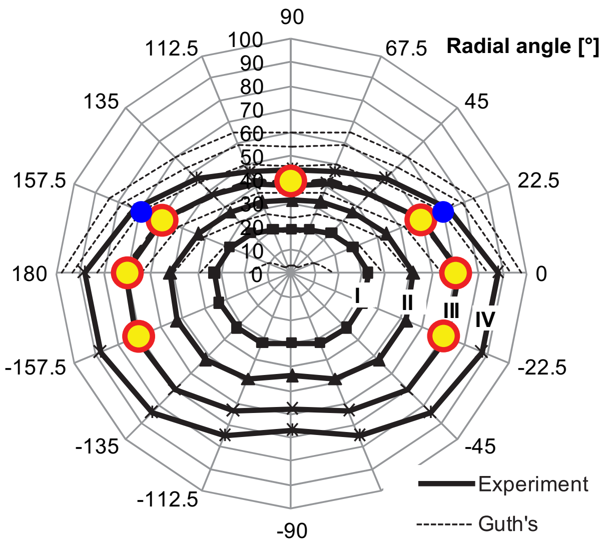

Figure 41: Glare source positions marked on the polar coordinate diagram from Figure 21. The blue spots marks the constructed position, indicating the error.

source had the largest Stroop interference (0.064) for glare sensitives and the third largest for glare insensitives (0.024). The left top glare source was ranked sixth in both groups (0.043 and 0.020 respectively). It could also be argued that since the head was not in a fixed position with a chin rest, how accurate would all this attention to detail be anyway? A fixed head position would be ideal, but it can become uncomfortable with time, so in this particular experiment the experimenter would observe the participants initial position and comment to place the head in a certain area. This was considered to be sufficient in this case.

7.3 Manual on/off order

While the participants were doing the Stroop tasks, the experimenter would control the on/off order of the glare sources behind the wall with manual toggle switches. The order of the first round was noted and attempted to be reversed in the second run to make sure a glare source would not end up in the same place in the order to account for participant fatigue. A few times this was noticed to occur anyway during the experiment and was always too late to correct. When counted during the analysis, 8 of 16 experiments each had one of this type 1 of error (participant #3, #4, #5, #8, #9, #10, #11 and #13).

Ideally, glare sources would not even be close in the order, such as number 5 in the first run and number 6 in the second run. This type 2 error occurred 36 times on 14 of 16 experiments (participant #3, #5, #6, #7, #8, #9, #10, #11, #12, #13, #14, #15, #16 and #19). 5 experiments had 1 type 2 error (participant #6, #0, #13, #16 and #19), 3 had 2 errors (participant #5, #8 and #9), 1 had 3 errors (participant #15), 4 had 4 errors (participant #3, #11, #12 and #14) and 1 had 6 errors (participant #7).

The ideal order of both runs was achieved with participant #18 where every glare source had at least a difference of 3 places in order between first and second run. This order is advised to use for every participant either manually, automatically or semi-automatically in similar experiments to achieve the best balance and avoid any potential experimental bias. See the order in annex E.

7.4 Benchmark tests

One of the bigger issues with verifying a potential measurable influence from discomfort glare on task performance has been the benchmark test carried out as the two first rounds before the two runs begin. The benchmark mean response time (RT) turned out to be slower than with any of the glare sources. This was unexpected as it was thought to have been either closer to the mean, to show no influence of the glare sources, or be quicker, indicating an influence. The fact that it was the slowest made it impossible to verify an influence and provide and answer to **RQ6**. It is speculated that since they were the first two rounds, they ended up as training rounds. It was thought that only the first round might show as training and the second round could be used in that case, but generally both rounds had slower performance.

It had also been considered to send a link to the participants to introduce them to an online concept test for them to try it, but that would give an unfair advantage to the participants who were not scheduled. To correct this in the future, it is suggested to introduce specific training rounds at the beginning of the experiment and then have a benchmark round at the start of each run, increasing the number of rounds from seven to eight per run, if not even more benchmark rounds are needed. The benchmark rounds could also just be mixed up in the order, providing no order advantage. This way participants can train first and the benchmark rounds gets treated the same way as the glare sources.

7.5 Unbalanced Stroop task

The Stroop task ended up having an unbalanced word and colour count, meaning some words and colours appeared more often than others. Of the 78 words per round, 39 would be “RED”, 26 would be “GREEN” and 13 would be “BLUE”. Of the 78 words, 13 would be written in red colour, 26 in green colour, and 39 in blue colour, showing the opposite balance of the word count. This imbalance was pointed out afterwards by several participants to hear if their eyes or mind was deceiving them. The number of congruent and incongruent pairs was balanced 50-50 with 39 of each pair. The error is a result of much time being allocated to build the experimental setup and too little getting to know and test the PsychoPy program. The error is based on the excel rows and columns PsychoPy reads as conditions to randomise in the test (see Figure 42). A column contained words and another the colours. The six different combinations were written and without giving it much thought all the combinations with the word “RED” was written first resulting in the colour red only appearing in the congruent condition. The green colour would only appear with the words “RED” and “GREEN”, and the blue colour appeared for all words. This unbalance is very likely to have influenced the number and types of errors. Most of the errors made are with reporting not matching either word or colour, and blue and green colours are generally the ones reported (see Table 9). Errors made in congruent and incongruent conditions are reasonably close with 263 (54%) and 227 (46%) errors respectively (16.4 and 14.2 errors on average). Errors where the response did not match the word accounted for 89 errors (18%, average 5.6 errors) while responses not matching either word or colour accounted for 401 errors (82%, average 25.1 errors). This might explain the surprising result of more errors made in congruent conditions when the opposite would be expected.

	A	B	C	D
1	Word	Colour	Congruent	Correct
2	RED	RED	1	left
3	RED	GREEN	0	down
4	RED	BLUE	0	right
5	GREEN	GREEN	1	down
6	GREEN	BLUE	0	right
7	BLUE	BLUE	1	right

Figure 42: Conditions used in PsychoPy.

Table 9: Analysis of types of wrong answers in the Stroop tasks.

	Wrong answers	Not matching word	Not matching word or colour	Congruent condition errors	Incongruent condition errors
Total (n = 16)	490	89	401	263	227
Mean	30.6	5.6	25.1	16.4	14.2

This result is speculated to be a product of the imbalance in the Stroop task, because participants realise some colours appear more often, they are more ready to report them. This has been dubbed the trigger-finger effect. To avoid this in the future, it is important to make sure the conditions excel sheet read by PsychoPy has equal representation in both columns.

7.6 Stroop task design

In this experiment, the word count was set to 78 words per round amounting to 156 words per glare source in order to achieve a total duration of 30 minutes. In other studies where the Stroop task has been used to test lighting, the word count seems to be lower, but the amount of repetitions is increased. In the study by Rodriguez et al. (2016) the word count is not mentioned specifically but they report "four blocks of 12 repetitions" for training and "eight blocks of 12 repetitions" for the test, where a block is thought to be equal to a run and repetitions equal to word count. This is equal to a word count of 48 words in training and 96 words in the actual experiment. If that is interpreted correctly, 156 words is reasonable compared to 96 words. It could be interesting to see if a smaller word count with more runs would have an effect, the pilot studies did not turn out much different in terms of response time, only in error rate, and they had only 60 words per glare source. A study by Moum and Högman (2015) used "48 trials" in two tests with different lighting, which is interpreted as 48 words per test. If interpreted correctly, this would mean that a bad run would influence the results, which is why this experiment has two runs with a mean response time derived from both.

After doing post-analysis research on the Stroop task, it is made clear that the task itself is not yet a clearly defined method. In a study by Salo and Robertson (2001), they set out to compare the classic clinical Stroop task, presented on sheets, and the modern version, presented on a computer. The classic version consisted of one sheet with words presented in incongruent colour conditions and another sheet with word presented in neutral black colour. Each sheet would have a matrix of words and the participant would have to read them out loud. It would only be possible to measure the time for the whole sheet and not for individual words. The Stroop interference (SI) would be calculated as the difference in response time between the two sheets. On a modern version of the Stroop task, the words are presented one by one, randomised, in the middle of a screen with the possibility of measuring response time (RT) for the individual words. With the rise of the modern version, studies had difficulties reaching the same conclusions as the classic version, and the research team wanted to test the variables.

In their first experiment, they tested whether differences could be measured between a computerized classic test with word matrix presentation in coloured stimuli blocks and neutral stimuli blocks (groups), a randomised test with single word presentation and a grouped test. In their second experiment, they tested different types of grouped neutral stimuli written either as similar nonword strings (XXX), dissimilar nonword strings (XXX, SSS, MMM) and as animal names (dog, bear, tiger). In their third experiment, they tested the influence of position shifting of the presented word where single random and single grouped words shifted location diagonally from word to word. Comparing the mean RT between all eight experiments, congruent conditions had a range of 0.473 – 0.601 s, neutral stimuli conditions a range of 0.491 – 0.659 s and incongruent conditions a range of 0.680 – 0.752 s. This resulted in a difference of 0.128 s, 0.166 s and 0.072 s respectively with the neutral stimuli condition showing the largest difference. The researchers concluded that the method and selection of neutral stimuli had an influence on the evaluation of performance. The neutral stimuli benchmark value is what the other RTs are compared to and the Stroop interference is calculated from. If it is unreliable then how can the test be trusted. They could not conclude anything on the location shifting tests. See annex F for an overview of their results.

Firstly, this study (Salo and Robertson, 2001) provides other response times to compare results to. The results of this experiment are in the exact same range as the results by Salo and Robertson (2001). It may be safe to conclude that discomfort glare is not causing an impairment of task performance no matter the position, answering both **RQ6** and **RQ7**. It might also question whether the Stroop interference is real or just a product of the design of the Stroop task. It might even question whether the Stroop task is suitable to measure performance in a lighting scenario, when psychology researchers are having difficulties quantifying and verifying their results. To answer the second part of **RQ6**, the Stroop task might not be suitable to measure influence from discomfort glare on task performance. Despite this, it is interesting that a difference between self-perceived glare sensitives and glare insensitives can still be measured, but a definitive answer to **RQ8** is difficult to provide.

Secondly, to obtain additional benchmark values for a future test, it would be advised to introduce neutral rounds as well, although which design to chose is unclear and would require additional literature reviewing. A neutral Stroop benchmark value would help verifying that the Stroop interference is in fact occurring, besides comparing RT of congruent and incongruent conditions of the same type of stimuli. Of course, this would have to be implemented in all rounds, benchmark rounds and in rounds with an active glare source. In the analysis, the inactive glare source benchmark value can be compared to rounds with an active glare source to establish whether discomfort glare has an influence on task performance.

A recent review by Scarpina and Tagini (2017) has called for more standardisation of Stroop colour and word tests and the scoring methods used to calculate results. Even if the test itself is the same, some studies might use different scoring methods, making it difficult to compare or can balance the factors wrong.

Designing a Stroop task is not a straightforward task it appears and might require more research and development before it can be applied to experiments testing for influence of an external stimuli besides the Stroop task itself.

8. Lighting Design Guidelines

Based on the knowledge gained through the literature review and personal experience during internship and student job, a few measures will be defined on how to avoid discomfort glare in projects.

8.1 Revised regulation

Europe revised its daylight standard in 2018 (DS/EN 17037:2018, Danish Standard, 2018) and has been in the process of revising the 12464-1 standard for indoor work space lighting for quite a while. The revision is entering a public hearing period from July 18th to September 17th where comments and concerns can be submitted. The suggested revision is highly relevant to discuss, since this is what to be expected of future lighting design in offices.

- Task area and immediate area are now specified in a horizontal, inclined and vertical position with background area still defined as being on the floor. This is interesting considering screens either functions as a inclined or vertical area combined with a horisontal desk area. If this applies to screens, it is uncertain if the immediate area (0.5 m wide band) should be regulated to 300 lux in a simulation whether a surface is present or not.
- The standard now refers to the 17037 standard to asses glare from windows.
- The UGR is now called R_{UGL} for Unified Glare Rating Limit. The values in tables in Clause 6 are based on the UGR tabular method and is stated cannot be applied to other uses of the UGR formula
- A short guideline on the considerations for the tabular method is now provided in the new annex B for both standard and non-standard situations, but the luminaire manufacturer must produce the UGR table. Without any third-party authentication organisation these tables might be still be falsified by unethical manufacturers. It is still important to experience the luminaire in person.
- A note is now included, stating that glare caused by daylight is different than from artificial sources regarding sizes of glare sources, complex luminance distributions and user acceptance. This is the same reason daylight glare was mostly left out of this thesis.

- A note states the R_{UGL} values are representing a likelihood of discomfort glare from low to high: 16, 19, 22, 25, and 28.
- A new definition for shielding against glare is presented for luminaires with optics in front instead of a direct view to the light source. A certain gamma-angle range (γ) defines the threshold for the luminaire luminance as the alpha-angle still does for direct view luminaires. This is welcome, since most modern luminaires uses optics.
- The section about flicker and stroboscopic effects has been updated. The phenomenon is called temporal lighting artefacts (TLA) relating to fluctuations in luminance close to the temporal threshold as previously described. The standard now refers to the testing methods and recommended limits found in the standards IEC TR 61547-1 and EN 61000-3-3. Apparently, they chose not to include the IEEE 1789-2015 standard discussed in this report. It is possibly mostly directed towards driver manufacturers.
- Clause 5 is now dedicated to lighting design considerations with recommendations for illuminance requirements, operation of lighting systems, energy efficiency, and variability of light. This section is a making it easier to understand and implement the standard by providing step-by-step guidelines on what to do and where to look. It puts in writing many of the important aspects of the user interaction with the visual environment to be considered except for just values in a table.
- Clause 6 includes all the table values for each scenario as the old standard but adds additional requirements for easy overview (see Figure 43). Boyce and Wilkins(2018) pointed out the absence of a maximum limit to illuminance and this is included. It is also positive that illuminance on walls and ceilings has gotten more attention.
- A new annex C informs about visual and non-visual effects of light. In part, this annex focuses on the visual environment and how the lighting of walls and ceiling influence users.

It is very positive to see more requirements specifically outlined and additional focus on the visual environment as a whole. Even though it is a little disappointing that discomfort glare is still based on the tabular method of UGR, but there is just not enough evidence that anything works better at the moment. It could be argued that knowledge and experience is the best way avoid glare in a project by knowing the luminaire and how to implement it.

Ref. no.	Type of task/activity area	$\bar{E}_{m,r}$ lx	$\bar{E}_{m,u}$ lx	U_o	R_a	R_{UGL}	$\bar{E}_z$ lx	$\bar{E}_{m,wall}$ lx	$\bar{E}_{m,ceiling}$ lx	Specific requirements
6.26.1	Filing, copying, etc.	300	500	0,40	80	19	100	100	75	
6.26.2	Writing, typing, reading, data processing	500	1 000	0,60	80	19	150	150	100	DSE-work, see 4.9. see 5.7 room brightness
6.26.3	Technical drawing	750	1 500	0,70	80	16	150	150	100	DSE-work, see 4.9. see 5.7 room brightness
6.26.4	CAD work stations	500	1 000	0,60	80	19	150	150	100	DSE-work, see 4.9.
6.26.5.1	Conference and meeting rooms	500	1 000	0,60	80	19	150	150	100	Lighting should be controllable.
6.26.5.2	Conference table	500	1 000	0,60	80	19	150	150	100	Lighting should be controllable.
6.26.6	Reception desk	300	750	0,60	80	22	100	100	75	
6.26.7	Archiving	200	300	0,40	80	25	75	75	50	

Figure 43: Office lighting regulation from the DS/EN 12464-1 revision (public hearing version). $E_{m,r}$ = min. maintained illuminance. $E_{m,u}$ = upper maintained illuminance. U_0 = min. uniformity. R_a = min. colour rendering index. R_{UGL} = max. UGR limit. E_z = min. cylindrical illuminance. $E_{m,wall}$ = min. average illuminance on walls. $E_{m,ceiling}$ = min. average illuminance on ceilings.

8.2 The visual environment

Boyce and Wilkins states: "*Lighting needs to be considered in relation to the visual environment in order to predict discomfort. Different groups of people take responsibility for décor and there can be little communication between them*" (Boyce and Wilkins, 2018, p. 109). From personal experience, this seem true like a true statement to some extend. Architects, interior designers and lighting designers might sit in their separate departments rather than a complete team in one place. There are probably fewer interior designers and lighting designers than architects since the play a consulting role, so it makes sense for them to be separated.

The trouble is that the project team might make a change directly influencing the lighting design and its ability to meet regulation without consulting the lighting designer. This can happen due to strict deadlines, outside influence such as consulting engineers or just be forgotten. To improve on this, it is important that architects and interior designers get a better sense of what in the visual environment requires the attention lighting designers.

Surfaces are what makes up the boundaries of the visual environment. They can shield be simple obstruction and reflect light in different ways depending on texture, colour and glossiness (specular reflection). This gives surfaces an enormous power over how light distributes in a space. Surfaces both makes up the exterior shell (walls, floors, ceiling and windows), shielding from the outside environment, and interior utilities (tables, cabinets, screens etc.). Architects and interior designers are usually in charge of selecting the surface materials (defining the texture), surface treatment (defining the colour and glossiness) and utilities (tables, screens, additional décor). If a space get glass meeting walls installed, the paint on walls changes dramatically, floors get glossy finish etc. then the lighting designer is required to be in the loop of information and/or at meetings about this.

Geometric changes to a space can also be of concern for the lighting designer. If the ceiling height is changed due engineering requirements light sources might change their vertical position and decrease their ability to illuminate the floor or tables properly or put them in the visual field of a user somewhere. If the ceiling changes layout the light sources might be spread to far out and risk the same issues as a ceiling height change. Increasing the length and width of a space without considering the ceiling layout and light sources can lower the average illuminance of the space thereby changing the uniformity and contrast.

These are just examples of changes that might occur on the design phase of a project and how it can affect the lighting. The important lesson to learn from this is surfaces and space geometry highly influence lighting distribution and contrast.

In the literature review it was learned how the visual system adapts to the visual environment in terms of luminance and contrast. The revision of the 12464-1 standard puts more focus on this as well by implementing a range for illuminance (min. and upper maintained illuminance) and min. illuminance for walls and ceilings for each work scenario.

8.3 Digital analysis

Lighting design simulations in modern projects is usually performed in DIALux and it is reasonably competent at it. From personal experience though, it seems to lack a certain level modelling freedom and user customisation found in recent years with daylight analysis and the rise of Ladybug Tools.

Ladybug, Honeybee and the rest of the suite of free software programs has revolutionised the way engineers and architects do environmental building design. They build on several free and open-source analysis engines, most notably for lighting, the Radiance ray-tracing engine. Ladybug Tools provide plugins for the two major CAD programs Rhino and Revit and their visual programming interfaces Grasshopper and Dynamo respectively. Many architects and interior designers are working in these programs and Ladybug Tools has made it much easier to integrate environmental analysis in the regular workflow. Engineers no longer has to export between completely different programs wasting time ensuring the export went well or redoing it in the software itself. Similarly, no well suited 3D model export option in DIALux can make it time consuming to build a model of a project.

DIALux still has this issue. Sure, it is a quick program for trying out concepts, but it does not handle complex geometry and large project well. Moreover, DIALux uses radiosity as simulation method to simulate luminance distribution. According to Sawicki and Wolska (2015), this method can affect UGR calculations since it assumes perfect local diffuse reflections while excluding perfect and almost perfect specular reflection. Additionally, DIALux obtains the background luminance L_b from the simulated luminance distribution to calculate the UGR formula (5), but the luminance of the glare sources are obtained from the luminous intensity distribution (in candela) of the luminaire. From the study by Sawicki and Wolska (2015), it is unclear to what extend the luminaires is simulated other than the background luminance they contribute to. It is probably saving time in the simulation to use this method, but it seem like accuracy suffers because of it. In contrast, Radiance uses ray-tracing (Monte Carlo method) where direct illumination and specular reflections are calculated deterministically (F*ritz and Mcneil*, 2019). Discomfort glare does not exclusively occur from perfect specular surfaces, as the radiosity method assumes, so it is clear why other software turns to Radiance.

One of the best features of DIALux is the fast visualisation of how the lighting behaves, and it is tough to compete with the speed of this feature. A program called Enscape for Rhino and Revit is often used by architects and interior designers to walk around virtually in the 3D model and get an idea of how the design look. It is still not capable of showing lighting scenarios realistically and it is possible to tweak settings like a camera, distorting the realism a bit. This might change in the near future though since graphics card maker NVidia is now selling graphics cards with real-time ray-tracing capabilities. Combined with virtual reality, it might provide a future design and selling tool for lighting designers if 3D realism is brought to real-time viewing.

Slowly switching to either Grasshopper or Dynamo for lighting design will help develop innovative analytical tools created by the community of users, just as it has done for Ladybug Tools. It can ease the workflow from architect and interior designer to lighting designer and back, speeding up the design phase with quicker iterations of lighting analysis. As of now, the tools can only analyse illuminance and support IES files, but if more lighting designer could see the benefits of this type of workflow within architectural studio settings, the functionality might come.

8.4 Specifications

When many hours have been spent on a lighting design project it would be a shame to have poor implementation be the cause of discomfort glare in the end. The best way to ensure this does not happen is to be very precise when specifying the details of the design, its components and their installation. There are several aspects of a design that are important to specify but a few are crucial to be very specific about in relation to discomfort glare.

As a lighting designer it is possible to make sure the selected luminaire is not causing any glare due to the housing. This can be ensured by experiencing it firsthand, assurance from the manufacturer in documented writing, and/or checking the information provided by the manufacturer. Testing it digitally through software such as DIALux is an option, although it is not actually fulfilling the documentation requirement in the regulation, as the UGR thresholds are determined with the UGR tabular method and no other uses of the UGR formula can be applied. This is stated in current public hearing version of the revised 12464-1 standard, though it can still change. There are no standard defined on how to do it in DIALux, whether to place single viewpoints or in a grid and where. This can lead to shortcuts in the methods and still present the documentation with approved values. In the case that a luminaire is going to be retrofitted with LEDs, it is important to ensure that the housing can still shield against glare as the standard specifies. The luminaire was not built for the small, bright LED sources, and they might be visible in unpleasant ways. A mock-up model is the best way to test such a scenario.

When the right luminaire has been selected, the next crucial specification is how to power it. As described previously, the LED driver powering the LED chips are responsible for converting AC power to DC. The quality of this component can influence the output in a dynamic way, either through dimming or flickering. Dimming has a purpose both for user control and energy efficiency, but if the LED driver has the wrong specifications or is just poor quality, it can end up producing flicker by dimming. The easiest way to avoid uncomfortable flickering is to specify that the driver must fulfil the recommendations of the IEEE standard 1789-2015 as described earlier. The standard recommends to have the operating frequencies of the driver correspond to a modulation of less than 8% (for low risk level of flicker, LRL) or 3% (for no observable effect level of flicker, NOEL) unless the driver increase the frequency from supplied from the electrical grid (see Figure 10). This ensures the difference between minimum and maximum luminance of the flickering will be minimised and limit biological effects and detection of flicker in general illumination.

When dimming is specified, it is recommended to be even more specific, because every single term is not regulated by a standard and sales representatives might make promises difficult to prove was false advertisement later on. It is good to know how low the dimming is required to go, because the voltage regulation methods each have their upsides and downsides. Pulse-width modulation (PWM) dimming is good at dimming to low levels but might produce flicker and noise in the process. Constant current (CC) dimming produces no flicker or noise and have a higher efficacy at lower levels (lumen/Watt), but is has poor regulation at low levels while potentially producing a colour shift in the LEDs. Some driver manufacturers produce drivers with a variable frequency, which makes flicker generation irregular and supposedly not perceivable while being good a dimming to low levels, generate low noise. Variable frequency drivers regulate with amplitude changes instead of turning the LED on and off at regular intervals as PWM.

If it is a requirement that dimming should be able to go all the way to dark, it is important to be clear that the metric is perceived light and not measured light, since they are not equal. If lighting is dimmed to 10%, the human visual system perceives 32% according to IESNA (Illuminating Engineering Society of North America). Dimmed to 1% is perceived as 10% light, and dimmed to 0.1% is perceived as 2-3% light. If dim-to-dark is required, it is recommended the specification states 0.1% measured and not 1% measured.

If the driver is specified as dim-to-dark and is digital, it is important to notice how many digital steps it regulates the output in. At low light levels, the visual system is extremely sensitive to changes in brightness, as described with the types of photoreceptors. The driver should be specified to have a step resolution of minimum 65.536 steps to ensure a smooth dimming curve. This is also called 16 bits (2^{16}). Anything less than a 16 bit step resolution risks creating perceivable changes when dimming at low light levels.

If tunable white is specified, it is even more important to specify the right driver. Tunable white light sources consists of two LED chip, one for warm light and one for cold light. When changing from warm to cold and vice versa the driver is basically dimming one down and dimming one up.

When the right driver has been selected, the controller or dimmer for the space can be specified. This is the controller the user of the space will interact with and the interior designers might have an idea for how is should look. But looks is not everything. It is important to know how the controller behaves in terms of dimming curve and how the driver responds to it. The dimming curve and response curve can be either linear or logarithmic. The end goal is to end up with linearly perceived light. Because of this, the controller is required to be linear if the driver is logarithmic and vice versa. A popular standard digital control language is DALI which has a linear curve, meaning the driver must be logarithmic or programmed to be if possible. DALI offers an interface where individual luminaires of a design is addressable and can be controlled and programmed. If dim-to-dark is specified, it is important to ensure the DALI controller features the whole range of set points (1-254) since set point 1-85 is responsible for 0%-10% perceived light.

Following the method of specifying the technical aspects of a lighting design will ensure the lowest risk of introducing discomfort glare in a design by poor implementation.

9. Conclusion

This master thesis set out to uncover the complexities of peripheral discomfort glare from the perspective of a lighting designer with little knowledge of the subject. In reviewing the literature it became clear that the human visual system is highly specialised in adapting to the visual environment.

Light is turned from photons to images by a complex signal chain starting with the photoreceptors in the eyes, transforming it to neural signals, filtered and interpreted in specific centres of the brain. Peripheral discomfort glare can occur in the conditions where the visual system is operating around its thresholds, whether it be poor visibility, overstimulation or distraction. Regulation has been agreed upon in Europe to ensure work spaces have sufficient light installed for users to enjoy a well lit visual environment to be productive in. Regulation of general illumination and uniformity makes sure the objective brightness in a space is controlled and well distributed. Specific regulation of discomfort glare uses the predictive glare model called unified glare rating (UGR), the most recent of the predictive models for small sources, to avoid brightness from light sources creating a luminance imbalance in the visual field of users.

It is no secret that UGR is not perfect at predicting glare. The background luminance is separated from the glare source luminance in the formula, which seems counter-intuitive. The position index became a special focus of the thesis, since it was based on 70 year old experiments and was only mapped for the upper visual field which seemed inadequate. With inspiration from a Korean and a British study, an experiment was built to test whether discomfort glare had an influence on performance task on display screen equipment (DSE) and where in the visual field in it would influence performance the most. The experiment was carefully planned through 3D modelling of the glare source positions and sizes. The visual task, used to measure the performance of the participants, proved difficult to select. Studies had shown that a cognitively demanding visual task could increase glare tolerance, so to reflect the cognitive demand of a true work scenario, the Stroop task was selected. The Stroop task measures a response time (RT) for a congruent condition (word matching colour) and an incongruent condition (word not matching colour) and the difference in RT is called the Stroop interference (SI). The SI is generally accepted as a measure of cognitive attention. Choosing this as the visual task had the added benefit of avoiding any preference evaluations from participants, since studies had shown a stimulus range bias as well as an anchor bias and how challenging it was to avoid these in an experimental design.

The experiment met some challenges when running, most notably the test program PsychoPy refusing to run the test on one computer for two days until a different computer was brought in. Additionally, the Stroop task had unfortunately been designed with an imbalance of words and colours presented on the screen, resulting in a trigger-finger-effect where participants responded with a colour not matching either the word or colour actually presented. This was by far the most common mistake showing the importance of keeping the choices for response balanced. The on/off order of the glare sources was not as consistent as wanted and suggestions for the ideal order was made for a hypothetical repetition of the experiment. The two side top glare sources was unfortunately misplaced a little. Exept for the word/colour imbalance, it was difficult to determine whether these affected the results.

16 participants completed this experiment, which took about 30 minutes each. The results showed the benchmark response to have the slowest response time (RT). This was unfortunate since the benchmark would have been used to check whether discomfort glare had an influence no matter the position, which was made impossible to answer. The results showed the Stroop interference (SI) in effect but it was unclear how significant it was to any SI general mean. A research question was adopted from a study to test if self-perceived glare sen-

sitives were influenced more than self-perceived glare insensitives. The results showed glare sensitives to have a higher SI than glare insensitives as the inspirational study had concluded, though the SIs were smaller in comparison, probably due to differences in sample size. The results found no evidence to conclude any glare source position had a higher influence on task performance than others.

It was discussed whether the Stroop task was fit to measure performance when exposed to external stimuli such as discomfort glare. The Stroop interference (SI) seemed to be real, but post-analysis research showed that not even psychologists could agree on a standard for testing the SI itself, let alone any other external stimuli introduced to the task.

The knowledge learned from the literature review informed the experimental design process to learn and show how difficult it can be for researchers to design experiments trying to quantify peripheral discomfort glare and develop scientifically proven predictive glare models. The literature review also inspired to define a few different measures lighting designers, and related colleagues in the architectural world, can take to avoid peripheral discomfort glare in projects. First measure was getting an understanding of the revisions for the 12464-1 indoor work places lighting standard to construct a workflow around it. Second measure was an appeal to architects and interior designers to better understand how their designs influences light, and how any changes in geometry and surfaces can impact how lighting is distributed in a space. Third measure was staying critical to the current state of lighting simulation software, staying updated on where it goes in the future, and consider how workflow and the lighting design community could potentially benefit from switching to software developed through community cooperation. Fourth and last measure outlined the importance of delivering detailed specifications for luminaire, LED drivers, dimming features and controllers to ensure correct implementation of a lighting design.

10. References

References retrieved with the AAU library paid subscription service include a link requiring a user from AAU to pass through. This means the links include ".zorac.aub.aau.dk". Only two publishing sites are used, www.sciencedirect.com and www.journals.sagepub.com. if it is necessary to use the link without an AAU user, remove the ".zorac.aub.aau.dk" part from the link and edit the link to match one of the two sites in use. Te be able to read the article this way requires a different user.

Bay, A., Nielsen, E. L., Fontoynont, M., Lumbye, A., Osterhaus, W., Kessler, L. (2017). *Glare and Energy for Lighting*, El-Forsk research project (number 348-009). Retrieved from El-Forsk February 22nd, from https://elforsk.dk/projektdatabase/energieffektivt-lys-gennem-blaendingskontrol

Bellchambers, H. E., Burt, W., Frith, D., Grundy, J. T., Hewitt, H., Hopkinson, R. G., ... (1962). T*he Development of the IES Glare Index System: Contributed by the Luminance Study Panel of the IES Technical Committee*, Transactions of the Illuminating Engineering Society, Vol. 27(1), (9-26). Retrieved from Sage Publishing/Journals February 22nd (2019), from https://journals-sagepub-com.zorac.aub.aau.dk/doi/pdf/10.1177/147715356202700103 (AAU library paid subscription).

Boyce, P. R. (2014). *Human Factors in Lighting* (3rd edition), Boca Raton, Florida, USA: CRC Press (Taylor & Francis Group). ISBN: 978-1-4398-7489-9 (e-book - PDF)**.**

Boyce, P. R., & Wilkins, A. (2018). *Visual discomfort indoors*, Lighting Research & Technology, Vol. 50(1), (98-114). Retrieved from Sage Publishing February 2nd (2019), from https://journals-sagepub-com.zorac.aub.aau.dk/doi/full/10.1177/1477153517736467 (AAU library paid subscription).

Clear, R. D. (2013). *Discomfort glare: What do we actually know?,* Lighting Research & Technology, Vol. 45(2), (141-158). Retrieved from Sage Publishing/Journals February 21st (2019), from https://journals-sagepub-com.zorac.aub.aau.dk/doi/full/10.1177/1477153512444527 (AAU library paid subscription).

Danish Standard (2011). *DS/EN 12464-1:2011 – Light and lighting – Lighting of work places – Part 1: Indoor workplaces*, Danish Standard (DS) & European Committee for Standardization (CEN). Retrieved from Danish Standard (DS) February 18th (2019), from https://sd-ds-dk.zorac.aub.aau.dk/Viewer/Standard?ProjectNr=M241664&Status=92.20&VariantID=41&Page=0 (AAU library paid subscription).

Danish Standard (2018). *DS/EN 17037:2018 – Daylight in buildings*. Danish Standard (DS) & European Committee for Standardization (CEN). Retrieved from Danish Standard (DS) February 18th (2019), from https://sd-ds-dk.zorac.aub.aau.dk/Viewer/Standard?ProjectNr=M308488&Status=60.60&VariantID=41&Page=0 (AAU library paid subscription).

Davis, Nick (-). *What you need to know before your next LED design*. Power Electronic News. Retrieved May 26th (2019), from https://www.powerelectronicsnews.com/problems-solutions/what-you-need-to-know-before-your-next-led-design

Describing Variability. Courses.Lumenlearning.com [data analysis education]. Retrieved May (2019), from https://courses.lumenlearning.com/boundless-statistics/chapter/describing-variability/

Einhorn, H. D. (1979). *Discomfort glare: a formula to bridge differences*, Lighting Research & Technology, Vol. 11(2), (90-94). Retrieved from Sage Publishing/Journals February 22nd (2019), from https://journals-sagepub-com.zorac.aub.aau.dk/doi/pdf/10.1177/14771535790110020401 (AAU library paid subscription).

Fritz, R., & Mcneil, A. (09:50, January 4th, 2019). *About Radiance*. Rad-Site | Radiance-online.org [software]. Retrieved May 28th (2019), from https://www.radiance-online.org/about

Ghasemi, A., & Zahediasl, S. (2012). *Normality Tests for Statistical Analysis: A Guide for Non-Statisticians*, International Journal of Endocrinology & Metabolism, Vol. 10(2), (486-489). Retrieved from National Center for Biotechnology Information (NCBI) May 18th (2019), from https://www.ncbi.nlm.nih.gov/pmc/articles/PMC3693611/

Hirning, M. B., Isoardi, G. L., & Cowling, I. (2013). *Discomfort glare in open plan green buildings*, Energy and Buildings, Vol. 70 (427-440). Retrieved from Elsevier Science Direct February 10th (2019), from https://www-sciencedirect-com.zorac.aub.aau.dk/science/article/pii/S0378778813007603 (AAU library paid subscription).

Hopkinson, R. G. (1972). *Glare from daylighting in buildings*, Applied Ergonomics, Vol. 3(4), (206-215). Retrieved from Elsevier Science Direct February 26th (2019), from https://www-sciencedirect-com.zorac.aub.aau.dk/science/article/pii/0003687072901020 (AAU library paid subscription).

How to calculate solid angle of a rectangledetector of 20 cm x 10 cm? (April, 2015-January 2017). Math.Stackexchange.com [mathematics online forum]. Retrieved March (2019), from https://math.stackexchange.com/questions/1244429/how-to-calculate-solid-angle-of-a-%20rectangular-detector-of-20cm-x-10cm

How to Find a Coefficient of Variation (2019). Statistics How To [data analysis education]. Retrieved May (2019), from https://www.statisticshowto.datasciencecentral.com/probability-and-statistics/how-to-find-%20a-coefficient-of-variation/

Hulsmans, G. (2019). *How to choose the right LED driver when it comes to perfect dimming & flicker? ...and what about camera compatibility, dynamic white, lighting controls and IoT?* [PowerPoint slides]. Retrieved personally from Gé Hulsmans (director specifier service at EldoLED LED drivers) February 28th (2019) through e-mail.

IEEE-SA,The Institute of Electrical and Electronics Standards Association (2015). *IEEE recommended practices for modulating current in high-brightness LEDs for mitigating health risks to viewers – IEEE Std. 1789-2015*. ISBN: 978-0-7381-9644-2 (PDF), 978-0-7381-9645-9 (print). Retrieved March 10 (2019), from http://www.bio-licht.org/02_resources/info_ieee_2015_standards-1789.pdf

Iwata, T., & Tokura, M. (199*7). Position Index for a glare source located below the line of vis*ion, International Journal of Lighting Research and Technology, Vol. 29(3), (172-178). Retrieved from Sage Publishing/Journals February 10th (2019), from https://journals-sagepub-com.zorac.aub.aau.dk/doi/pdf/10.1177/14771535970290030801 (AAU library paid subscription).

Kent, M. G. (2016). *Temporal Effects in Glare Response* (Doctoral dissertation, The University of Nottingham, Nottingham, United Kingdom. Retrieved from ProQuest Dissertations Publishing March 1 (2019), Dissertation number: 10625993, from https://search-proquest-com.zorac.aub.aau.dk/docview/1916426658?pq-origsite=primo (AAU library paid subscription).

Kent, M. G., Fotios, S., & Altomonte, S. (2018). *An Experimental Study on the Effect of Visual Task on Discomfort Due to Peripheral Glare*, LEUKOS - The Journal of the Illuminating Engineering Society, Vol. 15(1), (17-28). Retrieved from Taylor & Francis Online January 19th (2019), from https://www.tandfonline.com/doi/full/10.1080/15502724.2018.1489282 (AAU library paid subscription).

Kim, W., Kim, J. T. (2010a). *Effect of Background Luminance on Discomfort Glare in Relation to the Glare Source Size*, Indoor Built Environment, 19(1), (175-183). Retrieved from Sage Publishing/Journals February 26th (2019), from https://journals-sagepub-com.zorac.aub.aau.dk/doi/abs/10.1177/1420326X09358006 (AAU library paid subscription).

Kim, W., Kim, J. T. (2010b). *A distribution chart of glare sensation over the whole visual field*, Building and Environment, Vol. 45(4), (922-928). Retrieved from Elsevier Science Direct February 14th (2019), from https://www-sciencedirect-com.zorac.aub.aau.dk/science/article/pii/S036013230900256X (AAU library paid subscription).

Kim, W., Kim, J. T. (2011c). *A Position Index Formula for Evaluation of Glare Source in the Visual Field*, Indoor Built Environment, 20(1), (47-53). Retrieved from Sage Publishing/Journals March 7th (2019), from https://journals-sagepub-com.zorac.aub.aau.dk/doi/abs/10.1177/1420326X10389267 (AAU library paid subscription).

Logadóttir, A., Christoffersen, J., & Fotios, S. A. (2011a). *Investigating the use of an adjustment task to set the preferred illuminance in a workplace environment*, Lighting Research & Technology, Vol. 43(4), (403-422). Retrieved from Sage Publishing/Journals January 19th (2019), from https://journals-sagepub-com.zorac.aub.aau.dk/doi/abs/10.1177/1477153511400971 (AAU library paid subscription).

Logadóttir, A., Fotios, S. A., Christoffersen, J., Hansen, S. S., Corell, D. D., & Dam-Hansen, C. (2011b). *Investigating the Use of an Adjustment Task to Set Preferred Colour of Ambient Illumination*, Color Research and Application, Vol. 38(1), (46-57). Retrieved from Wiley Online Library January 19th (2019), from https://onlinelibrary-wiley-com.zorac.aub.aau.dk/doi/full/10.1002/col.20714 (AAU library paid subscription).

Lowson, J. C., (1981). *Practical application of the Einhorn (CIE) Glare Index formula,* Lighting Research & Technology, Vol. 13(4), (169-191). Retrieved from Sage Publishing/Journals February 24th (2019), from https://journals-sagepub-com.zorac.aub.aau.dk/doi/pdf/10.1177/096032718101300401 (AAU library paid subscription).

Luckiesh, M., & Guth, S. K. (1949). *Brightness in Visual Field at Borderline Between Comfort and Discomfort (BCD)*, Illuminating Engineering, Vol. 44(11), (650-670). Retrieved February 22nd (2019), from https://www.brikbase.org/sites/default/files/ies_035_0.pdf

MacAdam ellipse (11:21, April 9th, 2019). Wikipedia.com [online community encyclopedia]. Retrieved May 27th (2019), from https://en.wikipedia.org/wiki/MacAdam_ellipse

Moum, Å., & Högman, L. (2015). *New light on willpower: Can blue light strengthen self-control?*, Psykologi III (Stokholms Universitet - Psykologiska Institution). Provided personally through e-mail via supervisor.

Nothing but background after start, no demos working either (April, 2019). Discourse.PsychoPy.org [PsychoPy online forum]. Retrieved April (2019), from https://discourse.psychopy.org/t/nothing-but-background-after-start-no-demos-working-either/7373

Peirce, J. (2019). PsychoPy (version 3.0.7) [software]. Retrieved March 18th (2019), from https://www.psychopy.org/

Petherbridge, P., & Hopk*inson, R. G. (1950). Discomfort Glare an*d the Lighting of Buildings. Transactions of the Illuminating Engineering Society, Vol. 15(2), (39-79). Retrieved from Sage Publishing/Journals February 24th (2019), from https://journals-sagepub-com.zorac.aub.aau.dk/doi/pdf/10.1177/147715355001500201 (AAU library paid subscription).

Planning and calculation tips (Glossary): Quantities, units and their significance. Fagerhult.com [luminaire manufacturer]. Retrieved February (2019), from https://www.fagerhult.com/knowledge-hub/planning-and-calculation-tips/

Remington, L. A. (2012). *Clinical Anatomy and Physiology of the Visual System* (3rd edition). St. Louis, Missouri, USA: Butterworth Heinemann (Elsevier Inc.). ISBN: 978-1-4377-1926-0.

Rodriguez, R. G., Garretón, J. A. Y., Pattini, & A. E. (2016). *Glare and cognitive performance in screen work in the presence of sunlight*, Lighting Research & Technology, Vol. 48(2), (221-238). Retrieved from Sage Publishing/Journals February 22nd (2019), from https://journals-sagepub-com.zorac.aub.aau.dk/doi/full/10.1177/1477153515577851 (AAU library paid subscription).

Salo, R., Henik, A., & Robertson, L. C. (2001). *Interpreting Stroop Interference: An Analysis of Differences Between Task Versions*, Neuropsychology, Vol 15(4), (462-471). Retrieved from American Psychological Association PsycNET May 20th (2019), from https://psycnet-apa-org.zorac.aub.aau.dk/fulltext/2001-05289-005.html

Sawicki, D., & Wolska, A. (2015). *Discomfort glare prediction by different methods*, Lighting Research & Technology, Vol. 47(6), (668-671). Retrieved from Sage Publishing/Journals February 2nd (2019), from https://journals-sagepub-com.zorac.aub.aau.dk/doi/full/10.1177/1477153515589773 (AAU library paid subscription).

Scarpina, F., & Tagini, S. (2017). *The Stroop color and word test*, Frontiers in Psychology Vol. 8, article 557. Retrieved from National Center for Biotechnology Information (NCBI) May 13th (2019), from https://www.ncbi.nlm.nih.gov/pmc/articles/PMC5388755/

Scheir, G. H., Donners, M., Geerdinck, L. M., Vissenberg, M. C. J. M., Hanselaer, P., & Ryckaert, W. R. (2018). *A psychophysical model for visual discomfort based on receptive fields*, Lighting Research & Technology, Vol. 50(2), (205-217). Retrieved from Sage Publishing/Journals January 7th (2019), from https://journals-sagepub-com.zorac.aub.aau.dk/doi/full/10.1177/1477153516660606 (AAU library paid subscription).

Sine Wave. Chegg.com [online study portal]. Retrieved May 27th (2019), from https://www.chegg.com/homework-help/definitions/sine-wave-4

Standard Deviation. Statistics.Laerd.com [data analysis education]. Retrieved May (2019), from https://statistics.laerd.com/statistical-guides/measures-of-spread-standard-deviation.php

Sørensen, Kai (January, 2012). *Foredrag om UGR metoden* [PowerPoint presentation]. Provided personally by Kai Sørensen through e-mail.

TCO Development (2018). *TCO Certified*. Retrieved March 10th (2019), from https://tcocertified.com/certification-documents/

TCO Development (2018). *TCO Certified Generation 8, for displays*. Retrieved March 10th (2019), from https://tcocertified.com/files/certification/tco-certified-generation-8-for-displays.pdf

TCO Development (2018). *TCO Certified Generation 8, for notebooks*. Retrieved March 10th (2019), from https://tcocertified.com/files/certification/tco-certified-generation-8-for-notebooks.pdf

*Testing for Normality using SPSS Stati*stics. Statistics.Laerd.com [data analysis education]. Retrieved May (2019), from https://statistics.laerd.com/spss-tutorials/testing-for-normality-using-spss-statistics.php

Tregenza, P., & Loe, D. (2014). *The Design of Lighting* (2nd edition). Abingdon, Great Britain: Routledge (Taylor & Francis Group). ISBN: 978-0-415-52246-5.

A. Glare source position measurements

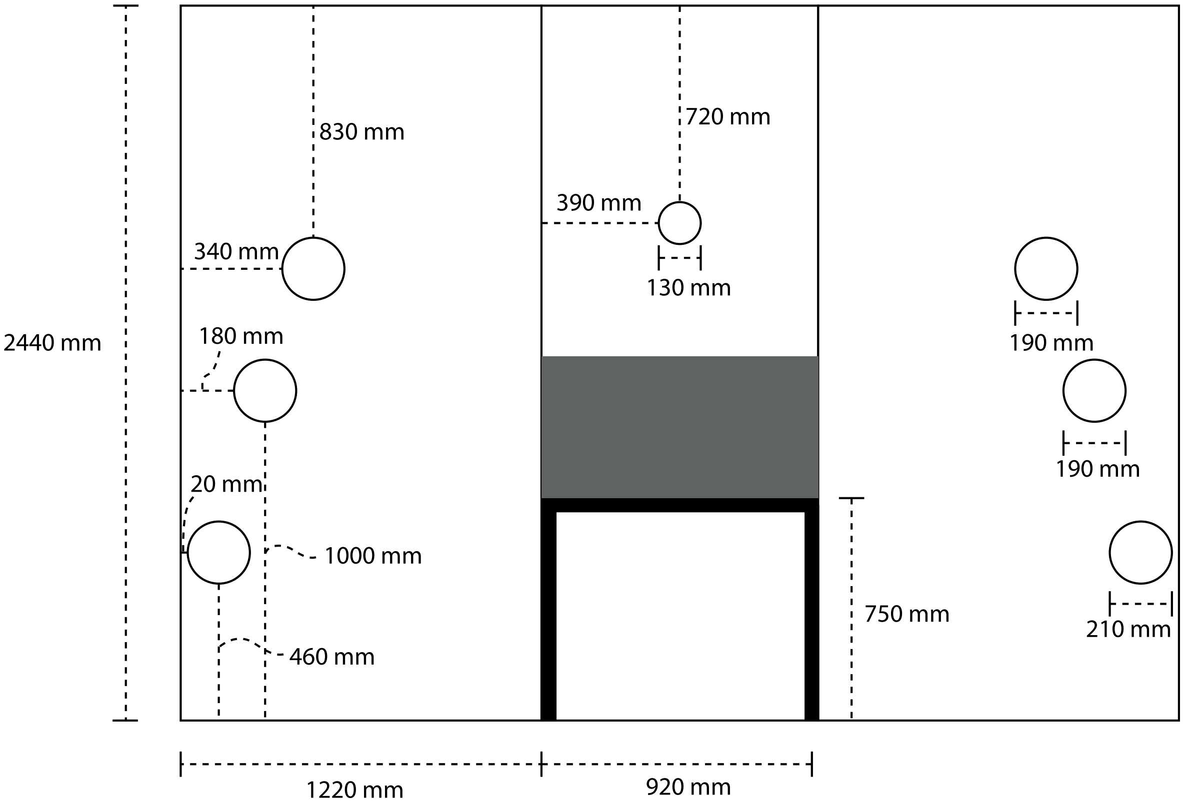

B. Light Lab measurements

Green area = tables; Blue area = behind wall screen (out of sight);

Red dots = room side wall measurements

Floor level illuminance measurements, 0 mm:

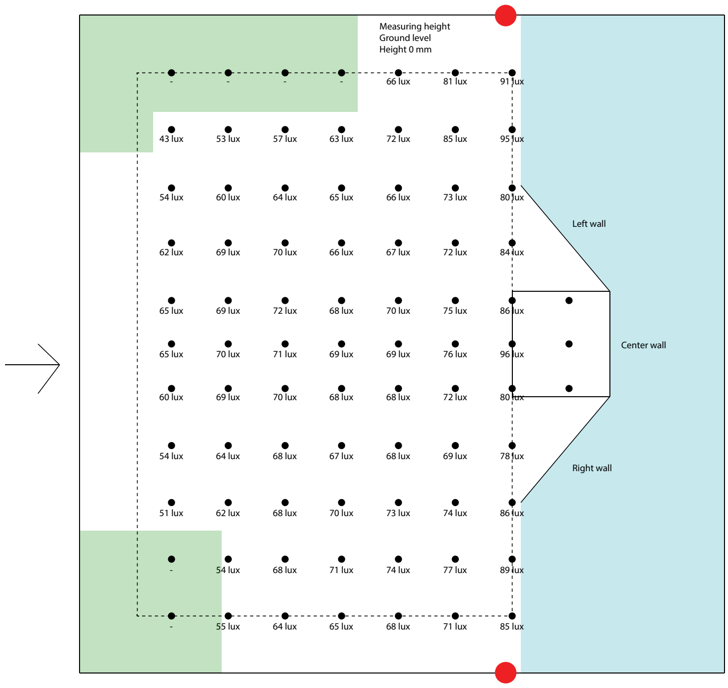

4,959 lux / 71 points = 70 lux on average

Table level illuminance measurements, 750 mm:

6,338 lux / 80 points = 79 lux

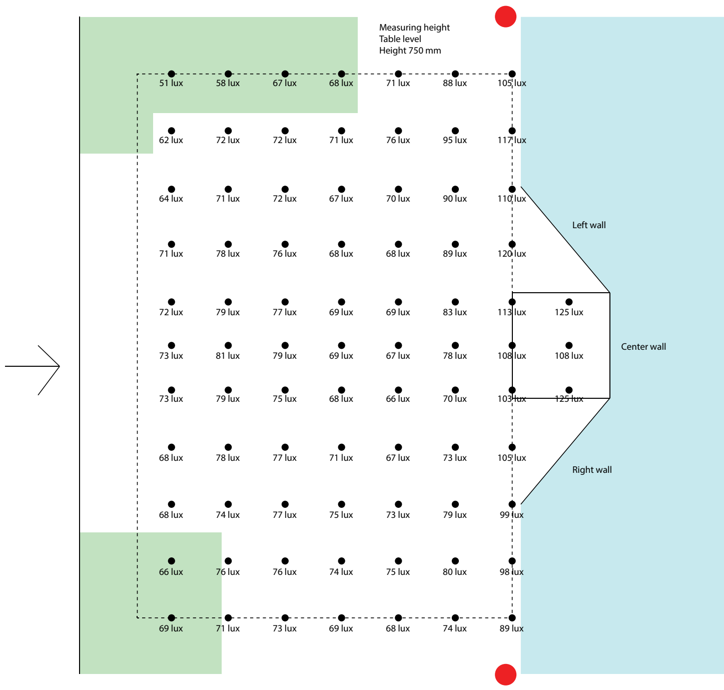

Screen wall measurements, luminance:

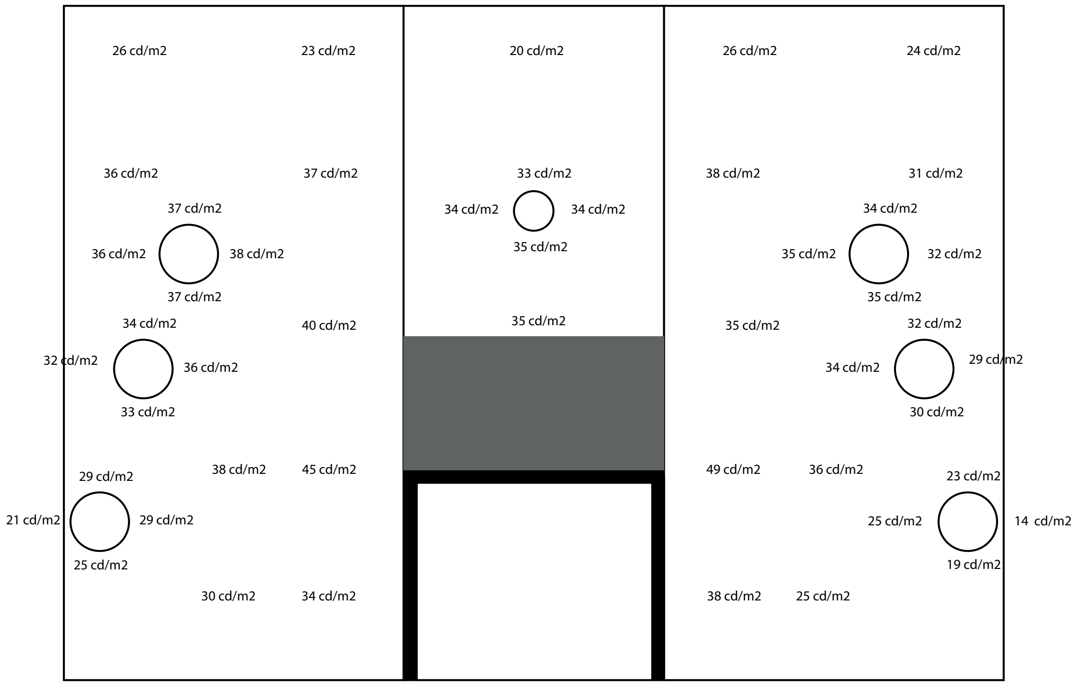

Screen wall measurements, illuminance:

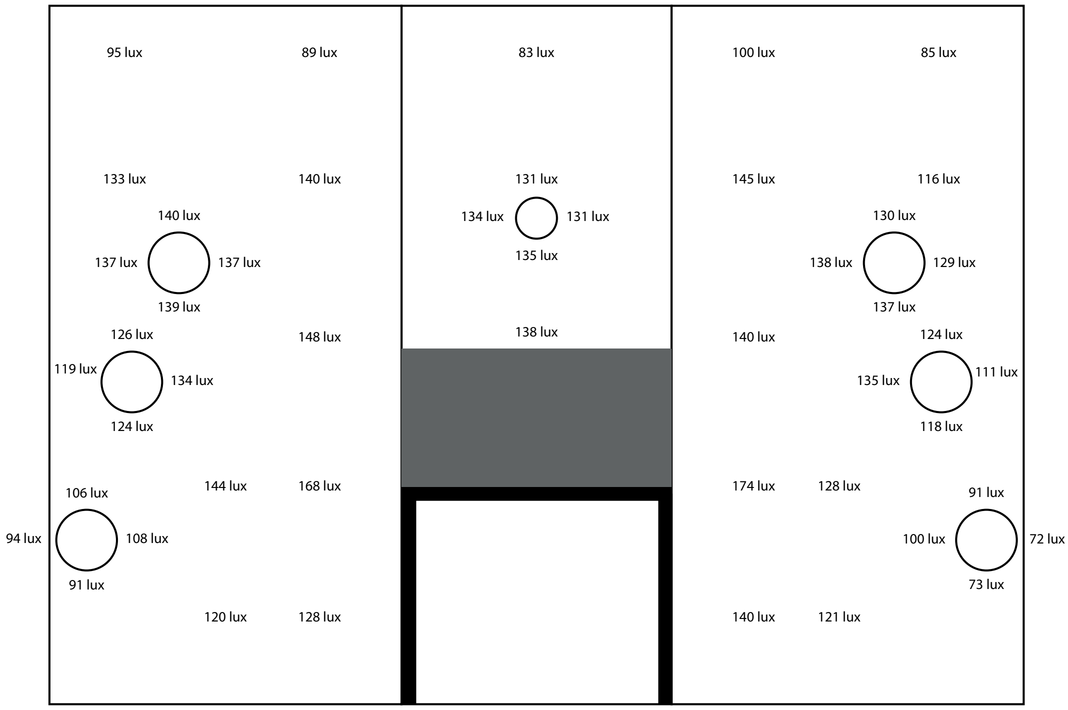

Room side wall luminance and illuminance (red dots)

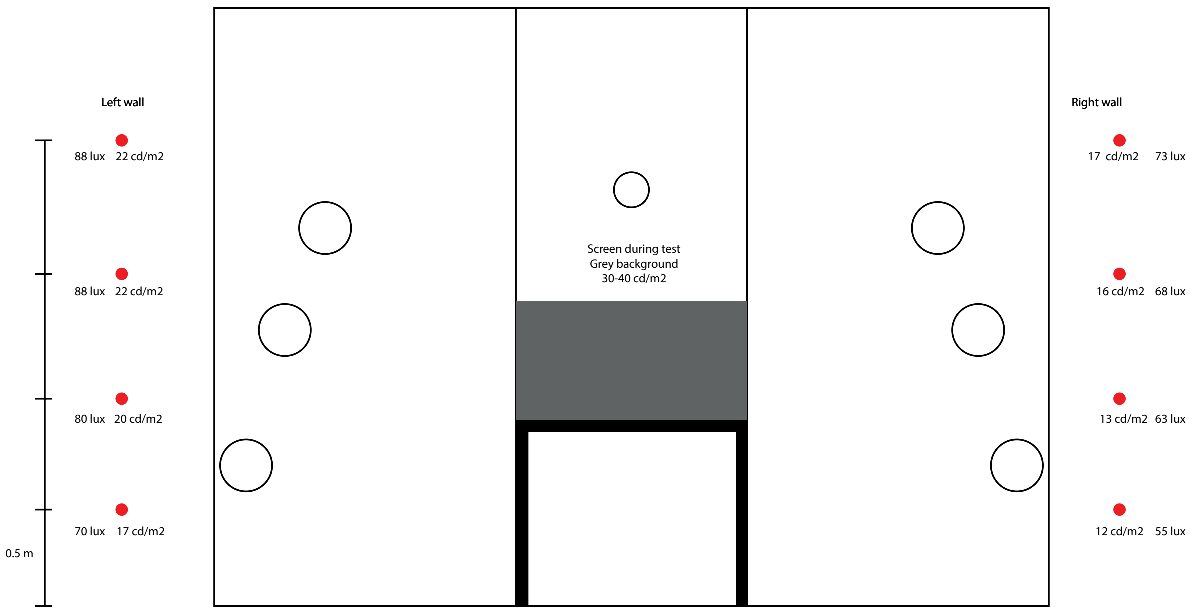

Glare source measurements, luminance:

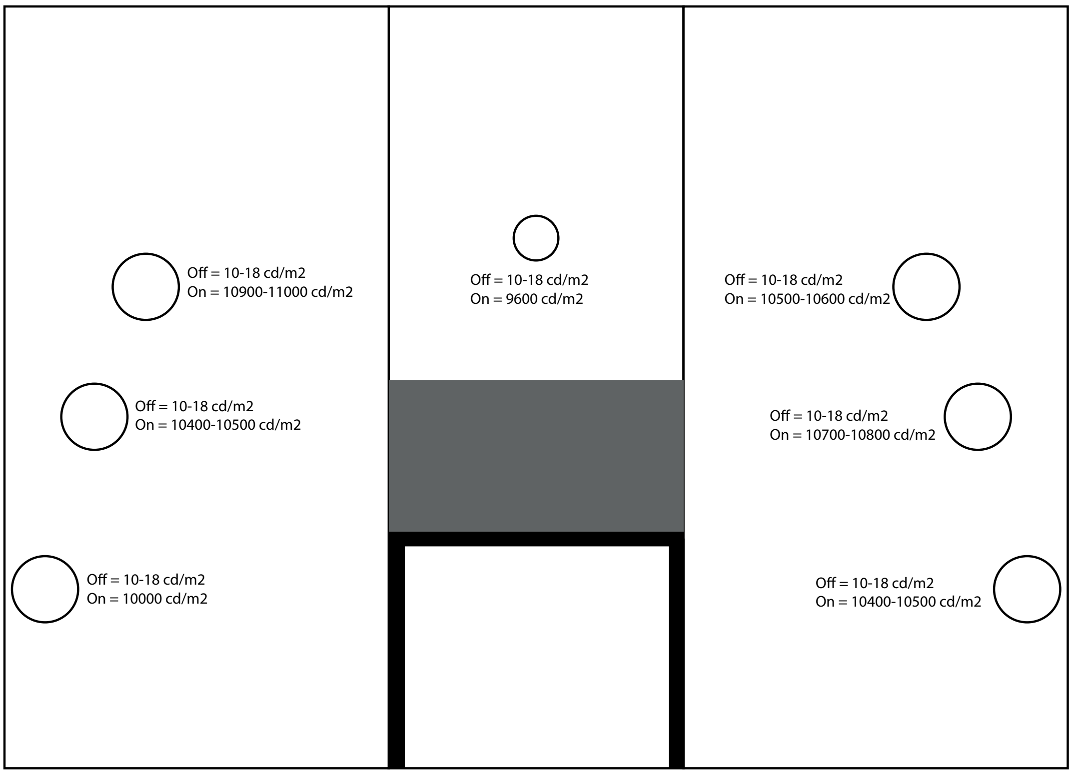

C. Participant poster

AALBORG UNIVERSITY
COPENHAGEN

LIGHTING DESIGN

TEST SUBJECTS WANTED FOR EXPERIMENT ON PERIPHERAL DISCOMFORT GLARE

Imagine the following scenario

You are working on your computer and suddenly it's getting harder to concentrate because a bright light source in your visual field is bothering you. Despite attempts to ignore it or change posture, you have to change place or find some method of shielding the light source.

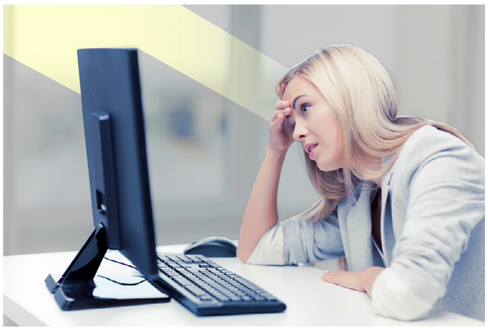

This is a typical experience of discomfort glare and can be very distracting or even uncomfortable when working. This experiment will attempt to measure if it is impairing one's task performance when exposed to peripheral discomfort glare and if so, where in the visual field does it influence performance the most.

<u>Cake is offered in return.</u>

Participation is anonymous.

Duration: approx. 30 min
Period: 8/4 - 14/4

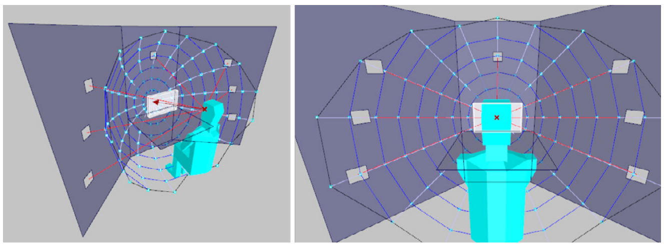

Address:
Aalborg University Copenhagen
A. C. Meyers Vænge 15
2450 Copenhagen

Contact:
Mads Mårbjerg
mads.maarbjerg@gmail.com

D. Result diagrams

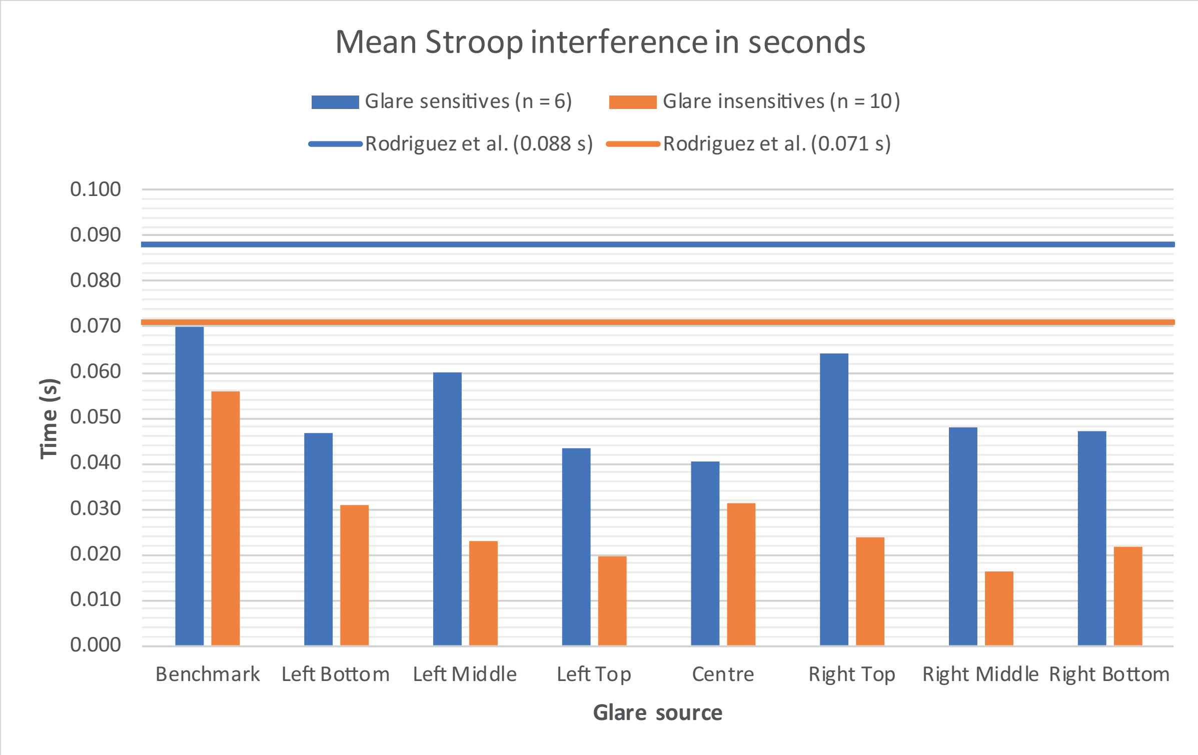

Figure D1: Mean Stroop interference in seconds for self-reported glare sensitives and glare insensitives.

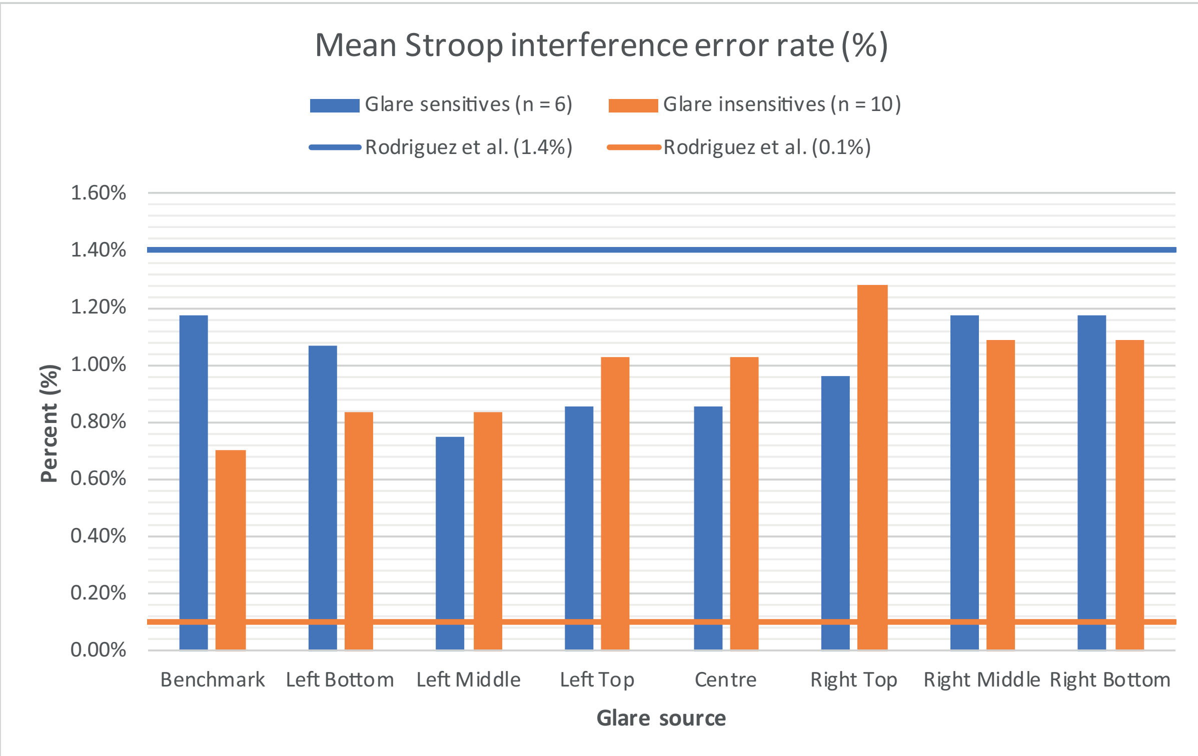

Figure D2: Mean Stroop interference error percentage for self-reported glare sensitives and glare insensitives.

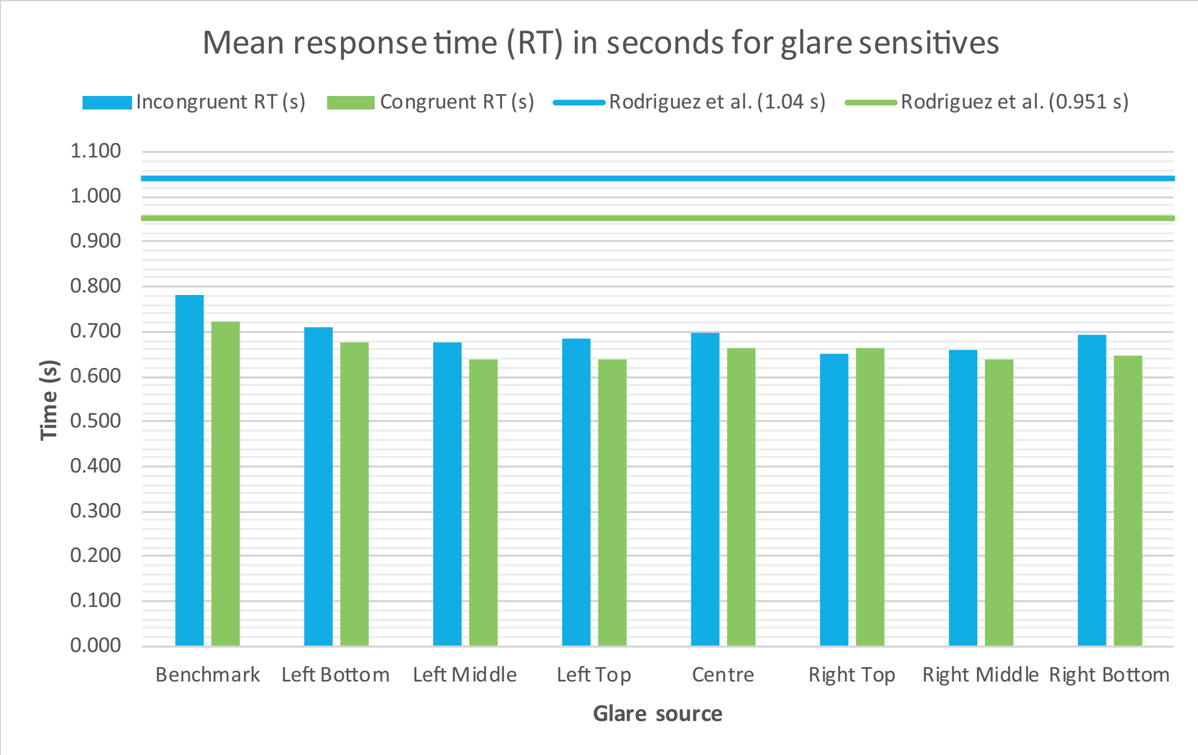

Figure D3: Mean response time in seconds for self-reported glare sensitives (bright colours) in incongruent conditions (blue) and congruent conditions (green).

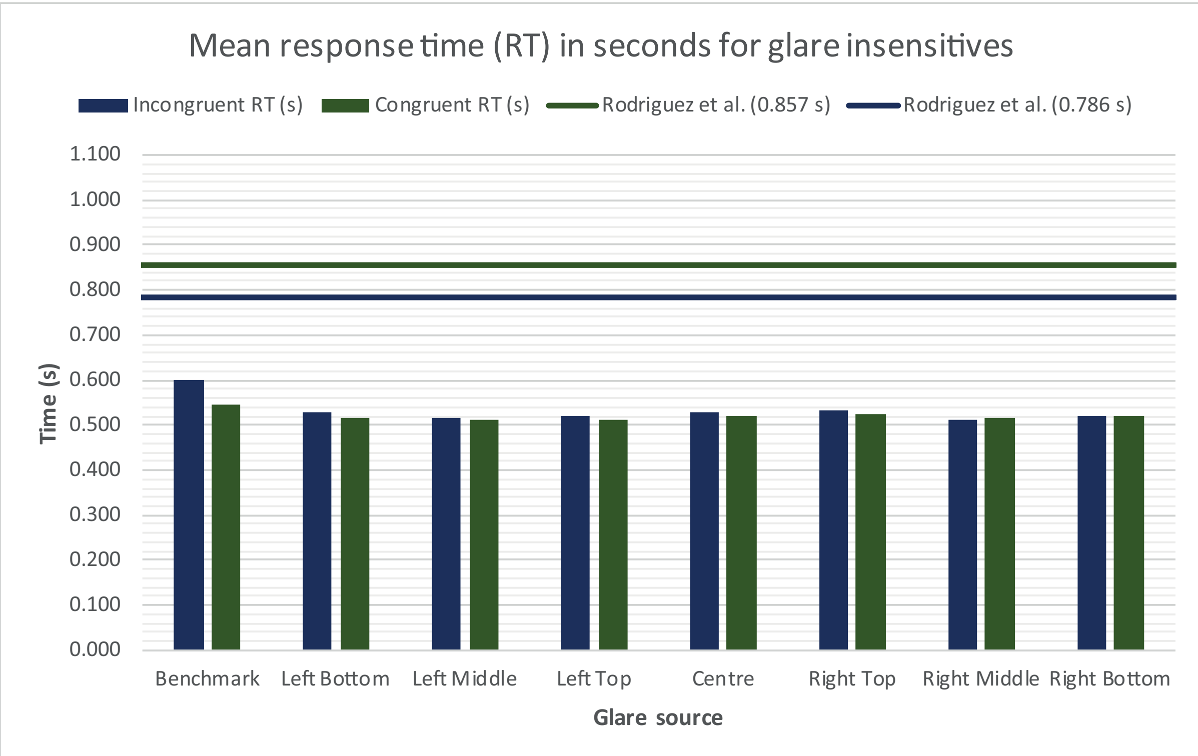

Figure D4: Mean response time in seconds for self-reported glare insensitives (dark colours) in incongruent conditions (blue) and congruent conditions (green).

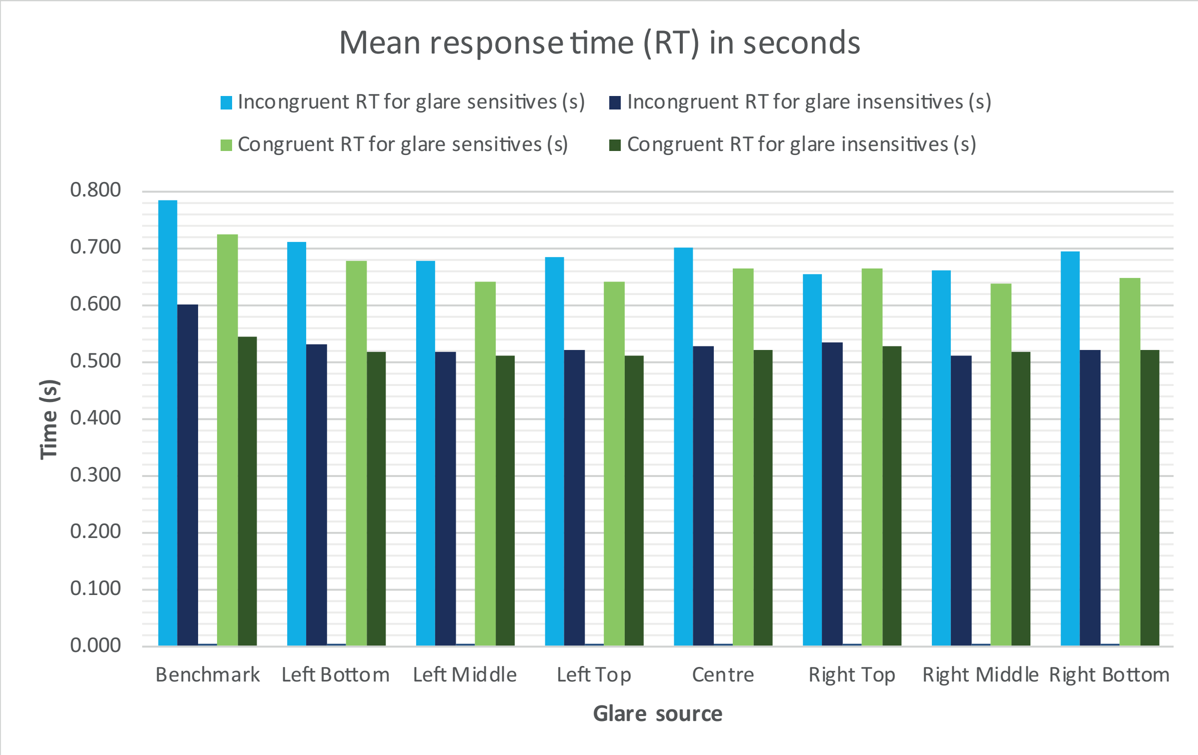

Figure D5: Mean response time in seconds for self-reported glare sensitives (bright colours) and glare insensitives (dark colours) in incongruent conditions (blue) and congruent conditions (green) for comparison.

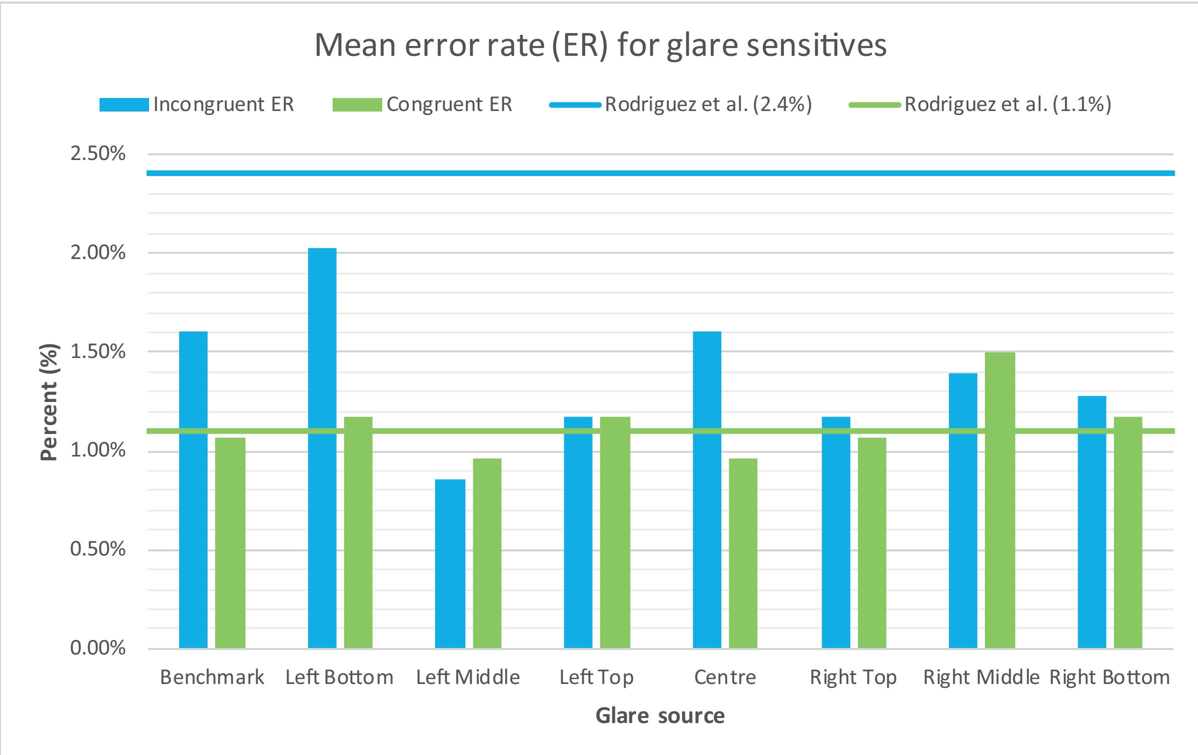

Figure D6: Mean error rate for self-reported glare sensitives (bright colours) in incongruent conditions (blue) and congruent conditions (green).

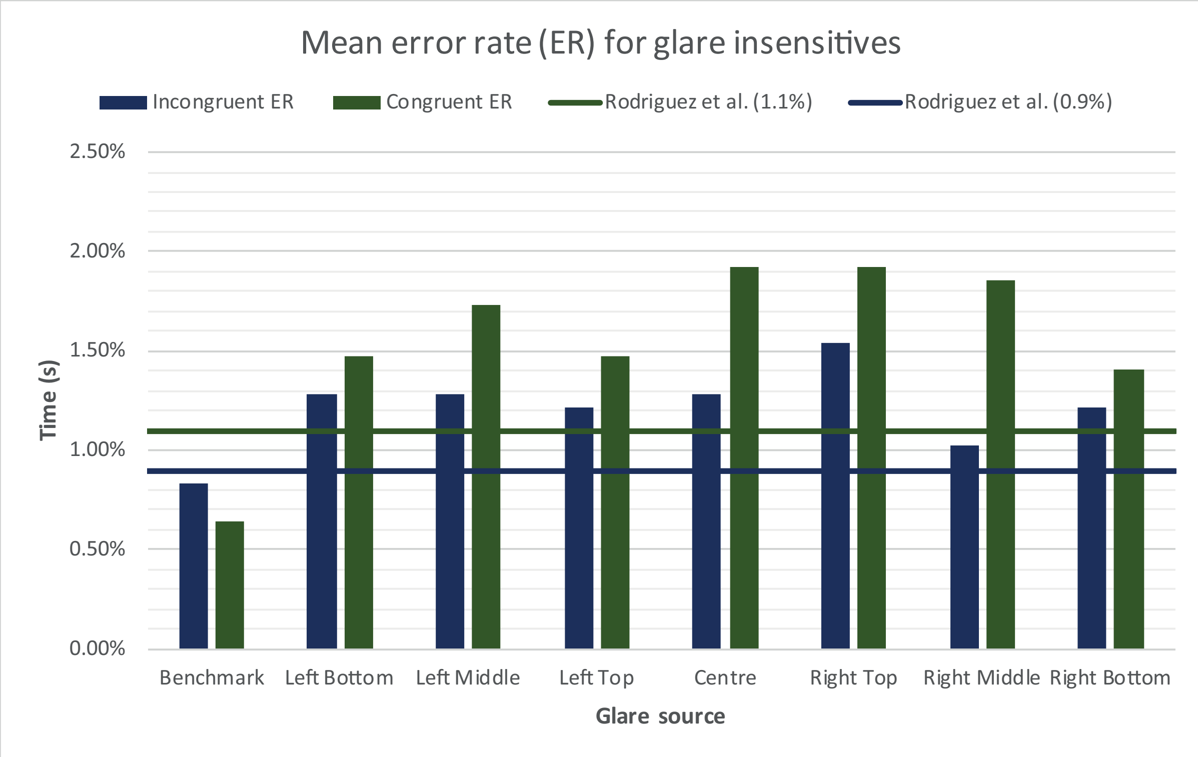

Figure D7: Mean error rate for self-reported glare insensitives (dark colours) in incongruent conditions (blue) and congruent conditions (green).

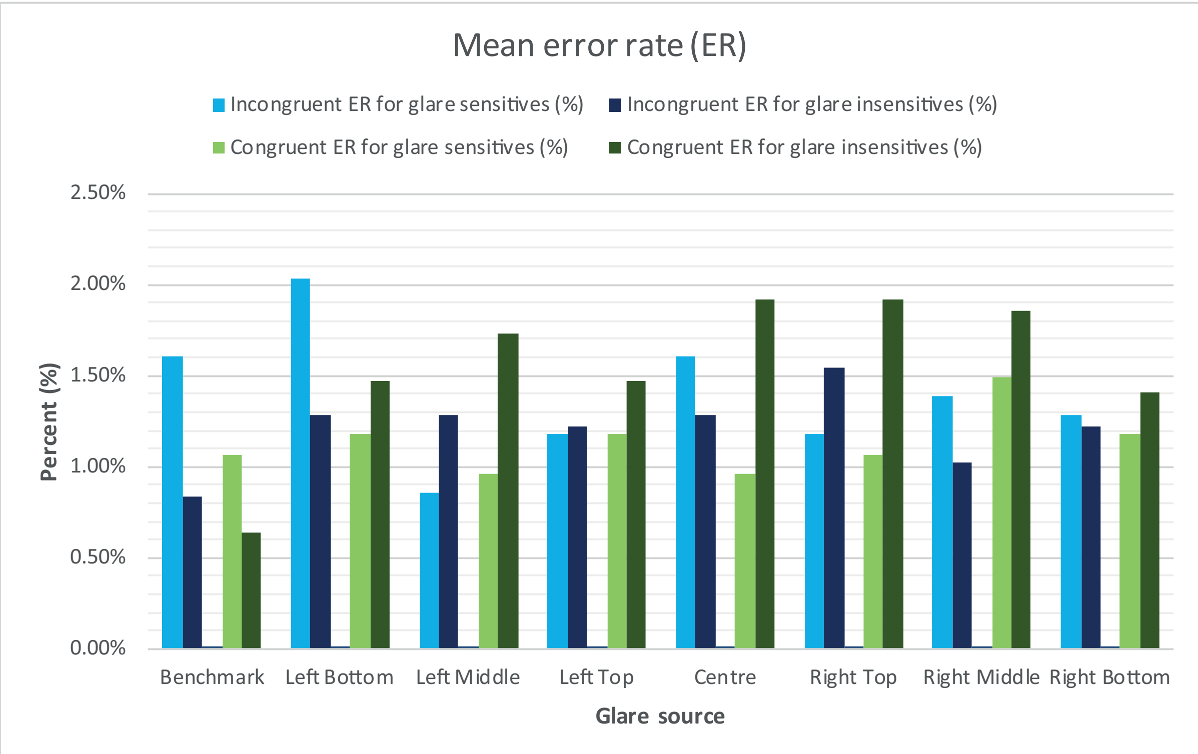

Figure D8: Mean error percentage for self-reported glare sensitives (bright colours) and glare insensitives (dark colours) in incongruent conditions (blue) and congruent conditions (green) for comparison.

E. Ideal on/off order

A4 sheet to keep track of the manual on/of order of the glare sources during the experiment. The numbers on this sheet represent the best order to follow to make sure each glare source is placed with a difference of at least three places in the order between the two runs. A source placed in the last half of the order in the first run will be shifted around in the second run to a position in the first halft of the order. It was the best combination found in the post-experiment analysis but unfortunately only achieved with one participant.

Test subject number : ______________________

Date and time: ______________________

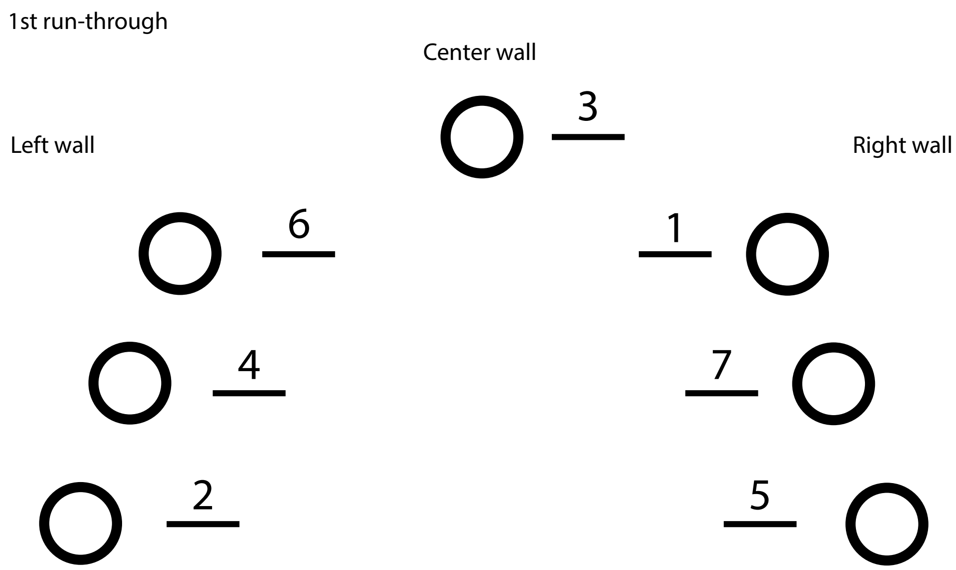

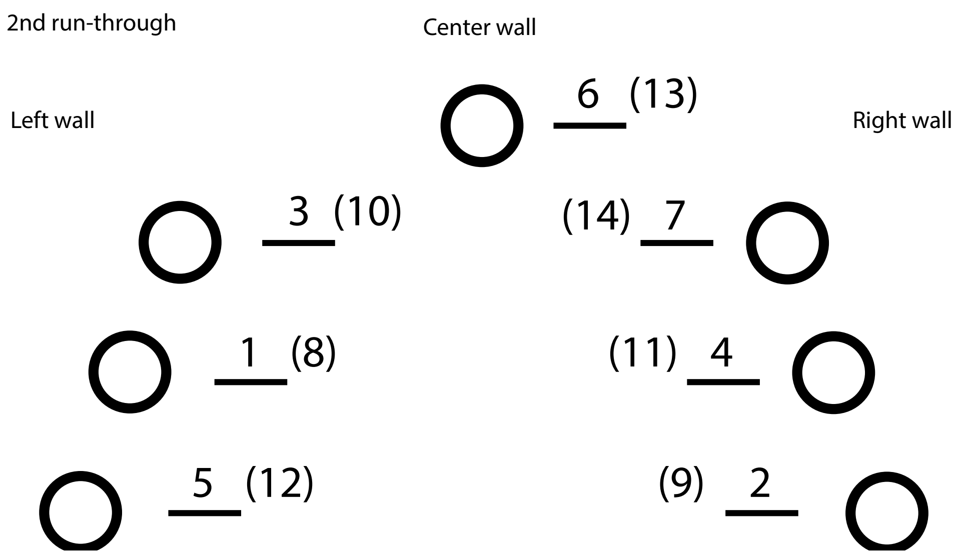

F. Stroop task design

Figure F1: Experiment 1A: Computerized clinical (classic) version – word matrix, blocked. Experiment 1B: Random single-trial version - single words, random. Experiment 1C: Blocked single-trial version - single words, blocked. Experiment 2A: Neutral testing – similar nonword strings (XXX), single word, blocked. Experiment 2B: Neutral testing – dissimilar nonword strings (XXX, SSS, MMM), single word, blocked. Experiment 2C: Neutral testing – animal names (dog, bear, tiger, monkey), single word, blocked. Experiment 3A: Location shift - diagonal, random. Experiment 3B: Location shift – diagonal, blocked.

	Congruent		**Neutral**		**Incongruent**	
	Mean RT (s)	SD	Mean RT (s)	SD	Mean RT (s)	SD
Experiment 1A	0.473	0.080	0.491	0.062	0.680	0.116
Experiment 1B	0.580	0.078	0.587	0.069	0.681	0.077
Experiment 1C	0.488	0.081	0.553	0.074	0.713	0.102
Experiment 2A	0.547	0.064	0.624	0.060	0.745	0.075
Experiment 2B	0.544	0.069	0.637	0.057	0.752	0.079
Experiment 2C	0.555	0.058	0.659	0.059	0.750	0.093
Experiment 3A	0.601	0.099	0.612	0.095	0.726	0.136
Experiment 3B	0.505	0.098	0.563	0.080	0.706	0.108

Differences between maximum and minimum values:

Congruent: 0.473 – 0.601 s = 0.128 s

Neutral: 0.491 – 0.659 s = 0.166 s

Incongruent: 0.680 – 0.752 s = 0.072 s

Salo, R., Henik, A., & Robertson, L. C. (2001). *Interpreting Stroop Interference: An Analysis of Differences Between Task Versions*, Neuropsychology, Vol 15(4), (462-471). Retrieved from American Psychological Association PsycNET May 20th (2019), from https://psycnet-apa-org.zorac.aub.aau.dk/fulltext/2001-05289-005.html

G. Shapiro-Wilk normality test

Testing a data set for normal distribution is standard in most papers as with the study by Rodriguez et al. (2016), where they used a Shapiro-Wilk test to test their data for normal distribution. The Shapiro-Wilk test is well-suited for experiments with small sample sizes such as this one (*Testing for Normality...*, 2019). Testing for normal distribution can assist in evaluating the accuracy of the data as well as guide in which statistical tests to apply onwards, since certain statistical tests rely on the assumption of normal distribution. It is apparently a problem with some scientific literature to have errors in their statistical assumptions (Ghasemi and Zahediasl, 2012). Because of this, these results reserved for readers wishing to scrutinize the data and results while not being discussed in the report.

The data was tested for normal distribution with Shapiro-Wilk tests in SPSS. In order for the data to be considered normally distributed, the significance value has to be above 0.005. If it is below, then the data deviates significantly from a normal distribution. Congruent and incongruent reaction times for all participants showed to be normally distributed (sig. >0.005), but the Stroop effect reaction time showed only the benchmark, left top source and right bottom source to be normally distributed, while the rest deviated too much from the mean (sig. <0.005). Rodriguez et al. (2016) do not clearly present their findings of the Shapiro-Wilk test in a table, and it seems most of their variables was not normally distributed, at least not the ones in the diffuse daylight scenario the results are compared to. Nonetheless, it is perceived as a positive result for this experiment.

See next page for tables.

Table G1: Response time for congruent conditions along with results from the Sharpiro-Wilk normality test.

Congruent response time								
	Response time (s)			Shapiro-Wilk test			Normality add-ons	
	Min.	Mean	Max.	Stat.	df	Sig.	Skew.	Kurtosis
Benchmark	0.451	0.612	0.834	0.945	16	0.418	0.507	-0.538
Left bottom	0.410	0.576	0.747	0.946	16	0.428	0.362	-0.619
Left middle	0.403	0.559	0.743	0.973	16	0.884	0.190	0.531
Left Top	0.439	0.559	0.711	0.963	16	0.720	0.226	-0.834
Centre	0.394	0.575	0.736	0.959	16	0.652	0.158	-0.204
Right top	0.421	0.577	0.755	0.970	16	0.846	0.437	0.132
Right middle	0.421	0.562	0.712	0.974	16	0.902	0.227	-0.493
Right bottom	0.405	0.567	0.705	0.978	16	0.945	-0.091	-0.489

Table G2: Response time for incongruent conditions along with results from the Sharpiro-Wilk normality test.

Incongruent response time								
	Response time (s)			Shapiro-Wilk test			Normality add-ons	
	Min.	Mean	Max.	Stat.	df	Sig.	Skew.	Kurtosis
Benchmark	0.449	0.669	0.931	0.985	16	0.991	0.175	-0.309
Left bottom	0.413	0.597	0.832	0.933	16	0.267	0.254	-0.703
Left middle	0.378	0.576	0.787	0.977	16	0.938	0.162	0.516
Left Top	0.418	0.581	0.735	0.960	16	0.655	-0.023	-1.153
Centre	0.399	0.592	0.742	0.955	16	0.577	-0.193	-0.827
Right top	0.429	0.579	0.752	0.962	16	0.705	0.119	0.065
Right middle	0.387	0.567	0.769	0.981	16	0.970	0.203	-0.339
Right bottom	0.426	0.587	0.826	0.961	16	0.684	0.684	0.466

Table G3: Response time for stroop interference along with results from the Sharpiro-Wilk normality test.

Stroop interference								
	Response time (s)			Shapiro-Wilk test			Normality add-ons	
	Min.	Mean	Max.	Stat.	df	Sig.	Skew.	Kurtosis
Benchmark	0.002	0.061	0.104	0.934	16	0.282	0.075	0.808
Left bottom	0.003	0.037	0.093	0.852	16	0.014	0.773	-1.004
Left middle	0.001	0.037	0.145	0.822	16	0.005	1.892	4.735
Left Top	0.003	0.028	0.086	0.910	16	0.115	1.031	1.108
Centre	0.003	0.035	0.179	0.704	16	0.000	2.462	7.000
Right top	0.001	0.039	0.105	0.824	16	0.006	0.961	-0.586
Right middle	0.004	0.028	0.069	0.895	16	0.067	0.601	-1.024
Right bottom	0.001	0.031	0.121	0.834	16	0.008	1.809	4.150